Investigation of excipients for the stabilization of HSV-2 vaccine candidate ACAM529

by

Julia Manalil

A thesis
presented to the University of Waterloo
in fulfillment of the
thesis requirement for the degree of
Master of Applied Science
in
Chemical Engineering

Waterloo, Ontario, Canada, 2018

Author's Declaration

I hereby declare that I am the sole author of this thesis. This is a true copy of the thesis, including any required final revisions, as accepted by my examiners.

I understand that my thesis may be made electronically available to the public.

Abstract

Herpes simplex virus type 2 (HSV-2) is a highly infectious pathogen that causes genital ulcerative disease and it affects millions of people worldwide. ACAM529 is a promising new live replication-deficient vaccine candidate against the virus. Vaccine stability during the upstream production processes is an issue so there is a great need for developing an effective stabilization buffer that will protect the vaccine during the process. The purpose of this work was to study the characteristics of ACAM529 and identify excipients that would protect the vaccine from inactivation in liquid solution short-term.

To establish a baseline of ACAM529 stability for further improvements, three lots of purified ACAM529 with differing purification protocols were characterized: Lot A, Lot B and Lot C. Plaque assays were used to determine the titer of each lot, SDS-PAGE was used to analyze the albumin content, and transmission electron microscopy (TEM) was used to image the virus. Lot C was found to have the highest titer at $5.2 \pm 0.6 \times 10^7$ PFU/ml and albumin concentration at approximately 8 g/L compared to Lot A ($3.4 \pm 0.6 \times 10^6$ PFU/ml and 0.5-1 g/L, respectively) and Lot B ($2.1 \pm 0.4 \times 10^7$ PFU/ml and <0.13 g/L, respectively). TEM imaging revealed a high prevalence of unenveloped compared to enveloped virus and some clumping of virus particles, however no differences could be identified between the lots. In addition, a time course assay was developed to study the stability of ACAM529 over 120h. Lot C was found to be more stable than Lot A and Lot B, especially at lower temperatures. Lot A and Lot B showed similar levels of stability at 2-4°C and 25°C.

To screen for ACAM529 stabilizers in liquid solution, various defined and complex solutions used in cell culture for virus production were studied using a time course assay. The addition of 0.01%-10% FBS to the reference buffer resulted in improvements to Lot B stability at 27°C, with minimal titer loss after 120h occurring with 1% FBS. The addition of 0.05-5 g/L rHSA to the reference buffer for

Lot B improved viral stability at 2-4°C in a concentration-independent manner. However, at 27°C, 0.5-5 g/L rHSA significantly reduced the stability, where increasing concentrations of rHSA lead to decreasingly stable virus. Low concentrations of rHSA (0.05 g/L) improved stability at 27°C. The addition of 10% conditioned OptiPro SFM resulted in a slight improvement to stability over a period of 120 hours at 27°C, however the same amount of fresh medium resulted in no change to stability. The addition of 0.1x-1x CLC supplements to the buffer resulted in dramatic decreases to ACAM529 stability at 27°C, especially in the first 24h. Lastly, Pluronic F68 (PF68) at concentrations below the critical micelle concentration (CMC), significantly improved viral titers after 120h, with maximal stability achieved at a concentration of 0.1% PF68.

Lastly, other excipients that have been implicated in enhancing the stability of protein and lipid-based products were investigated for ACAM529 stabilization. An acidic buffer (pH 5) condition caused an improved initial infectivity of the virus when titered with the plaque assay, however it had a negative impact on long-term stability compared to buffers in the range of pH 6-7. The replacement of 10% (w/v) sucrose with 10-30% (w/v) trehalose in the reference buffer did not result in changes to viral stability at pH 6-7 at 27°C. Also, the addition of 0.01-0.1 M L-arginine (along with the resulting increase in buffer ionic strength with the addition of Cl^- ions) and 0.1x-1x non-essential amino acid solution (NEAA) did not significantly affect the stability of ACAM529.

This work showed that it was possible to improve the stability of ACAM529 in the current liquid buffer. The highest level of stability was achieved with the addition of 1% FBS. The addition of 0.05 g/L rHSA or 0.1% PF68 also significantly improved the virus stability and these compounds have the added benefits of having a defined chemical composition compared to FBS and being a safer alternative.

Acknowledgements

I would like to thank our industry partners at Sanofi Pasteur for the opportunity to work on the ACAM529 vaccine candidate. They provided funding and materials, especially the complementary Vero cell line and purified ACAM529 product used in this work. I would especially like to thank Arno Zeiser and Patrick Farrell for taking the time to transfer materials and for their advice, input, and guidance on aspects of the project.

For technical assistance, I would like to thank: Dr. Raymond Legge for allowing the use of his plate reader; Mishi Groh for her training and invaluable advice on transmission electron microscopy; and Dr. Guy Guillemette for his training and expertise when using his CD spectrometer.

I would also like to thank the past and present members of the Aucoin lab for technical and many other types of support. Namely, I would like to acknowledge Stanislav Sokolenko for his reliable knowledge in statistics, data analysis, and R. And Megan Logan for being an incredible colleague and friend, for without whom, this thesis would not have been possible. I would especially like to thank her for providing training in all things Vero and ACAM529, as well as for providing me with sample R codes and helping me troubleshoot data analysis with R. She has also been a valuable sounding board for ideas throughout my Masters.

Lastly and most importantly, I would like to thank my supervisor, Dr. Marc Aucoin, for giving me the opportunity to work with him. He has offered valuable guidance and support throughout this work and also provided the opportunity for me to explore many new avenues that would not have been possible otherwise. Studying in chemical engineering has been an exciting challenge and the transition was made that much smoother with his help.

To my parents,

John and Jessy Manalil.

Table of Contents

List of Figures

List of Abbreviations

ACAM529	HSV-2 vaccine candidate with genes UL5 and UL29 deleted (same as dl5-29)
AIDS	Acquired immunodeficiency syndrome
CD	Circular dichroism
CLC	Cholesterol lipid concentrate solution
CMC	Critical micelle concentration
dl5-29	See ACAM529
DMEM/F12	Dulbecco's modified Eagle medium: nutrient mixture F-12
DMSO	Dimethyl sulfoxide
DNA	Deoxyribonucleic acid
DPBS	Dulbecco's phosphate buffered saline
FBS	Fetal bovine serum
HIV	Human immunodeficiency virus
HSV-2	Herpes simplex virus type 2
HVEM	Herpesvirus entry mediator
MEM	Eagle's minimum essential medium
MRW	Mean residue weight
NEAA	Non-essential amino acids
PEG	Polyethylene glycol
PF68	Pluronic F68
PFU	Plaque forming unit
rHSA	Recombinant human serum albumin
SDS-PAGE	Sodium dodecyl sulfate polyacrylamide gel electrophoresis
SFM	Serum-free media
TEM	Transmission electron microscopy
TFF	Tangential flow filtration
Vero	African green monkey kidney epithelial cell line
VLP	Virus-like particle

Chapter 1
Introduction

The prevalence of herpes simplex virus type 2 (HSV-2) globally is a major cause for concern. It is a highly infectious and contagious sexually transmitted disease affecting over 400 million people worldwide as of 2012 [1] and there is currently no cure for this life-long affliction. It is the leading cause for genital ulcerative disease, resulting in fever, body aches, swollen lymph nodes and, most notably, painful recurring lesions on the skin and mucosal layers surrounding the genitalia [2]. In addition to the physical ailments caused by the virus, the psychological effects are also significant as the social stigma associated with the disease can cause distress and ultimately decrease quality of life. Though it is rarely a life-threatening disease in adulthood, transmission of the virus to neonates during birth runs the risk of causing neurological disease and it is frequently lethal [3]. Furthermore, active shedding of HSV-2 significantly increases the susceptibility to infection by human immunodeficiency virus (HIV), leading to the life-threatening condition, acquired immunodeficiency syndrome (AIDS) [4,5]. It is clear from its high prevalence and numerous risks that an effective and affordable vaccine against HSV-2 is necessary.

There have been numerous attempts at developing an efficacious vaccine with some currently undergoing clinical trials [6,7]. The HSV-2 virus is an enveloped double-stranded DNA virus and there are many strategies for vaccine development. Subunit vaccines containing the glycoproteins naturally embedded in the viral envelope, such as GlaxoSmithKline's gD-2 [8], and Chiron's gD-2 and gB-2 [9] containing vaccine candidates, have thus far failed to illicit an effective broad immune response. DNA and single-replication vaccines have shown more promise as they were found to be more immunogenic [7]. One promising candidate vaccine is ACAM529, a live replication-deficient HSV-2 virus with two DNA replication associated genes, namely U_L5 and U_L29, deleted from its genome. Its effective immunogenicity relies on its ability to establish an acute infection in host cells and express

several potentially antigenic viral proteins that can be displayed by the infected cell to elicit an immune response [10]. To maintain the safety of the vaccine, the virus fails to amplify whole viral particles and lacks the ability to establish a more permanent latent infection [11]. ACAM529 was first developed by Dr. David Knipe's research group at Harvard Medical School and is currently licensed by Sanofi Pasteur. It is produced in a recombinant Vero cell line containing a copy of the deleted genes missing in ACAM529 to complement the virus genome and its amplification. The viral product is then harvested and purified through various steps. The final purified product is then frozen before undergoing other downstream processing such as formulation and lyophilization [12].

The production and development processes expose ACAM529 to various conditions that are potentially harmful to the virus. ACAM529 contains a lipid envelope with glycoprotein spikes that are essential to its efficacy but these features also make the virus highly susceptible to inactivation. Enveloped viruses are notoriously less stable than their non-enveloped virus counterparts [13]. The glycoproteins are essential for viral attachment and entry [14] and thus it is crucial that the structure and function are retained by optimizing the surrounding environment. By extension, the integrity of the lipid membrane in which they are embedded must also be protected. However, the lipid membrane is especially vulnerable to changes in pH, temperature, osmotic pressures, ionic strength, and mechanical stresses such as shear forces [15]. ACAM529 is highly likely to be exposed to these factors during the manufacturing process. It is of great interest to study ACAM529 and devise methods to improve its stability.

1.1 Purpose

The purpose of this work is to develop a buffer for the stabilization of ACAM529 to prevent significant losses in viral titer during the purification process. The improved stability of ACAM529 would improve yields at the end of the manufacturing process and in turn, lower costs for the vaccine.

1.2 Hypothesis

By studying the differences in the stability profiles of various lots of ACAM529 that have been produced using different processes, a more directed approach towards stabilizing the virus is possible. For instance, compounds and solutions used during the cell culture for ACAM529 production have the potential to reveal novel excipients that stabilize the virus. Furthermore, it is hypothesized that strategies used in formulations for other lipid- and protein-based products could be applied to ACAM529 as it is an enveloped virus with glycoprotein spikes.

1.3 Objectives

The objectives of this research are as follows:

1. Characterize different lots of purified ACAM529 to establish a baseline from which improvements to the buffer can be made.
2. Screen for potential stabilizing agents in complex and defined solutions used for virus production in cell culture.
3. Identify and screen other stabilizers of interest that have been used for lipid- and protein-based products for the effective stabilization of ACAM529.

1.4 Outline

This thesis first presents a brief background about the biology of HSV-2, the development and production of the ACAM529 vaccine candidate, and a literature review on excipients used for protein and lipid-based biological stability. The next chapter, Chapter 3, summarizes the general materials and methods used throughout this work. Next, the following three chapters detail the findings of this research. Chapter 4 explores the characteristics of different lots of ACAM529, Chapter 5 investigates the stabilizing effects of various solutions and compounds used in cell culture, and Chapter 6 screens other commonly used excipients for their stabilization properties for ACAM529. A discussion about

the findings of this work is presented in Chapter 7 and concluding remarks about the research in Chapter 8. Lastly, recommendations for future research are presented in Chapter 9.

Chapter 2
Literature Review

2.1 Herpes simplex virus type 2

The highly infectious herpes simplex virus type 2 (HSV-2) is the major cause of genital ulcerative disease and according to the World Health Organization, an estimated 417 million people worldwide between the ages of 15 and 49 were affected in 2012 [1]. It persists to varying degrees in different populations, with the highest prevalence being in Africa (31.5% of the population in 2012), followed by the Americas (14.4%). The virus is capable of establishing latency in sensory neurons and activation leads to viral replication in epithelial cells. Infected individuals who are actively producing and shedding the virus easily transmit it through sexual contact and the established infection is life-long. Its high resilience in the host system can be attributed to its ability to establish a latent infection in host neuronal cells, allowing it to effectively evade the immune system [16]. The disease rarely causes life-threatening symptoms, however the more problematic aspect of HSV-2 infection is the increased susceptibility to HIV (human immunodeficiency virus) infection. HSV-2 infection sites actively recruit CD4+ cells to the surface, the preferred target of HIV, increasing the chance for an HIV infection. There is currently no cure for HSV-2 related disease but the disease and associated risks warrants the great need for an effective vaccine.

2.1.1 HSV structure

HSV is an enveloped double stranded DNA virus belonging to the herpesviridae family of viruses, all of which establish latency in their host. HSV-2 is further categorized into the alphaherpesvirinae subfamily, which also includes the closely related cold sore-causing virus, HSV-1. These viruses are so characterized due to their specificity for sensory neurons for latent infections, where HSV-1 targets the trigeminal ganglion (part of a cranial nerve), and HSV-2 the dorsal root ganglion (part of a spinal nerve). The extent to which HSV-1 has been studied in the literature far surpasses that of HSV-2, so

this literature review also describes aspects of HSV-1, relying on the high instance of homology between the two serotypes [2].

The HSV viral particle has four major components: the DNA core, the protein capsid, the tegument layer, and the lipid envelope embedded with glycoprotein spikes (Figure 2.1A).

2.1.1.1 DNA core

In electron spectroscopic techniques, the HSV genome appears as an electron-dense region in the core of the virus particle. The approximately155 kilobase pair (kbp) HSV-2 DNA genome is linear and double stranded. It is arranged as two regions of unique sequences denoted long (U_L) and short (U_S) regions, which are flanked by regions of inverted repeat sequences (Figure 2.1B). Gene products have been mapped to both the unique sequences and the inverted repeats. The full transcriptome and proteome of HSV has yet to be characterized in its entirety but the function of numerous gene products have been identified [2].

2.1.1.2 Viral capsid

The DNA is surrounded by an approximately 100 nm rigid icosahedral protein capsid made up of 12 pentamers and 150 hexamers arranged in a T=16 pattern. The capsid is generally quite robust, requiring SDS and heat for denaturation [17], and it is composed of viral protein 26 (VP26) (encoded by U_L35), VP23 (U_L18), VP19C (U_L38), and the major capsid protein VP5 (U_L19)[2]. It was found to be mostly uninfectious without the presence of the viral envelope [18] however, infectivity could be rescued by re-encapsulation with synthetic lipid envelopes [19]. Without the lipid envelope, the viral capsid lacks the proteins required cell entry.

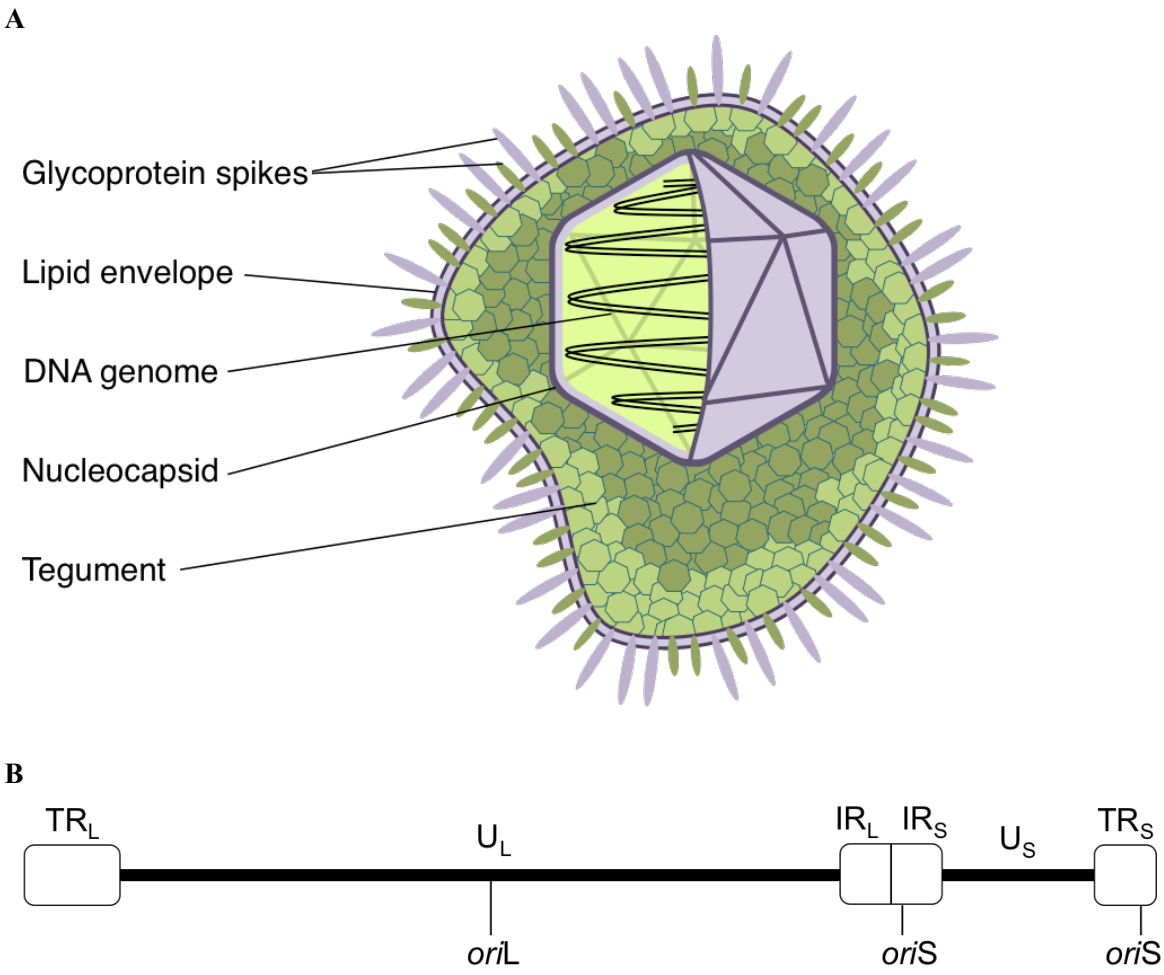

Figure 2.1 HSV virion and genome structure

A. Structure of a HSV virion. **B.** Schematic of the arrangement of the linear HSV DNA genome. Long and short unique sequences (U_L and U_S, respectively) are shown as thin lines. The terminal repeat and inverted repeat sequences flanking the U_L region (TR_L and IR_L, respectively), and flanking the U_S region (TR_S and IR_S, respectively) are shown as white boxes. The origins of replication are noted as *ori*L and *ori*S.

2.1.1.3 Tegument

Electron microscopic imaging revealed a distinct asymmetrical positioning of the capsid within viral particles and this is due to the complex network of proteins constituting the tegument layer [20]. The tegument is seen to cause a distinct polarity in viral particles in that the viral capsid is localized at one pole, whereas tegument proteins dominate the opposite pole. Later studies observed that cell-associated viral particles had a more symmetrical arrangement of the capsid within the tegument layer, which then becomes altered upon release into the extracellular environment [21]. Over time, the tegument of the released viral particle also becomes increasingly resistant to dissociation from the capsid with TritonX-100 treatment [21,22]. It is composed of over 18 viral proteins with functions related to capsid transport to the nucleus and viral DNA release (e.g. VP1/2 encoded by U_L36), viral transcriptional regulation (e.g. infectious cell protein 0 (ICP0), ICP4), and host gene regulation and immune evasion (e.g. ICP34.5, VHS (virion host shut-off encoded by U_L41)), among others [23]. The tegument has been further classified as an inner tegument layer acquired in the host cytoplasm with a diameter of approximately 120 nm, and an outer tegument layer acquired upon envelopment with a diameter of up to 160 nm [24].

2.1.1.4 Lipid envelope

The virus is enveloped in a lipid bilayer membrane acquired from the host cell. To generate the viral envelope, HSV was found to affect cellular lipid metabolism upon infection. A relatively early study in arterial smooth muscle cells found infection with HSV-1 promoted the accumulation of intracellular cholesterol [25]. A later study in Vero cells found that HSV-1 infection resulted in increases to cell size and the Golgi network, to ultimately increase the overall amount of lipid membranes throughout the cell to support viral envelopment [26].

The composition of the envelope can vary depending on the cell type [27] and there are several theories regarding the origin of the membrane, i.e. whether it is from the nuclear, Golgi, or cellular membrane.

The more widely accepted theory suggests that viral particles acquire Golgi-derived membranes [28] and there was evidence of similarity between the HSV envelope and the Golgi membranes. The envelope of HSV-1 produced in Vero cells was found to contain the phospholipids phosphatidylcholine (51.2%), phosphatidylethanolamine (29.8%), phosphatidylinositol (11.3%), phosphatidylserine (4.6%), sphingomyelin (3.1%), which were similar to concentrations in the Golgi membrane [29].

2.1.1.5 Glycoprotein spikes

The HSV envelope is embedded with several types of viral proteins that play a major role in viral pathogenicity. They are involved in viral entry mechanisms, cell-to-cell spread of virus [14], egress pathways, and mediation of cell-cell fusion [2,30]. The composition of the envelope proteins were observed to be independent of the host when two unrelated cell lines (baby hamster kidney (BHK) cells and HeLa cells) were used to produce HSV-1 [31]. There are approximately 11 glycoproteins on the viral envelope, including gB, gC, gD, gE, gG, gH, gI, gK, gL, and gM, as well as some non-glycosylated proteins such as U_L20 and U_S9 [2,30,31]. Electron microscopy of HSV particles shows the glycoproteins as protruding spikes that vary in their dispersion around the viral particle [20]. Glycoprotein B appears as T-shaped and clusters (approximately14 nm), whereas gC (approximately 24 nm) is more widely dispersed. The most abundant glycoprotein, gD (8-10 nm) also clusters but in a distinct irregular pattern [32].

2.1.2 Virus replication cycle

Primary infection by HSV typically occurs at the mucosal layer but it has been shown to infect a wide variety of cell types [32]. The virus replication cycle in host cells typically takes 18-24h and it is quite complex. It involves several stages: attachment, entry, amplification, assembly, and egress.

2.1.2.1 Attachment and entry

The first step in the virus replication cycle of HSV is attachment to the host cell membrane and this is accomplished by the interaction of HSV glycoproteins to several potential receptors. Glycoprotein B (or gC to a lesser extent) binds to glycosaminoglycan chains (GAGs), preferably heparan sulfate, on the host cell membrane to anchor the particle to the surface and bring gD into closer proximity to its specific receptors [33]. The binding of gB to GAGs is not essential to infection but it greatly enhances the infectivity of the virus [34].

The HSV-specific receptors found naturally on the host cell membrane include the herpesvirus entry mediator (HVEM), nectins, and 3-O-sulfated heparin (3-OS HS). The receptors recognized by HSV-2 gD are HVEM, nectin-1, and nectin-2. In comparison, HSV-1 gD binds HVEM, nectin-1, and 3-OS HS, but does not typically bind nectin-2 [35]. HVEM is part of the tumour necrosis factor receptor superfamily and is the principal receptor. It is found on many cell types including epithelial and more commonly, on T lymphocytes (i.e. T cells). Nectin-1 and -2 are cell adhesion molecules, part of the immunoglobulin superfamily, and they are found in a variety of cell types including epithelial cells, fibroblasts, and neuronal cells [34].

The interaction between gD and its receptors induces a conformational change in gD that activates the gH-gL heterodimer complex. This, in turn, activates gB into its fusogenic form which initiates fusion of the viral and cellular membranes and release of the viral capsid and tegument into the cytoplasm [36].

Whether the fusion of the lipid membranes occurs at the plasma membrane or in cellular endosomes is cell-type dependent. Entry of Vero (African green monkey kidney) and HEp-2 (human epithelial type 2) cells by HSV predominately occurs at the plasma membrane. However in CHO (Chinese hamster ovary) and HeLa cells, HSV is taken up by the cells through endocytosis and membrane fusion occurs in both a pH-dependent or pH-independent manner [37]. Regardless of the manner in which the virus enters the cells, the same glycoproteins are involved [2].

Upon release of the tegument and capsid into the cytoplasm of the cell, the outer tegument proteins are shed and the capsid is transported to the nucleus along microtubules via the host cell motor protein, dynein [23]. Inner tegument proteins (e.g. pU_L36) are involved in the targeting of the viral particle to a nuclear pore complex where the capsid is docked and DNA is released through the pore into the host cell nucleus [38,39].

2.1.2.2 Amplification

The primary objective of the virus is self-amplification. This is initiated in the host nucleus and uses both viral and cellular factors. Once the viral DNA has entered the nucleus, a variety of viral products, such as proteins, noncoding RNAs, and micro RNAs, are produced in a complex and coordinated manner [2]. The immediate-early or α genes are those expressed first and in the absence of viral protein synthesis. The highest rates of synthesis are detected between 2-4 hours. The α genes autoregulate their expression, as well as induce the expression of early or β genes, which reach peak synthesis rates between 6-12 hours after infection. Both α and β genes then induce the expression of late or γ genes. The expression of γ genes, unlike α and β genes, is affected by DNA synthesis to differing degrees [2]. For example, the expression of true late genes (γ_2 genes), such as U_L38 (codes capsid protein VP19C) and U_L44 (codes gC), requires DNA synthesis. Late in the infection cycle, the γ gene products repress the expression of α and ß genes.

In addition to amplifying viral proteins, the genome must also be amplified. Viral DNA replication occurs between 3-15 hours after infection within replication compartments in the nucleus and involves seven β genes [2]. First, the origin-binding protein (coded by U_L9) binds the origin of replication sites in the genome, *ori*L or *ori*S (Figure 2.1B), and begins to unwind the double stranded DNA. ICP8, a single-stranded DNA binding protein (coded by U_L29), is recruited to stabilize the unwound DNA. Both proteins signal the recruitment of the helicase-primase complex (composed of

U_L5, U_L8 and U_L52) and the viral polymerase complex (composed of U_L30 and U_L42) to initiate DNA synthesis [2].

2.1.2.3 Assembly and egress

Assembly of the HSV particles is initiated within the replication compartments with capsid assembly. Newly synthesized and partially assembled capsid proteins localize into the nucleus from the cytoplasm, where they are fully assembled. Once the capsid is formed, one copy of the linearized double stranded viral DNA is packaged into each capsid through a portal complex [40] and the resulting particle is designated as a mature nucleocapsid.

Viral egress is the next step in the infection cycle and it requires the acquisition of the tegument layer and envelope around each mature nucleocapsid. As mentioned in section 2.1.1.4, it is still widely contested where the virus acquires its lipid envelope, however the more accepted mechanism is the envelopment-de-envelopment-re-envelopment process. The first envelopment occurs at the inner nuclear membrane. Mature nucleocapsids bind to inner tegument proteins; VP1/2, pU_L37, VHS, VP22 and VP16, and these interact with the inner tails of viral glycoproteins embedded in the inner nuclear membrane [23]. A primary envelope is acquired as the virion buds into the perinuclear space and this process requires the viral proteins pU_L31 and pU_L34, which constitute the nuclear egress complex (NEC).

The enveloped primary virion is subsequently de-enveloped at the outer nuclear membrane through membrane fusion, mediated by gB, gH-gL heterodimer complex, and pU_S3 [41]. The nucleocapsid is released into the cytoplasm where it acquires its inner tegument proteins, including pU_S3, pU_L36, and pU_L37. Tegumentation proceeds as the virion is transported to the trans-Golgi network (TGN) where it acquires the outer tegument [28]. Tegument protein pU_L48 interacts with several outer tegument proteins, such as pU_L41, pU_L46, pU_L47, and pU_L49 [42], as well as with the cytoplasmic regions of

glycoproteins gB, gD, and gH, which are embedded in Golgi membranes [43]. The outer tegument is further anchored to the membrane by pU_L11, pU_L16, and pU_L21 [23], where pU_L11 was shown to interact with the envelope glycoproteins gD and gE in HSV-1 [44] and envelope protein pU_L56 in HSV-2 [45]. The TGN is the site of secondary envelopment as the virus buds into the vesicles. The final stage of egress is the release of the enveloped virus particles and this occurs through cellular exocytotic pathways [23].

Newly released viruses tend to associate with cellular membranes and thus, cell-to-cell spread of the virus relies heavily on interactions between adjacent cells [46]. Glycoproteins gE and gI, which localize to the lateral surfaces of cells where junctions are present [47], play an essential role in cell-to-cell spread [14]. Deletion of either glycoprotein reduced plaque sizes in monolayers of human fibroblasts however in Vero cells, the reduction in plaque size was less apparent [48].

2.2 ACAM529 vaccine candidate

2.2.1 Development of dl5-29

The double deletion replication-deficient HSV-2 mutant, ACAM529, was first developed by Dr. David Knipe's research group at Harvard Medical School. The immunogenic success of a live HSV-1 mutant with a deletion in gene U_L29 in protecting mice from HSV-1 associated disease [49,50] drove the research towards creating a similar mutant in HSV-2. The HSV-1 U_L29 deletion mutant was able to infect permissive cells and express alpha and beta genes, but was unable to produce progeny virus as ICP8, the U_L29 gene product, plays a key role in gene expression and genome synthesis. ICP8 is the major viral DNA-binding protein and it mediates the unwinding of the double stranded DNA and stabilizes the single strands. It is also involved in the transcriptional regulation of gamma genes [2]. Virus was only amplified in complementary Vero cells engineered to express the U_L29 gene product [49,50].

It was observed that de novo synthesis of viral proteins was a key factor towards a strong immunogenic response in mice. The HSV-1 U_L29 deletion mutant had stronger immunogenic properties than an ICP4 deletion mutant, which could only express some alpha genes. Furthermore, a UV-inactivated HSV-1 virus was not an effective vaccine against an HSV-1 challenge [49]. The U_L29 deletion in HSV-1 and -2 behaves similarly [10]. In HSV-2 U_L29 mutants (dl29), viral DNA replication was not detected but significant expression of some late genes (ICP5, ICP15, ICP25, gB, gD) was detected. gB and gD, important targets for anti-HSV immunity, were detected at only slightly lower levels than wildtype virus.

To reduce the probability that the virus could revert back to a wild type virus, a second gene, U_L5 was deleted in addition to U_L29 in HSV-2 (dl5-29) [51]. The U_L5 gene product is part of the helicase-primase complex involved in viral DNA synthesis [2]. Similar to the dl29 virus, the dl5-29 virus only replicated in complementary Vero cells engineered to express the missing genes, in this case U_L5 and U_L29 [51]. The dl5-29 virus showed similar expression of viral genes as the wild type HSV-2 strain (186 syn $^+$-1) in both monkey (Vero) and human (HEL299 or human embryonic lung fibroblast, and MRC-5 or medical research council strain 5 human fetal lung fibroblast) cell lines but at lower levels for some late proteins such as gB, ICP5, and ICP25 [51]. In mice infected with dl5-29, vaginal shedding was significantly reduced and the virus notably failed to establish a latent infection in mouse neuronal cells [11].

2.2.2 Virus manufacturing

Virus manufacturing involves several stages (Figure 2.2). Essentially, virus is produced during upstream processes, concentration and purification is achieved during downstream processes, then the final product is packaged. Below, the upstream and downstream processes are briefly discussed.

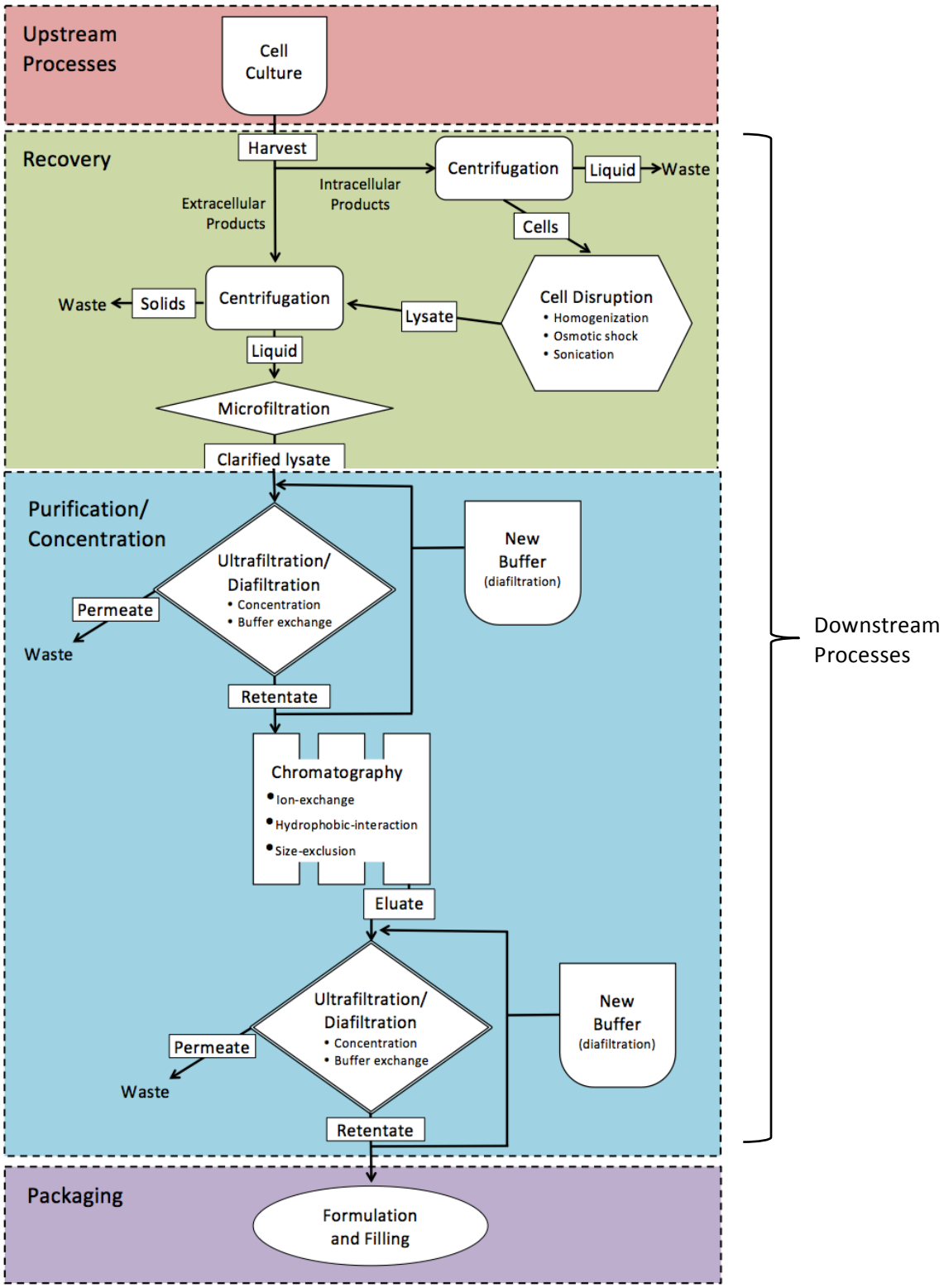

Figure 2.2 Downstream processes for large-scale virus manufacturing.

2.2.2.1 Upstream processes

Virus vaccine production requires an animal cell line (or insect cell line for some systems) for amplification. The upstream process generally involves culturing the cells to the appropriate density, inducing virus production in the cells, and after sufficient time, harvesting the culture to obtain maximum virus yield.

The cell line may either be anchorage-dependent, where a surface is required for proliferation, or it may grow in suspension. Most animal cell lines are anchorage-dependent, however they are not ideal for scale-up and are more labour-intensive. Large surface areas are required for culturing higher cell densities and a detachment step is necessary for passaging [52]. Some cell lines, especially tumour-derived cell lines, can be adapted to grow in suspension. Suspension cell lines are more ideal for scale-up since they can be passaged by dilution and can be grown to higher density in solution. Shear forces are one concern however, due to the mixing required for suspension cultures [52].

Cells are grown to the appropriate density by optimizing parameters such as pH, temperature, dissolved oxygen, pressure, and nutrient supply. It is more advantageous to use chemically defined culture media and supplements as not only do they reduce batch-to-batch variability, but the risk of containing harmful pathogens is reduced, unlike with animal-derived serums [13]. This is especially a concern for products intended for clinical applications.

Once the desired cell density has been achieved, virus production is induced. The cell line may either be stable, where it is engineered to contain the necessary genetic material to produce virus, or it may produce virus transiently. For transient cell lines, induction by for example providing the necessary DNA plasmids, or infecting with the virus, is necessary for production [52]. The multiplicity of infection (MOI) is the ratio of virus particles to cells and ideally, the lowest MOI for optimal virus production is used to induce production. The culturing parameters may also be altered during production for optimal output and this is specific for each type of virus product. After incubation, the culture is

harvested at the optimal time for maximal product yield and the virus undergoes downstream processing.

2.2.2.2 Downstream processes

Upon harvest, the next step in manufacturing is recovery, where the virus is separated from cell debris and other solid contaminants. This process is simplest if the virus is secreted or buds into the extracellular space. The virus can be harvested by sedimentation of the cells using centrifugation and collecting the supernatant. This is the gold standard for clarification of the solution and is optimized for maximal removal of cells with minimal cell lysis [53]. If the virus tends to adhere to the cell surface, which is the case with HSV, an eluting agent can be used. Dextran sulfate is an analog of heparin, an HSV receptor used for cell attachment prior to infection. ACAM529 recovery was increased when dextran sulfate was used in the harvesting media [12].

If the virus is intracellular, it can be liberated by subjecting the cells to lysis-inducing stresses such as high pressure (homogenizers), osmotic shock, or sonication. In addition to releasing the virus into solution, cell disruption also releases other intracellular impurities, such as cellular DNA and proteases, which must be removed in subsequent steps and further complicates the purification process [53]. Removal of host cell DNA is often achieved using enzymes. Benzonase digests DNA into smaller molecules so that it can be removed more readily and in turn reduce the viscosity of the solution. Benzonase treatment prior to filtration reduced membrane fouling and improved the step yield of ACAM529 [12]. Microfiltration is then used to remove any large or solid contaminants.

The next step in downstream processing is to reduce the working volume and remove dissolved impurities from the clarified lysate. Ultrafiltration uses a porous membrane to allow water and small dissolved particles to pass through (permeate) while retaining larger-molecular weight particles, such as the virus (retentate). Concentration of the virus can therefore be achieved using ultrafiltration. For

large-scale processes, ultrafiltration using tangential flow filtration (TFF) is commonly used [54]. Unlike with conventional or dead-end filtration, where the flow of the solution is perpendicular to the porous membrane, in TFF the flow of the solution is parallel to the membrane. This reduces membrane fouling because the parallel flow is able to effectively wash the membrane of accumulating particles. However there are increased shear forces due to the high flow rates required [54].

Once the working volume has been reduced, a buffer exchange step is often subsequently performed using diafiltration. The new buffer is added to the inlet of the TFF step to wash and displace culture media and small molecule impurities from the virus solution. This buffer is typically optimized for maximal product stability while also being tailored for specific subsequent purification steps [54]. For ACAM529, a typical stabilization buffer contains 10% (w/v) sucrose, 10 mM L-histidine, 50 mM potassium glutamate, 160 mM NaCl, pH 7 [12].

The final stage in downstream processing is purification and polishing. The virus is separated from impurities based on specific physical properties. Column chromatography can be used to separate based on ionic strength (ion-exchange chromatography), hydrophobicity (hydrophobic interaction chromatography), or size (size-exclusion chromatography) [54]. Ion exchange and hydrophobic interaction chromatography are absorptive chromatography techniques, which contain beads that are engineered to interact with or bind to chemicals. They are then gradually eluted from the column and the fraction containing the virus is collected. Size-exclusion chromatography contains a porous stationary phase that allows small molecules to enter and this effectively slows the rate at which they pass through the column. Larger particles elute faster because they are not able to enter the pores. Chromatography techniques require optimization to ensure the matrix adequately captures the virus with minimal inactivation, while reducing the adsorption of contaminants. The subsequent elution of

the virus from the column also needs to be optimized for maximal recovery of active virus [53]. Once the product is adequately purified, it is then prepared for final formulation and packaging.

2.3 Components of stabilization solutions

Biologics that contain lipid membranes, such as ACAM529, are particularly more thermolabile than their protein counterparts. The membrane is sensitive to changes in the environment such as osmotic pressures, ionic strength, surfactant concentrations, shear stresses, and temperature [13]. They can also be easily damaged by ice crystal formation encountered during freezing and can be dissociated using detergents [55]. ACAM529 also contains several glycoproteins embedded in the lipid membrane whose function is essential to the vaccines antigenicity. To maintain their structure and function, proteins require specific pH, ionic strength, and temperature conditions [56]. The key components of a stabilization solution are an appropriate buffering agent to maintain the ideal pH, and various excipients that help protect the biological material from unwanted chemical and physical reactions, while also maintaining the correct osmolarity and ionic strength.

The following sections explore various components of liquid stabilization buffers for biological products with lipid membranes, as well as protein-based biologics. Literature on liquid formulation of enveloped vaccines is lacking, as lyophilization is the method of choice for storage.

2.3.1 Buffer pH

The pH of the solution has been regarded as an important attribute to control, especially for protein and peptide products, as it has an effect on both chemical and physical degradation pathways. For example, certain pH conditions can promote unwanted acid-base catalyzed reactions, deamidation of asparagine and glutamine residues, and charge variations that cause structural unfolding [57]. These reactions can ultimately lead to the loss of vaccine antigenicity.

Buffering agents commonly used include citrate, acetate, phosphate, Tris, amino acids such as histidine and glycine and buffer in the range of 3-10. Careful selection of buffering agents is necessary as the buffer ions may interact with the protein in both stabilizing and destabilizing pathways. Some buffers such as phosphate-buffered solutions are particularly prone to temperature induced pH shifts [58] and others are susceptible to degradation upon exposure to light or trace metals such as citrate [56]. Tris buffer was found to stabilize retrovirus better than phosphate buffered saline due to its superior pH stability, especially at freezing temperatures in both liquid and freeze-dried form [59]. Phosphate buffers are particularly ill suited for freezing because the base (Na_2HPO_4) crystallizes faster than the acid (NaH_2PO_4) causing pH drops. Buffers which do not crystallize but form amorphous systems have less changes in pH [57].

The buffering agent in the ACAM529 reference buffer is 10 mM histidine, pH 7 [12], with $pK_a = 6.04$ for the imidazole side chain. In the range of pH 5.5-7, histidine was found to have optimal buffering capacity (0.47-0.49 micro equivalents of acid or base required to change the pH of the system by one unit per micromole of buffering agent (μEq/μmol)) [60]. At pH 7-8, the buffering capacity was significantly reduced to 0.16 μEq/μmol.

2.3.2 Buffer ionic strength and osmotic pressure

The ionic strength of a solution is an important factor when considering the stability of enveloped products and care should be taken to control this. It was shown to be important for optimizing the charge interactions between phospholipid moieties in lipid membranes. Monovalent and divalent cations increase the strength of the membranes of *E. coli* and synthetic liposomes with increasing ionic concentration [61]. Ionic strength also has an effect on buffering capacity. Self-buffering monoclonal antibody (mAb) solutions had a 25-35% difference in buffering capacity between pH 8.0-5.0 when NaCl concentrations were increased from 10 mM to 160 mM. Histidine, however, was minimally affected by this ionic strength change, with only 15-10% difference [60].

Ionic strength also has a direct effect on the osmotic pressure of a solution and can thus cause shrinkage or swelling. An enveloped influenza vaccine experienced shrinkage and membrane perturbations in a hyperosmotic solution but when the viscosity of the solution was increased with methylcellulose, the osmotic stress effects were minimized [62]. Significant inactivation of HSV-2 was seen with rapid drops in osmotic pressure (from dilution) but not with a gradual drop [63]. Conversely, high osmotic pressures can effect the environment within the capsid of enveloped virus. The ability of HSV-1 to eject its viral DNA contents from capsids was directly hindered by an increasing concentration of polyethylene glycol (PEG) that increased the external osmotic pressure [38].

2.3.3 Stabilizers

Many pathways for inactivation and product loss can be mediated through stabilizers. Proteins and lipid-based biologics are susceptible to numerous degradation pathways and remedying this is a more complex challenge. Product loss may occur from unfavourable chemical reactions, aggregation, or from adhesion to container surfaces or air-liquid interphases caused by hydrophilic or electrostatic interactions [64]. This can have a profound effect on product yield, as it can lead to irreversible denaturation or reduce the bioavailability of the product.

2.3.3.1 Preferential exclusion

A broad range of excipients has been identified with the ability to stabilize proteins and this suggests that specific binding effects between the protein and excipient are not involved. The preferential exclusion theory postulates that excipients are excluded from the protein and this promotes a stronger interaction between the protein and solvent to produce a hydration shell [65]. This state favours the native structure of the protein since unfolded proteins would have more surface area and thus a higher chemical potential than the native state. The interaction and binding between excipients and proteins, such as that with arginine or lysine and RNase A, decreases the transition temperature and thermal

stability of the protein compared to when excipients are excluded, such as with trehalose [66]. However, with increased temperatures, trehalose was also found to bind to the native state of RNase A but this binding was observed to be stabilizing and protected the enzyme from thermal inactivation [67].

2.3.3.2 Sugars and other carbohydrates

Sugars and other carbohydrates are widely used stabilizers for their effect on preferential exclusion in liquid solution and also because they are effective cryoprotectants. Disaccharides remain amorphous during freeze-drying, where they are thought to form a glass around the product [55,68]. An amorphous matrix is preferred over crystalline due to the increased risk of damage to lipid membranes from crystal formation. They are also thought to protect products from damage induced by lyophilization by taking the place of water in hydrogen bonds to polar surfaces on proteins and with the carbonyl groups of lipid membranes, allowing them to maintain their native structure [69,70].

Several disaccharides, such as lactose, maltose and cellobiose, and all monosaccharides are reducing sugars and they are typically avoided for formulation. Reducing sugars tautomerize to an open chain form where the aldehyde group undergoes a Maillard reaction with free amino groups on proteins, altering charge, conformation, and degradation rates [71]. The Maillard reaction between glucose and amino side chains of the protein therapeutic, human relaxin, was found to be the major cause of instability. However, trehalose and mannitol prevented this reaction [72].

Conversely, sucrose and trehalose are non-reducing sugars. The anomeric carbons involved in the glycosidic bond prevents the molecule from reverting to the open-chain. However, in acidic conditions, sucrose has been shown to hydrolyze into its monomeric constituents, glucose and fructose, which are both reducing sugars [73]. This becomes relevant during freezing, because uneven freezing of the solution may create microenvironments with elevated proton concentrations, thus

reducing pH. In nature, sucrose and trehalose act as osmolytes to protect intercellular environments from harsh temperatures and low water levels [56].

Sucrose is widely used in vaccine formulations [13,55,74] and it is present in the stabilization buffer for ACAM529. A phosphate buffered sucrose solution improved the stability of several enveloped virus after freezing and warmer temperature storage (4°C and 20°C). It was found to be a superior stabilizer to sorbitol for cytomegalovirus (CMV), varicella-zoster virus (VZV), respiratory syncytial virus (RSV), and HSV-1 [75]. Another increasingly popular disaccharide used in formulation is trehalose [55,66,67,69,70,72,76,77] and it has been shown to have superior properties over sucrose. Trehalose has a higher viscosity than several sugars, including sucrose, and it has superior stabilization properties for numerous proteins. The stabilizing effect on the protein enzymes pyrophosphatase and on glucose 6-phosphate dehydrogenase using 0.5 M trehalose was similar to that with 1.5 M sucrose [69]. The superior stabilizing effect of trehalose over sucrose is not universal. It is dependent on the specific product to be stabilized, as sucrose-containing solutions have been shown to perform better than or similar to trehalose-containing solutions [55]. During lyophilization, mannitol and polyethylene glycol (PEG) were observed to crystallize and were not able to offer any protection for the recombinant human protein Factor XIII. Dextran is able to form an amorphous phase with the protein but this is not enough for protection. Trehalose and sucrose are both able to form a glass around the protein and form hydrogen bonds with the protein in place of water, which is more protective [78].

Sugars, sugar alcohols, and other compounds have also been shown to have membrane-stabilizing properties. The membrane integrity was deemed to be an essential characteristic for measles virus stability [79]. The infectivity of a measles viral vaccine was improved with the excipients mannitol, myo-inositol, proline, malic acid, or gelatin. Lactose, malic acid, and gelatin-containing formulations protected against temperature induced swelling of the virus. Mannitol and malic acid were also shown to function as membrane hydration inhibitors and proline decreased the overall change in membrane

hydration. Increased membrane hydration increases the polarity and thus reduces the stability of lipid membranes [79]. In another study, trehalose and glycine were found to reduce membrane hydration effects at higher temperatures for an enveloped influenza VLP [77].

2.3.3.3 Amino acids

The role of amino acids in solution can by multifold. They are often used as anti-aggregation agents, anti-oxidants, and buffering agents as described previously. Aggregation was seen to be a major issue with influenza VLPs so glycine and the secondary amine and diol, diethanolamine, were used to reduce aggregation. They had a neutral effect on the tertiary structure of the protein spikes, suggesting that particle aggregation was prevented by directly interfering with protein-protein interactions [77].

Arginine has been widely used in protein stabilization solution for its ability to reduce aggregation. Chromatography techniques used in mAb production were improved using 1 M arginine. Protein aggregation was reduced and elution efficiencies from the chromatography columns were increased [80]. L- and D-arginine have also been used to elute measles virus off the surface of erythrocytes. L-ornithine, which is similar in structure to arginine except the guanidine group is replaced by an amino group, was 75% as efficient at elution as arginine [81]. Arginine and lysine also improved the solubility of the protein: tissue plasminogen activator [57]. The mechanism by which arginine prevents aggregation is hypothesized to be due to the three methylene groups which form a hydrophobic region. Exposed hydrophobic regions on a protein, such as aromatic side chains, are prone to induce aggregation and unfolding. The methylene group in arginine can bind to hydrophobic regions on the protein, stabilizing the structure and preventing further unfolding [82,83].

Oxidation can often be the major cause of the denaturation of protein products, especially those high in methionine, cysteine, tryptophan, tyrosine, and histidine [84]. Histidine prevents oxidation by free radicals. The addition of histidine to a liquid formulation for an adenovirus vaccine, which was shown

to be susceptible to oxidation, improved its stability during long term storage at 4°C [85]. The thermal stability of a lipoprotein hepatitis B vaccine was also improved with histidine. They tried several ionic excipients but found histidine and lactate to perform best, with succinate and malate having little to no effect [86].

2.3.3.4 Surfactants

Non-ionic surfactants are commonly used as a stabilizer to prevent protein aggregation. Surfactants are amphiphilic compounds that have both a hydrophobic and hydrophilic region. They adsorb to interfaces, such as air-liquid, solid-liquid, or liquid-liquid, and stabilize compounds that tend to denature or aggregate at these interfaces. When these aggregates go back into solution, it induces further aggregation and eventually precipitation [56,57]. Polysorbate 20 (or Tween 20) and polysorbate 80 (or Tween 80) are commonly used to protect proteins from aggregation [56]. For example, Tween 20 significantly reduced recombinant human interferon-γ adhesion to air-liquid interphases [87]. Genapol PF-10, a block co-polymer of polypropylene oxide (hydrophobic) and polyethylene oxide (hydrophilic), has been shown to prevent insulin surface adsorption and ultimately decrease aggregation [88].

Surfactants, though useful as anti-adsorption and anti-aggregation agents, also interact with and disrupt membranes. Decreased stability was observed with a lipid envelope-containing hepatitis B vaccine when Tween 80 was used [13]. They are frequently used for cellular membrane lysis and for uncoating of enveloped virus for studies [19], though at higher concentrations. Surfactants assemble into micelles when the concentration in the bulk aqueous solution reaches the critical micelle concentration (CMC).

2.3.3.4.1 Pluronic F68

Pluronic F68 is a non-ionic tri-block co-polymer surfactant belonging to the family of Pluronics composed of terminal polyethylene oxide (PEO) regions that are hydrophilic and a central polypropylene oxide (PPO) region that is hydrophobic. Pluronic F68 specifically has an average molar mass of 8400 g/mol and is ~80% polyethylene oxide by mass. On average, one tri-block has a total of 152.73 hydrophilic ethylene oxide units and 28.97 hydrophobic propylene oxide units (e.g. PEO_{76}-PPO_{29}-PEO_{76}). It is commonly used in large-scale animal cell culture as it has the ability to reduce the association of cell membranes with bubbles from sparging, and to protect the membranes from hydrodynamic forces such as shear stress [89]. The mechanism by which it achieves increased membrane stability is either through membrane adsorption or insertion. One study showed that its increased hydrophilicity compared to other Pluronics favoured lipid membrane association over membrane insertion during short (4h) incubations [90]. It is theorized that shorter hydrophobic regions restrict membrane insertion but instead favour the lateral coverage of the membrane, which has been implicated in sealing membrane defects and protecting against leakage [91]. Pluronic F68 has also been demonstrated to be taken up by chondrocytes and CHO cells [92], however in this case, it was unclear whether the polymer was adsorbed to the surface or inserted into the lipid membranes.

2.3.3.5 Lipids and cholesterol

Many enveloped virus contain high levels of cholesterol in their lipid membranes. Cholesterol enrichment was necessary for HIV [93] and HSV-1[94] infectivity. Cholesterol is also used in liposomes as they confer an increased stability by protecting the bilayers from mechanical breakage [95]. However, due to the nonpolar nature of cholesterol, increased levels were shown to decrease the overall surface charge and ion-lipid interactions in synthetic membranes [96]. This reduction in ion-lipid interaction would then decrease the strength of the membrane as mentioned above [61].

2.3.3.6 Proteins: albumin

Proteins, especially gelatin and albumin, have been used extensively as stabilizers. They have proven to be fantastic anti-adhesion stabilizers as they can compete with the biological product of interest to adsorb to surfaces and reduce the amount of product loss. A disadvantage to these stabilizers, however, is that they are often animal derived and gelatin has been reported to cause anaphylactic reactions [97,98]. Recombinant forms of albumin are therefore gaining more popularity.

Recombinant human serum albumin (rHSA) is another alternative to albumin. rHSA produced in rice was found to be similar in structure and biochemistry as plasma-derived human albumin [99] and it was found to protect enveloped virus in liquid formulation [100]. During production, viral products are generally more stable in the culture media due to the presence of many protective agents required by the cells such proteins, lipids, and amino acids. When FBS, was added to liquid solutions of gammaretroviral or lentiviral vectors, an improved infectivity and reverse transcription activity was observed [100]. After studying the specific components of FBS, the researchers found that a recombinant human serum albumin (rHSA) was sufficient for gamma retroviral stability and a combination of rHSA and lipoproteins for lentiviral stability.

One of the major roles of albumin, which is predominantly alpha-helical in structure, is to bind and transport materials through the circulatory system and it has been well documented to bind various types of compounds [101]. It has 7-9 fatty acid binding sites, and two drug-binding sites known as Sudlow's site I and II [101,102]. Bound ligands can have competitive or allosteric effects on the binding of other compounds to albumin and furthermore, it can cause conformational changes in secondary structure (reduced alpha helical content) and tertiary structure (domain rotations in relation to each other). The ability of albumin to bind drugs often increases the drug solubility and half-life *in vivo* [103]. Albumin has also been shown to have antioxidant properties, either by binding radical scavengers, or sequestering transition metal ions with pro-oxidant activity [104].

2.3.3.6.1 Circular dichroism spectroscopy

Circular dichroism (CD) spectrometry is a popular technique used for rapid protein structural analysis. It relies on the property that asymmetrical molecules absorb left- and right-handed polarized light to differing degrees, resulting in an elliptically polarized light, and the ellipticity is highly dependent on the chemical environment of the molecule [105,106]. Spectra in the far UV region (190-250 nm) are predominantly due to the peptide bond and it can be used to determine protein secondary structure. Alpha-helices display strong negative peaks around 208 nm and 222 nm, and a positive peak at 193 nm. Antiparallel beta-pleated sheets show negative peaks at 218 nm and positive peaks at 195 nm. Disordered or random coils display negative peaks around 195 nm and have very low ellipticity above 210 nm [106]. Spectra in the near UV region (260-320 nm) are due to aromatic amino acid side chains: tryptophan causes peaks between 290-305 nm, tyrosine between 272-282 nm, and phenylalanine between 255-270 nm [105]. The analysis of near UV spectra of proteins is not sophisticated enough to give specific structural insights however it can be extremely useful for comparative studies. For example, it is often used to assess the proper folding of recombinant protein by comparing its near UV CD spectra to that of the wild type protein [99].

2.4 Summary

ACAM529 is a live replication-deficient viral vaccine against the disease caused by HSV-2. The efficacy of the vaccine relies on its ability to infect and produce potentially immunogenic viral proteins in the host cell. It is therefore essential that the lipid envelope of the virus and embedded glycoproteins required for cell entry are protected during the manufacturing process. There are numerous types of compounds that can be used as stabilizing excipients for protein and lipid-based biological products. Though their mechanisms of stabilization are not fully understood, specific types of excipients have been implicated in preventing deactivation events such as particle aggregation, surface adsorption, oxidation, and membrane disruption. Formulations are often specific to the product of interest so it is important to screen several types of compounds to identify stabilizing excipients.

Chapter 3
Materials and Methods

This chapter describes the approaches used to study ACAM529 stability and provides details on the general techniques and materials used in this body of work.

3.1 Viral vaccine candidate

The vaccine candidate ACAM529 is a live herpes simplex virus type 2 with two genes, U_L5 and U_L29, deleted from its genome, rendering it replication-deficient in susceptible cells. It was first developed by Dr. David Knipe (Harvard Medical School, Boston, MA)[11,51] before being acquired by Sanofi Pasteur (Toronto, ON) for large scale production. Sanofi Pasteur has supplied several lots of frozen purified ACAM529, three of which were used in these studies: Lot A, Lot B, and Lot C.

3.2 Cell line

A complementary Vero cell line (African green monkey kidney epithelial cells) with the HSV-2 U_L5 gene and HSV-1 U_L29 gene cloned into its genome was used to propagate the virus. The cell line, developed by Dr. Knipe [11,51], was provided by Sanofi Pasteur and it was stored frozen in the vapour phase of liquid nitrogen in 1 ml aliquots at a concentration of $1x10^6$ cells/ml in culture media (Dulbecco's Modified Eagle Medium: Nutrient Mixture F-12 (DMEM/F12) (Corning) supplemented with 4 mM L-glutamine (Sigma-Aldrich), and 10% fetal bovine serum (FBS) (HyClone)) with 10% dimethyl sulfoxide (DMSO) (Sigma-Aldrich).

3.2.1 Initiating a cell culture

To initiate a cell culture, a frozen 1 ml vial was quickly thawed in a 37°C water bath and the DMSO-containing medium exchanged. The cells were diluted 1/10 in culture media, centrifuged at 800 rpm for 5 minutes, decanted, and resuspended in 20 ml fresh culture media. Cells were seeded at a concentration of ~$1.3x10^4$ cells/cm^2 on a 75 cm^2 tissue culture treated T-flask (Nunc, Thermo

Scientific) and incubated at 37°C with 5% CO_2 atmosphere until 80-90% confluency with media exchanges every 48-72h.

3.2.2 Cell passaging

Passages were performed when culture confluency reached 80-90%. The media was removed and cells were washed with Dulbecco's phosphate buffered saline (DPBS), then dissociated from the T-flask surface using TrypLE (Gibco) for 10 min at 37°C. The suspended cells were diluted with culture media, centrifuged at 800 rpm for 5 min to pellet the cells, and the media was removed then replaced with fresh media. Cell viability was determined using the trypan blue exclusion method. A small sample of the cells was diluted 1:1 in a 0.5% trypan blue solution (HiMedia) in DPBS and counted under a microscope using a hemocytometer. Cells were deemed to be alive if they were able to exclude the dye and cells were deemed dead if the dye was able to penetrate the cellular membrane. The cells were then diluted using culture media and seeded into fresh T-flasks at a concentration of 1.1-2.7x10^4 cells/cm^2.

3.3 Time course assay

A 5-day time course of virus activity at ambient temperatures was chosen as the key response variable for changes in conditions and formulation.

3.3.1 Buffer preparation and baseline formulation

A reference buffer typical for ACAM529 purification consisting of 10% (w/v) sucrose (Sigma-Aldrich), 10 mM L-histidine (Sigma-Aldrich), 50 mM potassium glutamate (Sigma-Aldrich), 160 mM sodium chloride (Sigma-Aldrich), pH 7 [12] was used throughout this work as a baseline control. Excipients were either added to the reference buffer or used to replace components, as specified. All buffers were prepared fresh for each time course assay.

3.3.2 Viral preparation

Frozen purified virus stock from Sanofi Pasteur was quickly thawed at 37°C and diluted 1/100 (see Appendix A) in fresh buffer and incubated at the appropriate temperature in 15 ml Falcon tubes (Corning). Tubes were covered in foil to reduce light exposure. To monitor viral stability, a small volume was removed for titration via the plaque assay. In most cases, titration was done immediately after sampling but for cases where sampling times were more frequent, the volume removed was frozen at -80°C for storage and then quickly thawed at 37°C prior to performing the plaque assay (see Appendix A). If frozen, in all cases, all samples taken at a specific time point were titered at the same time.

3.3.3 Viral titration: plaque assays

Viral titers during the time course assays were based on a measure of viral infectivity, an important attribute for the efficacy of the ACAM529 vaccine candidate. When HSV-2 infects a monolayer of susceptible cells, the infection causes plaques to form in the monolayer. At low virus densities, each plaque corresponds to a single virus, and the titer can be established as plaque forming units per ml (PFU/ml).

12-well tissue culture treated plates (VWR) were seeded with complementary Vero cells below passage 25 (see Appendix A) at a concentration of $3x10^5$ cells/well and incubated at 37°C with 5% CO_2 atmosphere for approximately 24 hours. The media was removed and cells were washed with DPBS. Serial dilutions of the virus were performed in 96-well plates (VWR) using culture media and 200 µL of viral dilutions were used to infect each well of the 12-well plate. Negative controls were included, where 200 µL of media was used instead of the viral dilution, to assess the quality of the cell monolayers. Plates were rocked every 15 min for 1 hour, then 1 mL/well of overlay media (DMEM/F12 with 4 mM L-glutamine, 1% (v/v) FBS, 100 Units/mL penicillin, 100 µg/mL streptomycin solution (Gibco), and 0.75% (w/v) methyl cellulose (Sigma-Aldrich)) was applied and

plates were incubated at 37°C with 5% CO_2 atmosphere for approximately 45-48 hours to allow for plaque formation. After incubation, media was aspirated and cell monolayers were dyed with crystal violet solution (12.9% crystal violet, 0.056% ammonium oxalate, 11.2% ethanol, 44% methanol) (Sigma-Aldrich) for 30 min, and then washed with deionized water. Plaques in the monolayer were counted manually and wells containing 20-220 plaques were used to determine the viral titer in units of plaque forming units (PFU) per mL as shown in equation [1]:

$$PFU\ per\ ml = \frac{\#\ of\ plaques \times dilution\ factor}{0.2\ ml} \quad [1]$$

To determine the log loss in titer after 120 hours, the logarithm of the average titer at 120 hours was subtracted from the logarithm of the average titer at 0 hours, as shown in equation [2]:

$$Log\ loss\ in\ titer = f(x, y) = \log(x) - \log(y) \quad [2]$$

where x is the average titer at 120 hours and y is the average titer at 0 hours. Equation [4] was used to determine the propagation of error, s_f (general formula shown in [3]) for the value obtained using equation [2]:

$$s_f = \sqrt{\left(\frac{\partial f}{\partial x}\right)^2 {s_x}^2 + \left(\frac{\partial f}{\partial y}\right)^2 {s_y}^2} \quad [3]$$

$$s_f = \sqrt{\left(\frac{1}{x \ln 10}\right)^2 {s_x}^2 + \left(\frac{1}{y \ln 10}\right)^2 {s_y}^2} \quad [4]$$

where x is the average titer at 120 hours, s_x is the associated standard deviation for x, y is the average titer at 0 hours, and s_y is the associated standard deviation for y. All data manipulation and plot generation was done with R [107–113].

3.4 TEM

Transmission electron microscopy (TEM) was used to visualize the structure of ACAM529. Formvar/carbon 200 mesh copper grids (Ted Pella, Inc., Redding, CA) were prepared by applying a 0.01% bovine serum albumin (BSA) (Sigma-Aldrich) solution for 30s and then removing the excess liquid. Virus sample was diluted 1/100 in 10 mM HEPES (BDH Chemicals) buffer, pH 6.6 then applied to the grid for 1 min. Excess liquid was then drained and the virus was fixed with 2% formaldehyde (Sigma-Aldrich) for 5 min. The grids were stained with 1% phosphotungstic acid (PTA) for 45s, drained, and left to dry overnight at 2-4°C. Samples were examined on a Philips CM10 transmission electron microscope at 25 000x to 60 000x magnification.

3.5 SDS-PAGE

Sodium dodecyl sulfate polyacrylamide gel electrophoresis (SDS-PAGE) was used to separate and visualize proteins in the purified viral product. Samples were diluted 1:1 in 2x SDS sample buffer (125 mM Tris-HCl (Bio-Rad) (pH 6.8), 4% (w/v) SDS (Sigma-Aldrich), 20% (v/v) glycerol (Bio Basic Canada), 5% (v/v) β-mercaptoethanol (Sigma-Aldrich), 0.2% (w/v) bromophenol blue (Sigma-Aldrich)) and incubated in a boiling water bath for 7 min before loading into 1 mm-thickness SDS-PAGE gels (12% acrylamide resolving gel with a 4% acrylamide stacking gel). PageRuler Unstained Protein Ladder (Thermo Scientific) and PageRuler Plus Prestained Protein Ladder (Thermo Scientific) were used to estimate protein size and either recombinant human serum albumin (rHSA) (Cellastim, Invitria) or BSA was used as a concentration reference standard. Gels were run at 175 V for approximately 1h in running buffer (25 mM Tris base (Bio-Rad), 190 mM glycine (Sigma-Aldrich), 0.1% (w/v) SDS, pH 8.3). Protein was visualized by staining the gels for 1.5h in Coomassie solution (0.05% (w/v) Coomassie R-250 (Bio-Rad), 10% (v/v) glacial acetic acid (Sigma-Aldrich), 40% (v/v) ethanol (Sigma-Aldrich)), and then destaining overnight in destain solution (10% (v/v) glacial acetic acid, 40% (v/v) ethanol).

3.6 CD spectrometry

Circular dichroism (CD) spectrometry was used to detect potential changes to albumin tertiary and secondary structure caused by thermal stresses or the addition of excipients. CD spectra were obtained on a Jasco J-715 CD spectrometer with the accompanying Spectra Manager software. Scans were done at room temperature in quartz SUPRASIL cuvettes (Hellma Analytics, Mullheim, Germany) with 0.1 cm path length for the far UV region (250 nm – 180 nm). Samples containing albumin were diluted with the appropriate buffer immediately before loading into the cuvette to a concentration of 0.5 g/L. The response time used was 0.125 s with a data pitch of 0.5 nm and a scan speed of 200 nm/min. A total of 25 accumulations were acquired for each run and cuvettes were rinsed thoroughly with DI water between runs. Buffer background scans without albumin were obtained to establish the baseline. All scans were smoothed using the Spectra Manager software "Means-Movement" method and the baseline spectra was subtracted from the albumin spectra. Molar ellipticity $[\theta]$ in degree cm^2 $dmol^{-1}$ was calculated according to equation [5] using the mean residue weight (MRW) value of 113 Da for albumin [114]:

$$[\theta]_\lambda = \frac{\theta \times MRW}{c \times l \times 10} \quad [5]$$

where θ is the measured ellipticity at wavelength λ (mdeg), c is the concentration of albumin in solution (g/L), and l is the path length (cm). Data was visualized by plotting the calculated molar ellipticity against the wavelength using R [107–113].

Chapter 4
Characterizing ACAM529

4.1 Chapter objective

Final material characterization in terms of quantification and stability is well established; however, both suffer when transferring to in-process analysis. Material concentration and composition can vary enormously at different stages of preparation. For a virus, the active ingredient is exposed to culture media with composition that varies with time and to fairly elevated temperatures. Following the amplification, the virus will be subject to shear stresses, gravitational forces, and osmotic shifts.

Production and purification processes for ACAM529 have resulted in virus with variable stability. In this chapter, various characteristics of three lots of virus were studied to form a baseline for subsequent analysis.

4.2 Materials and methods

4.2.1 Protein quantification using SDS-PAGE

To analyze the protein content in each of the viral lots, frozen stocks of Lot A, Lot B, and Lot C were quickly thawed at 37°C, serially diluted, then 5 µl was run on SDS-PAGE gels as described in Chapter 3. Recombinant human serum albumin (rHSA) dissolved in MilliQ water was used as the reference standard.

4.2.2 TEM imaging

Transmission electron microscopy (TEM) was used to visualize the structure of ACAM529 in Lot A and Lot C as described in Chapter 3.

4.2.3 Time course assays

4.2.3.1 Virus batch differences

To study the stability profiles of different batches of virus, frozen stocks of Lot A, Lot B, and Lot C were quickly thawed at 37°C and diluted 1/100 in triplicate into freshly prepared reference buffer at pH 7. The time course assay comparing Lot A to Lot B used incubation temperatures of 2-4°C (in the fridge) and 25°C, and samples were taken immediately after (0 hour), 24, 72, and 120 hours after diluting the virus to monitor the viral titer. The time course assay comparing Lot B to Lot C used incubation temperatures of 2-4°C, 27°C, and 37°C, and samples were taken immediately after (0 hour), 4, 8, 16, 24, 48, 72, and 120 hours after diluting the virus to monitor viral titer. Plaque assays were conducted as described previously in Chapter 3.

4.2.4 Stability modelling

4.2.4.1 First order exponential decay model

The stability profiles of Lot B and Lot C at 2-4°C, 27°C, and 37°C (described in section 4.2.3.1) were fit to the following first order decay model:

$$\frac{d}{dt} V(t) = -k \cdot V(t) \quad [6]$$

$$V(t) = V_0 \cdot e^{-k \cdot t} \quad [7]$$

where $V(t)$ is the viral titer (PFU/ml) at time t (h), V_0 is the initial viral titer at 0h, and k is the decay rate constant (h^{-1}). The model was fit using the Solver function in Microsoft Excel by minimizing the sum of squared differences between the experimental data and model. The constraint that was applied was that V_0 was held constant for each virus (an assumption that is reasonable at a given pH). To calculate the energy of deactivation (E_a in J mol^{-1}), the k values at each temperature were fit to the Arrhenius model:

$$k = A \cdot e^{-\frac{E_a}{R \cdot T}} \quad [8]$$

where A is the pre-exponential factor (h^{-1}), R is the gas constant (8.314 J mol^{-1} K^{-1}), and T is the temperature (K). An Arrhenius plot ($ln(k)$ vs. T^{-1}) was generated by plotting the linear form of the model:

$$\ln(k) = \ln(A) - \frac{E_a}{R \cdot T} \quad [9]$$

and E_a and A for each virus were calculated using the slope and y-intercept, respectively.

4.2.4.2 Double decay model

To better describe biphasic ACAM529 deactivation observed at lower temperatures, a double decay model was developed. It was proposed that there are two subpopulations of virus, each undergoing a different rate of decay. The first order exponential decay model [7] was adjusted to include an additional first order decay component as shown below, and was dubbed the double decay model:

$$V(t) = V_1 \cdot e^{-k_1 t} + V_2 \cdot e^{-k_2 t} \quad [10]$$

where V_1 and V_2 are the initial viral titers of subpopulation 1 and 2, respectively, and k_1 and k_2 are the respective decay rate constants. The model can be further simplified:

$$V(t) = V_0 \cdot y_1 \cdot e^{-k_1 t} + V_0 \cdot y_2 \cdot e^{-k_2 t} \quad [11]$$

$$V(t) = V_0\left(y_1 \cdot e^{-k_1 t} + y_2 \cdot e^{-k_2 t}\right) \quad [12]$$

$$V(t) = V_0\left(y_1 \cdot e^{-k_1 t} + (1 - y_1) \cdot e^{-k_2 t}\right) \quad [13]$$

where y_1 and y_2 are the fraction of the population that are subpopulation 1 and 2, respectively, and sum to a value of 1. The model was fit to the stability profiles of Lot B and Lot C at 2-4°C (described in section 4.2.3.1) using the Solver function in Microsoft Excel by minimizing the sum of squared differences between the experimental data and model.

4.3 Results

4.3.1 Virus stock albumin content, titer, and imaging

To compare the protein content in each of the viral lots, SDS-PAGE was conducted and the results can be observed in Figure 4.1A. The predominant protein in each lot had a similar molecular weight to the albumin standard. Viral proteins were in low quantitates relative to albumin and difficult to quantify using the Coomassie stain, even with undiluted samples (Appendix C). The PageRuler Prestained protein ladder estimated the correct expected size of albumin (approximately 66 kDa), however the PageRuler Unstained protein ladder consistently estimated the size of albumin to be higher than 70 kDa.

The albumin content in each lot was estimated by comparing the intensities of the appropriate band to that of the rHSA standard. The most abundant proteins in HSV-1 are capsid protein VP5, which has a molecular weight of 149.1 kDa, and tegument protein VP13/14, which has a molecular weight of 73.8 kDa (see Appendix C). Since these and other viral proteins were in low concentrations, their contribution to the intensity of the band for albumin was assumed negligent. Lot A contained approximately an order of magnitude more albumin than Lot B, with 0.5-1 g/L and <0.13 g/L, respectively (Figure 4.1B). Lot C, however, had the highest albumin content of the three lots, with approximately 8 g/L. The albumin content in each of the lots varied significantly.

To determine the titer of each of the virus stocks, plaque assays were performed and the results are presented in Figure 4.1C. Lot A had a titer of $3.4 \pm 0.6 \times 10^6$ PFU/ml, close to an order of magnitude lower than Lot B which had a titer of $2.1 \pm 0.4 \times 10^7$ PFU/ml. The titer of Lot C was significantly higher than the other two lots at $5.2 \pm 0.6 \times 10^7$ PFU/ml.

TEM was used to observe the physical properties of the virus and to determine whether there were physical differences between some of the lots. Lot A and Lot C were imaged and representative

images are shown in Figure 4.2 and Figure 4.3, respectively. In Lot A and Lot C, both enveloped virus and capsids lacking an envelope (naked capsids) were observed, with the latter being at higher prevalence. Enveloped viruses typically appear as round, irregular structures close to 200 nm with some displaying a white halo [17,24]. The inner structures (capsid and DNA core) are also typically visible with adequate penetration by the stain. Many of the enveloped viruses observed in Lot A and Lot B did not have highly visible capsids or DNA cores so the stain did not appear to penetrate (Figure 4.2B and Figure 4.3C). Many of the enveloped viruses were also observed in clusters (Figure 4.2B). In many cases however, it was difficult to discern between an enveloped virus and debris.

Naked capsids are icosahedral and typically appear very regularly shaped and approximately 100 nm. Several naked capsids were identified for both Lot A and Lot B and most had electron dense centers, indicating the presence of DNA (Figure 4.2A and C, and Figure 4.3A and D). A few displayed more uniform colour, suggesting an empty capsid (Figure 4.3B) and some appeared in clusters (Figure 4.3B). Several naked capsids were observed to be surrounded by an irregular material (Figure 4.2C) that could be the tegument layer peeling away [17]. Broken capsids were also observed and it was possible to see the penton and hexon capsomers that made up the capsid (Figure 4.2D). Due to the small size of the virus and difficulty in identifying enveloped virus, it was challenging to accurately make quantifiable observations, such as the enveloped virus to naked capsid ratio. Therefore, only qualitative observations were made with TEM and both Lot A and Lot C did not show any significant differences in physical characteristics using this method.

A

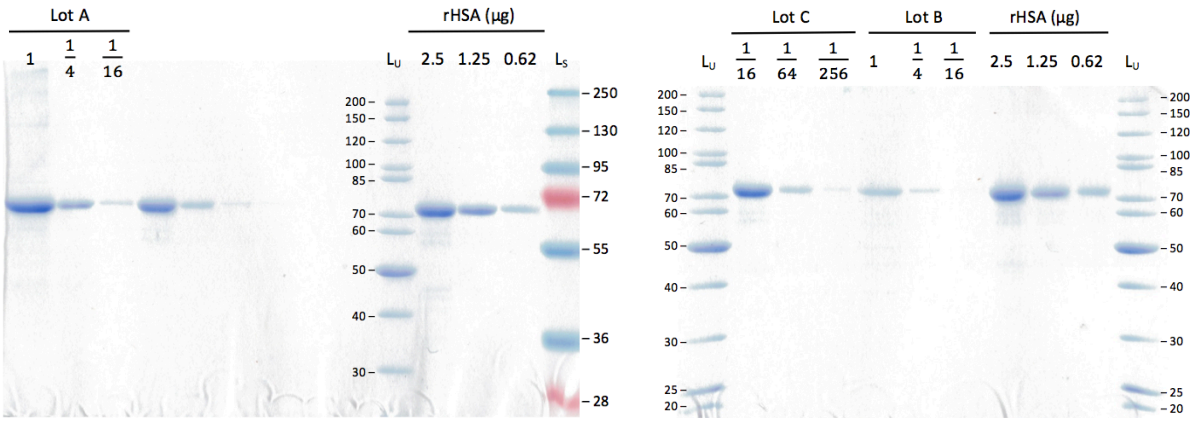

B

Virus	[Albumin] (g/L)
Lot A	0.5-1
Lot B	<0.13
Lot C	~8

C

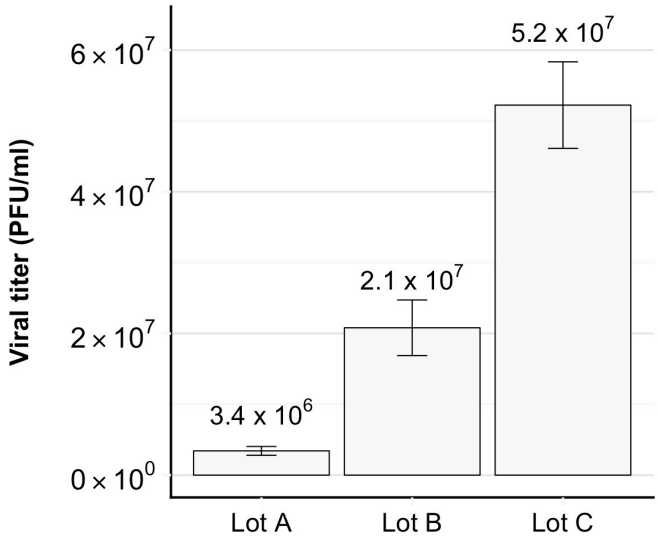

Figure 4.1 Analyzing differences in albumin content and titer in ACAM529 Lot A, Lot B, and Lot C.

A. SDS-PAGE gels of each lot of ACAM529. The dilution of each lot is indicated above the lanes. rHSA was used as a standard to estimate the albumin content and 5 uL of each sample was loaded. PageRuler Prestained (L_S) and Unstained (L_U) Protein Ladder were used with protein sizes indicated (kDa). **B.** The table summarizes the calculated albumin concentration in each lot of ACAM529, approximated by comparing band intensities to the rHSA standard. **C.** Plot of viral titers of each lot of purified ACAM529 as determined using plaque assays upon thawing frozen stocks.

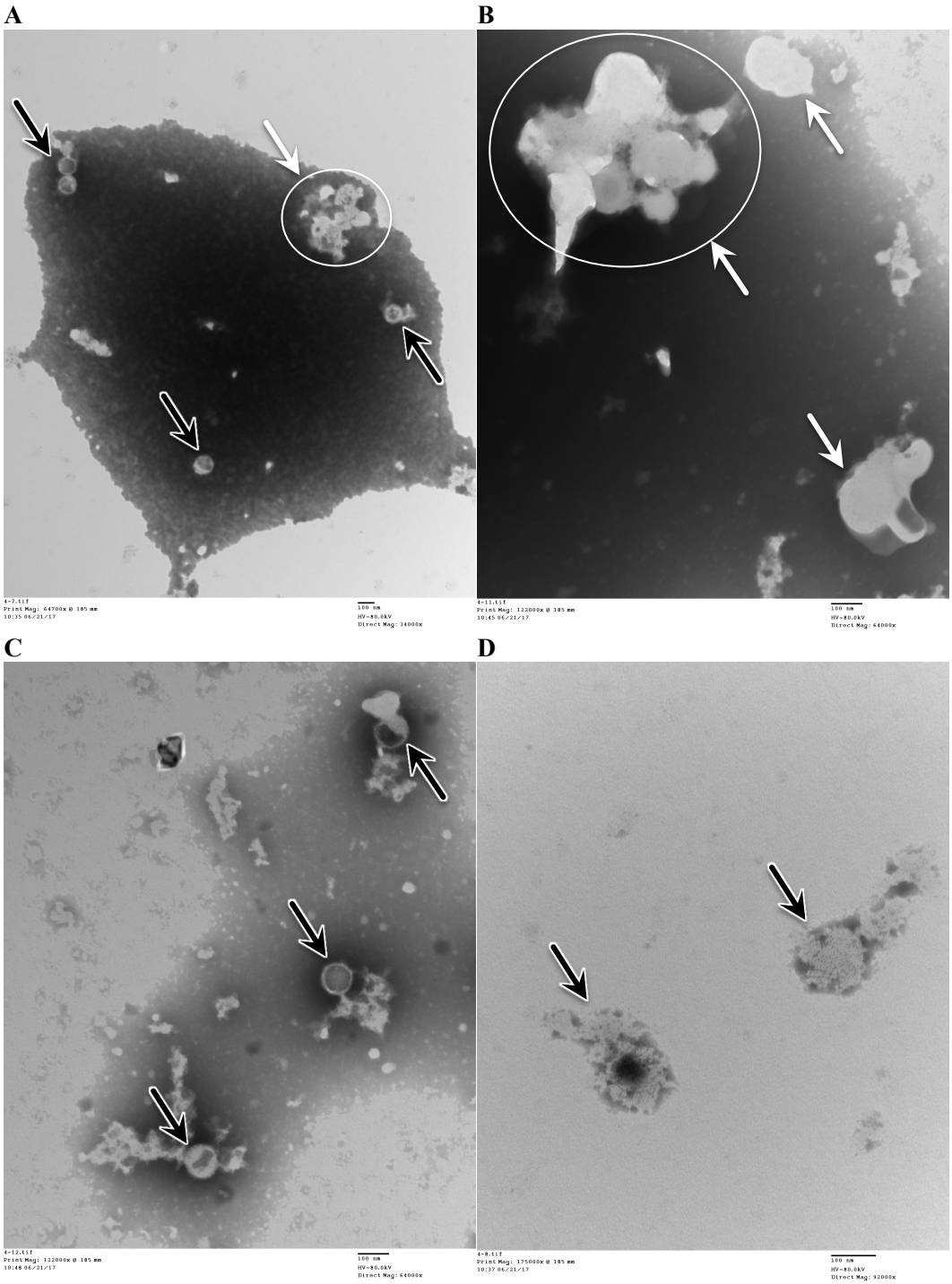

Figure 4.2 TEM imaging of ACAM529 Lot A.

Black arrows show capsids, White arrows show enveloped virus. Clusters are circled in the respective shade. Bars indicate 100 nm.

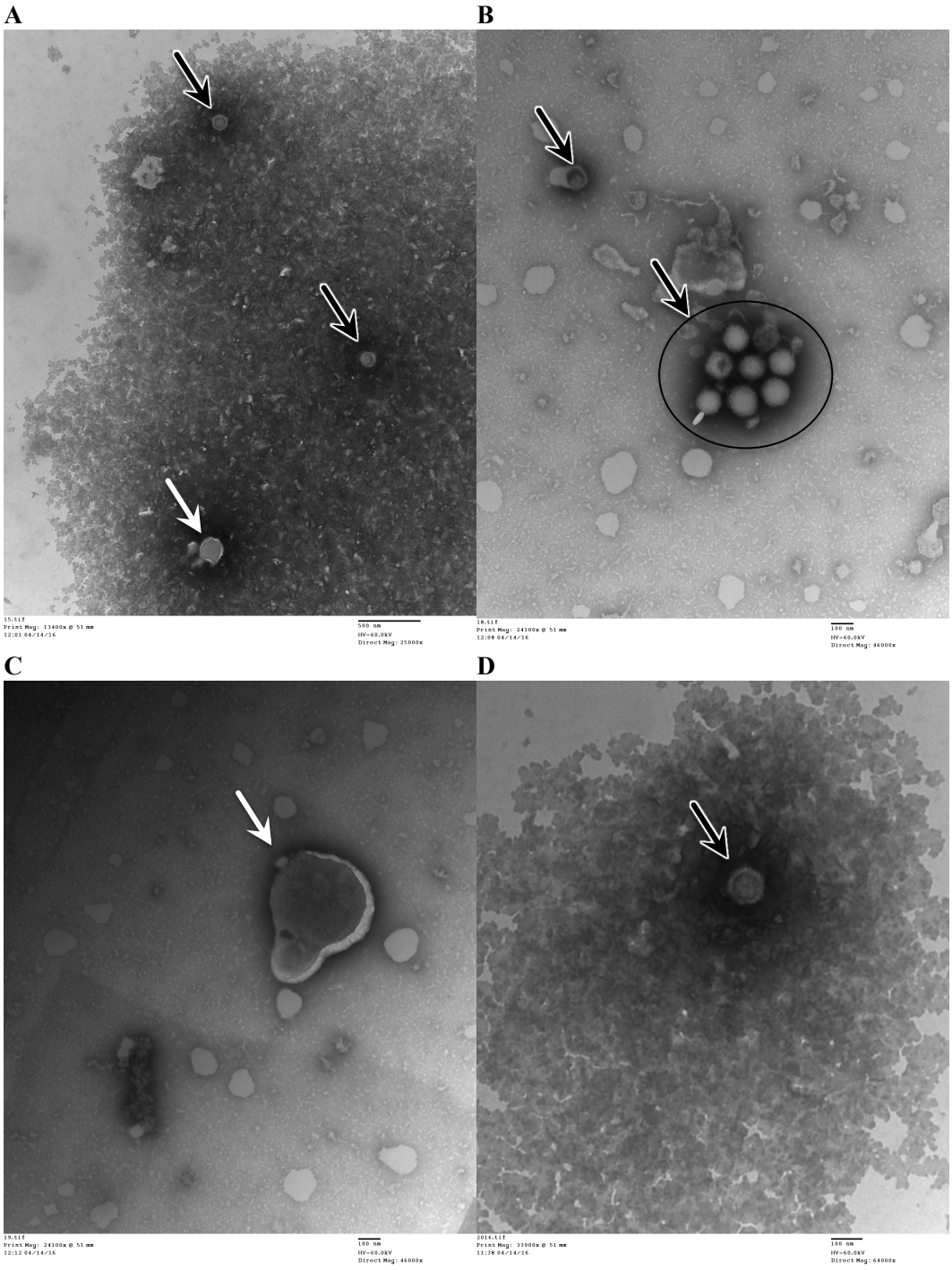

Figure 4.3 TEM imaging of ACAM529 Lot C.

Black arrows show capsids, white arrows show enveloped virus. Clusters are circled in the respective shade. Bars indicate 100 nm.

4.3.2 Comparing the stability of ACAM529 lots

To examine the differences in stability between lots, 120h time course studies were conducted. Comparisons of the stability profiles of Lot A and Lot B at 25°C in the first 72 hours revealed they were very similar (Figure 4.4A). However, the overall log loss in titer after 120h at 25°C for Lot A (0.63 ± 0.10 log loss) was lower than Lot B (0.84 ± 0.10 log loss) (Figure 4.4B). It should be taken into account that the calculation for the log loss in titer relies heavily on the first and last point of the experiment, whereas the time course assay provides more information about the stability. The time course stability profile in Figure 4.4A shows that their profiles were very similar except at 120h, where there is an increase in titer for Lot A, though there is relatively high variance in the value. This could have been caused by an error in the plaque assay titer and as a result, caused a decreased value in the calculated log loss in titer. These results suggest that there was no significant difference in stability between Lot A and Lot B.

Differences between ACAM529 Lot B and Lot C stability were similarly assessed. A time course assay was conducted at 27°C for 120h and the results are presented in Figure 4.4C and D. As seen previously, there was a steep initial decline in titer in the first 24h with both lots, followed by a less steep decline thereafter. It was evident that Lot C, which had 0.89 ± 0.07 log loss in titer, was significantly more stable than Lot B, which had 1.3 ± 0.11 log loss in titer.

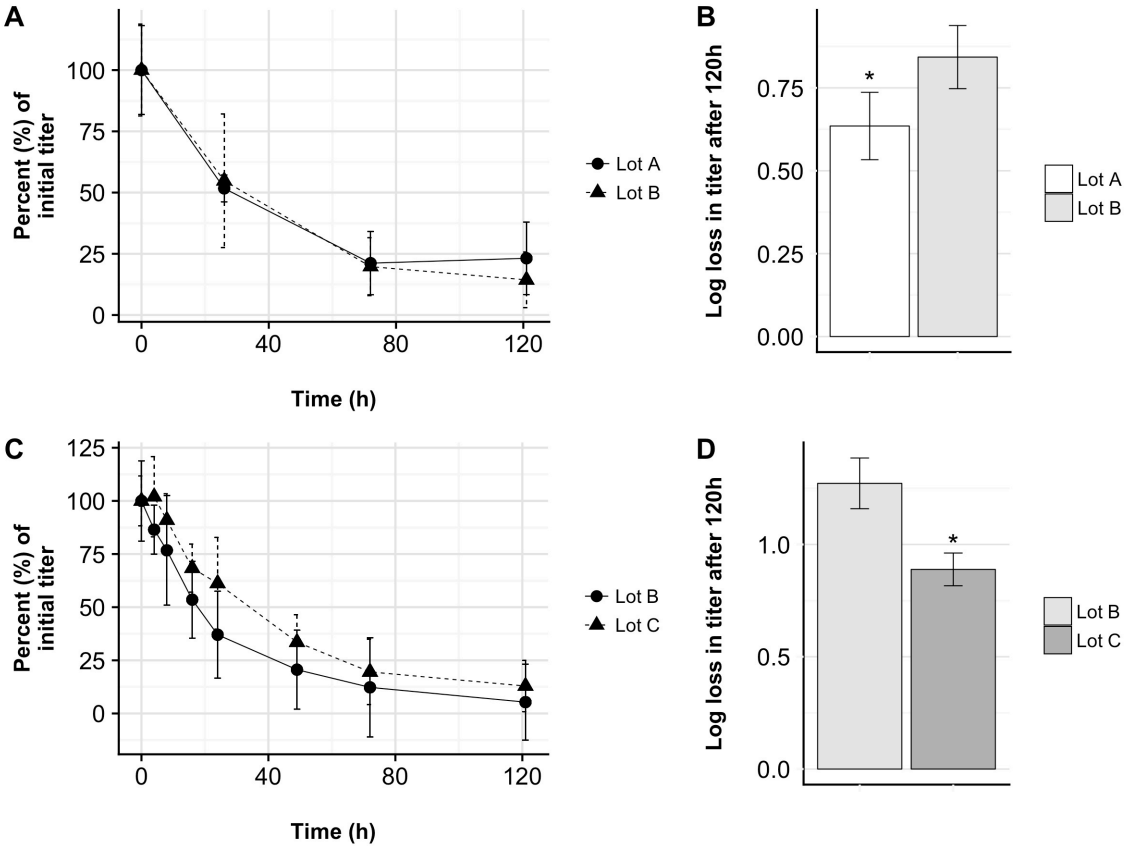

Figure 4.4 Comparing the stability of ACAM529 Lot A, Lot B, and Lot C.

Lot A and Lot B were diluted into the reference buffer and incubated at 25°C for 120h. Viral stability over time was monitored using plaque assays and reported as PFU/ml (**A**) and the total log loss in titer was determined (**B**). In a second experiment, Lot B and Lot C were diluted into the reference buffer and incubated at 27°C for 120h. Viral stability over time was monitored using plaque assays and reported as PFU/ml (**C**) and the total log loss in titer was determined (**D**). A significant deviation ($\alpha = 0.05$) from Lot B in the same experiment is noted with *.

4.3.3 Effect of temperature on ACAM529 stability

Enveloped viruses, such as ACAM529 are notoriously thermolabile and often experience elevated deactivation at higher temperatures. Here, time course assays were conducted to study the effect of temperature on the stability of different lots of ACAM529. The results are presented in Figure 4.5 (the data at 25°C and 27°C are the same as what was presented in Figure 4.4). The data is also presented in Appendix D (Figure D.1) in a way that allows for stability comparisons between the different lots at a given temperature.

The stability of each lot of ACAM529 studied here significantly decreased with increased temperature. In the first experiment, Lot A had 0.44 ± 0.09 log loss in titer at 2-4°C compared to 0.63 ± 0.10 log loss at 25°C (Figure 4.5A and B). In the same experiment (Figure D.1A and B), Lot B had 0.45 ± 0.09 log loss in titer at 2-4°C, which was not significantly different from the titer loss observed with Lot A, reiterating the results observed in the previous section that these lots have similar stability profiles.

In a separate experiment, the stability of Lot B and Lot C at 2-4°C, 27°C, and 37°C were compared. It was evident that Lot B was less stable than Lot C at all temperatures tested (Figure D.1C and D) and both lots were significantly more stable at lower temperatures (Figure 4.5C-F). The results also show that the difference in stability between the two lots becomes more pronounced at lower temperatures. At 2-4°C, the log loss in titer of Lot C was 0.46 ± 0.07 while the log loss in titer of Lot B was 0.77 ± 0.08. At 27°C, the log loss in titer of Lot C was 0.89 ± 0.07 while the log loss in titer of Lot B was 1.27 ± 0.11. Finally, at 37°C, the log loss in titer of Lot C was 1.72 ± 0.11 while the log loss in titer of Lot B was 1.94 ± 0.11. The processes used to produce Lot C have resulted in a significantly more stable virus, with the protective effects being enhanced at lower temperatures.

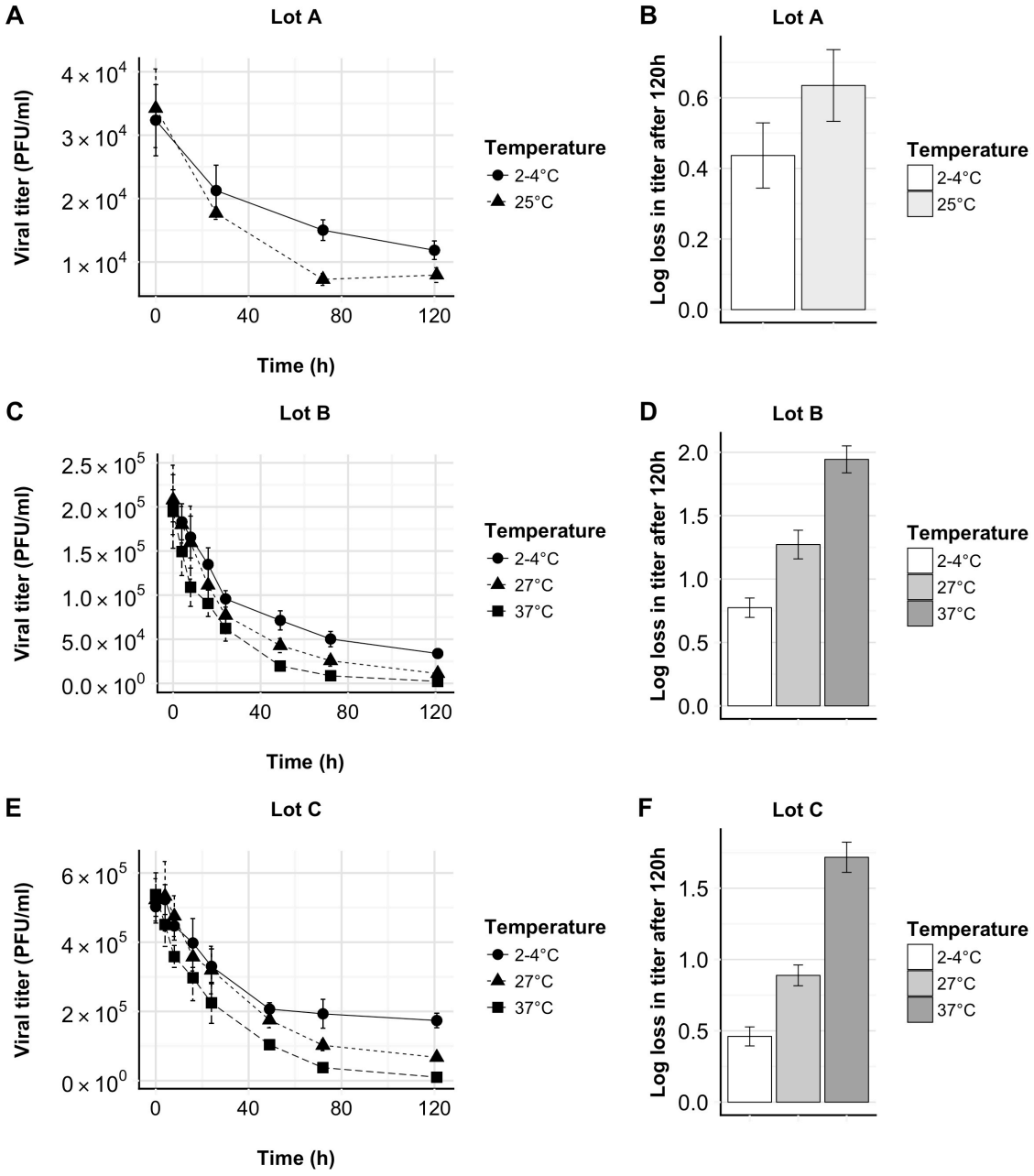

Figure 4.5 Effect of temperature on the stability of ACAM529 Lot A, Lot B, and Lot C.

Lot A was diluted into reference buffer and incubated at 2-4°C or 27°C for 120h. Viral stability over time was monitored using plaque assays and reported as PFU/ml (**A**) and the total log loss in titer was determined (**B**). In a second experiment, Lot B and Lot C were diluted into the reference buffer and incubated at 2-4°C, 27°C or 37°C for 120h. Viral stability over time was monitored using plaque assays and reported as PFU/ml (**C** and **E**, respectively) and the total log loss in titer was determined (**D** and **F**, respectively).

4.3.4 Stability profile modelling

4.3.4.1 First order decay kinetics

Modeling all aspects of viral decay is challenging, as there are numerous potential mechanisms involved, each mechanism with their own rate constants. Viral decay, however, typically follows a characteristic exponential decay [59,115]. The stability profiles of Lot B and Lot C at 2-4°C, 27°C, and 37°C were fit to the first order decay model expressed in equation [7]. The model was able to describe the decay curves at 27°C and 37°C adequately, with data for Lot B fitting slightly better overall than Lot C (Figure 4.6A). However at 2-4°C, the decay trend after 24h for both virus, but especially Lot C, did not fit the model as well. It was evident that the data better fit the model at higher temperatures than at lower temperatures. The V_0 values calculated by the model for Lot B (1.96×10^5 PFU/ml) and Lot C (5.23×10^5 PFU/ml) were similar to the average experimental titers for both viruses at 0h ($2.01 \pm 0.34 \times 10^5$ PFU/ml for Lot B, and $5.21 \pm 0.56 \times 10^5$ PFU/ml for Lot C) (Figure 4.6B). The k values for both virus increased with increased temperature, indicating an increased decay rate with higher temperatures. Also, the k values were lower with Lot C compared to Lot B, indicating that the latter decayed at a faster rate.

The energy of deactivation, E_a (J mol^{-1}), and pre-exponential factor, A (h^{-1}), were calculated using the Arrhenius model [8] (Figure 4.7). The energy of deactivation for Lot C (17.78 kJ mol^{-1}) was slightly lower than that of Lot B (18.42 kJ mol^{-1}). The pre-exponential factor, however, was twice as high in Lot B compared to Lot C (60.91 h^{-1} compared to 31.07 h^{-1}). This suggests that the factors contributing to the increased stability of Lot C over Lot B have an increased effect on A compared to E_a.

A

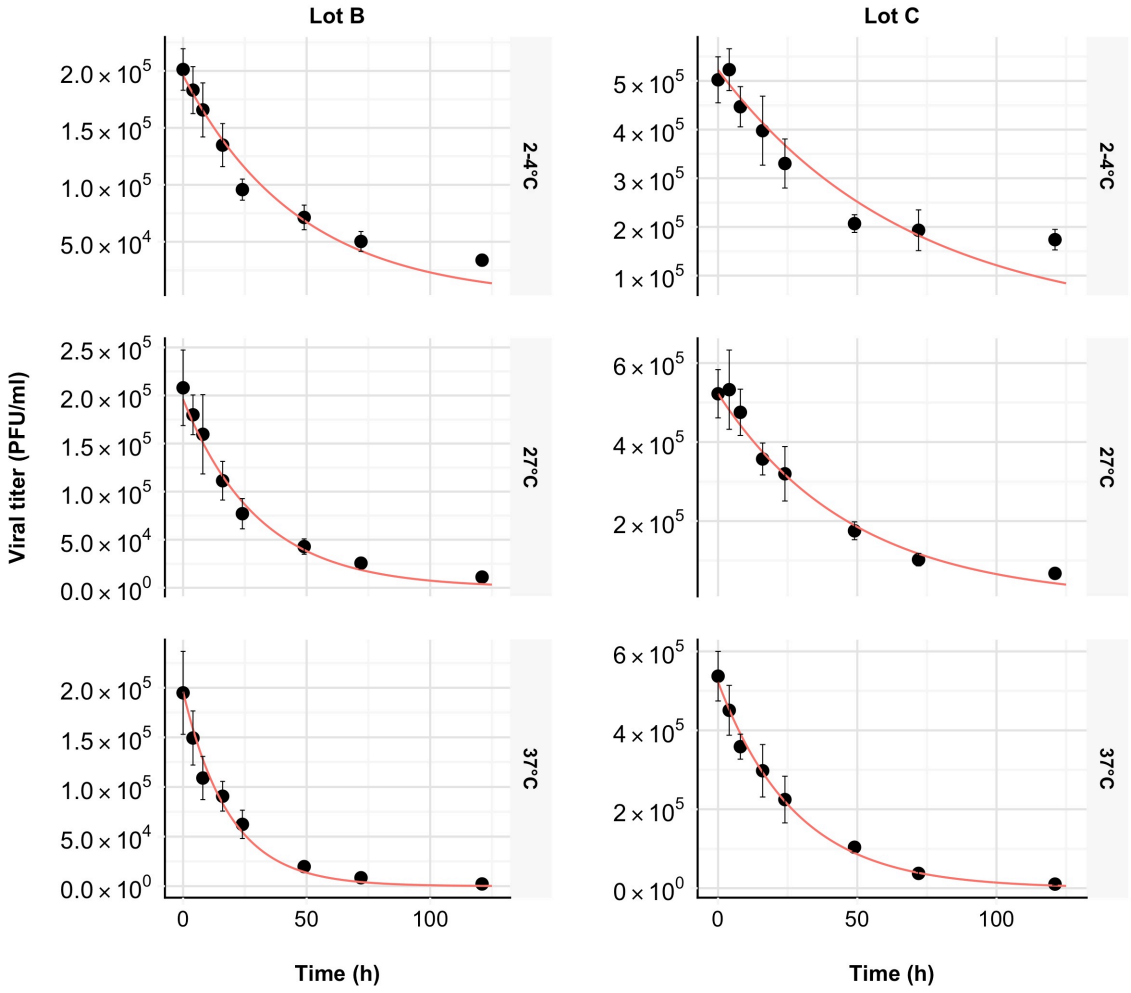

B

Virus Lot	Temp. (°C)	V_0 (PFU/ml)	k (h^{-1})	Sum of Squared Error $(PFU/ml)^2$
Lot B	2-4	1.96×10^5	2.14×10^{-2}	9.61×10^8
	27		3.27×10^{-2}	5.70×10^8
	37		5.34×10^{-2}	6.05×10^8
Lot C	2-4	5.23×10^5	1.46×10^{-2}	1.30×10^{10}
	27		2.08×10^{-2}	5.10×10^9
	37		3.61×10^{-2}	1.57×10^9

Figure 4.6 Fitting ACAM529 stability profiles to a first order exponential decay model.

Virus titer was plot against time and the data was fit to the first order exponential decay model: $\boldsymbol{V(t) = V_0 \cdot e^{-k \cdot t}}$ (**A**). The table summarizes the parameter values as calculated using Solver (**B**).

A

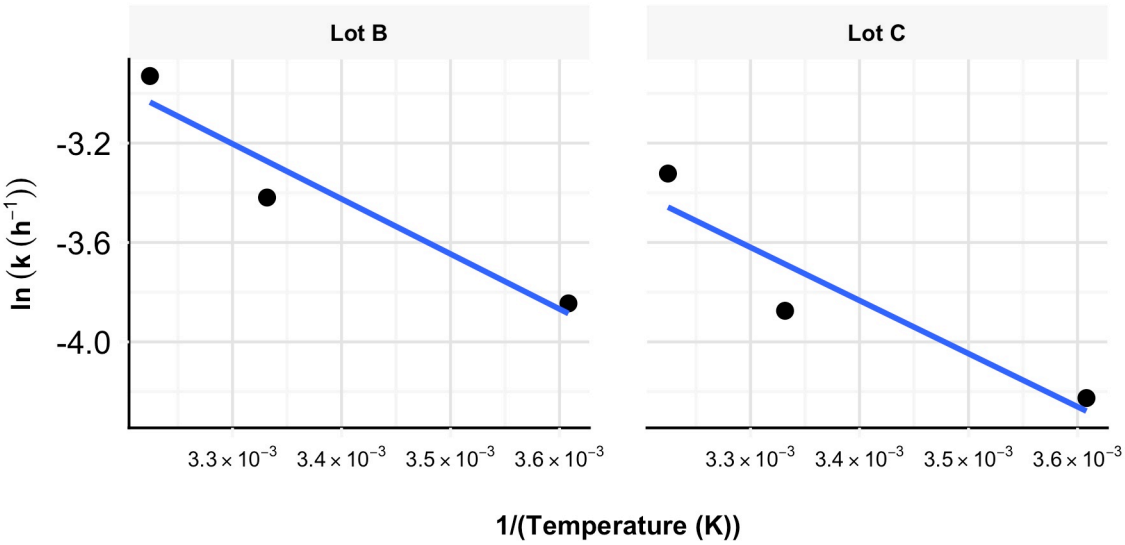

B

Virus Lot	E_a (kJ mol^{-1})	A (h^{-1})
Lot B	18.42	60.91
Lot C	17.78	31.07

Figure 4.7 Arrhenius plot for ACAM529 stability from a first order exponential decay model.

An Arrhenius plot was generated using the calculated k values at each temperature point (**A**) and the calculated energy of deactivation (E_a) and pre-exponential factor (A) are summarized in the following table (**B**). They were calculated using the slope and y-intercept, respectively.

4.3.4.2 Double decay model

To better model the stability profiles of ACAM529 at 2-4°C, a double decay model was tested. The stability profiles showed an initial steep decline in titer, followed by a less steep decline thereafter. The observed biphasic kinetics could be a result of two species of virus decaying at different rates. To reflect this phenomenon, the first order decay model was adjusted to include an additional first order decay component, as described in 4.2.4.2, and was dubbed the double decay model [13]. This model provided a better fit for the curves at 2-4°C compared to the first order decay model (Figure 4.8). Since the kinetics corresponding to k_1 and k_2 are similar, the larger value was called k_1. From the parameters, it can be seen that y_1, which corresponds to the fraction of the virus population affected by the deactivation reaction with k_1, was similar for both Lot B and Lot C (0.68 and 0.71, respectively). The y_2 values (calculated by subtracting y_1 from 1) were 0.32 for Lot B and 0.29 for Lot C. This suggests the same proportion of virus in both lots experienced each of the two reactions described by the model.

The parameter estimates for k were higher for Lot B than for Lot C, suggesting that some degradation pathways were minimized in Lot C. This was also observed with the first order decay model. The k_1 value for Lot B was 4.3 $x10^{-2}$ h^{-1}, while for Lot C, it was slightly lower at 3.2 $x10^{-2}$ h^{-1}. Conversely, the k_2 values were lower than k_1 and they differed greatly as Lot B had a value of 5.5 $x10^{-3}$ h^{-1}, while Lot C, had a value of 0 h^{-1}. This suggests that at 2-4°C, both lots contained a smaller subpopulation of virus (32% in Lot B and 29% in Lot C) that underwent deactivation at a slower rate, with Lot C containing a subpopulation that is stable for the duration of the experiment. The experimental data showed a plateau for Lot C after 48h incubation and this could be as a result of the stable sub-population.

A

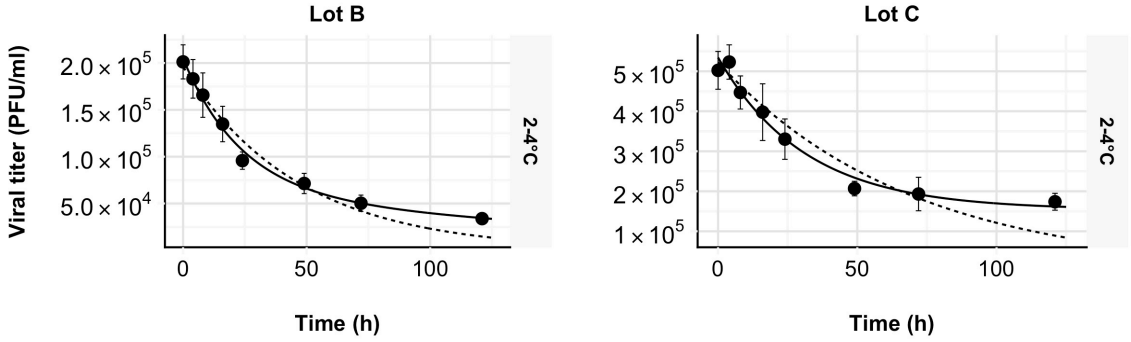

B

Virus Lot	V_0 (PFU/ml)	y_1	k_1 (h^{-1})	k_2 (h^{-1})	Sum of Squared Error $(PFU/ml)^2$
Lot B	2.05 x 10^5	0.68	4.3 x 10^{-2}	5.5 x 10^{-3}	2.05 x 10^8
Lot C	5.34 x 10^5	0.71	3.2 x 10^{-2}	0	3.31 x 10^9

Figure 4.8 Comparing the fit of a first-order decay model with a double decay model for ACAM529 stability at 2-4°C.

The curves shown in Figure 4.6 at 2-4°C are displayed again here for comparison purposes. For the double decay model, viral titer was fit to equation [13] (**A**). The dotted line (…) corresponds to the first order exponential decay model: $V(t) = V_0 \cdot e^{-k \cdot t}$, and the solid line (−) corresponds to the double decay model: $V(t) = V_0\left(y_1 \cdot e^{-k_1 t} + (1 - y_1) \cdot e^{-k_2 t}\right)$. The table summarizes the parameter values for the double decay model (**B**).

4.4 Chapter summary

In this chapter, various characteristics of three lots of ACAM529 were studied. First, the albumin content and titer of each lot was determined and two lots were imaged using TEM. Lot A had up to an order of magnitude more albumin content than Lot B. The titer of Lot A was an order of magnitude lower than Lot B. Lot C had much more albumin than either of the other two lots and also had significantly higher titer. TEM images of Lot A and Lot C showed a high prevalence of naked capsids in the samples and some instances of clumping of enveloped viruses and naked capsids. Enveloped viruses were difficult to distinguish, as there were not many instances of adequate stain penetration to identify the inner viral structures that would identify an enveloped virus. Differences between Lot A and Lot C were not discernable using TEM.

This chapter also explored the stability of the different lots of virus and observed the effects of temperature. Lot A and Lot B had similar stabilities at 2-4°C and 25°C. Lot C was significantly more stable compared to Lot B at 2-4°C, 27°C, and 37°C, with the difference being more apparent with decreasing temperatures.

Finally, the stability of the ACAM529 was modelled. A first order exponential decay model was adequate to describe the stability of Lot B and Lot C at 27°C and 37°C. The parameter estimates for the initial viral titer (V_0) were close to experimental values and in general, the decay rate constants (k) for Lot B were higher than Lot C and higher at higher temperatures. The energy of deactivation constants (E_a) were similar for both lots but the pre-exponential factor (A) for Lot B was twice as high as Lot C. At lower temperatures (2-4°C), a proposed double decay model, which describes the overall decay of two subpopulations of virus following first order exponential decay, was a better fit for the stability of Lot B and C. The parameter estimate for the ratio of subpopulations (y_1 and y_2) was similar for both lots and decay rate constants (k_1 and k_2) were higher for Lot B than Lot C. The value of k_2 for Lot C was 0 h^{-1}, indicating a subpopulation that was stable for the length of the experiment.

Chapter 5

Exploring Cell Culture Components for ACAM529 Stabilization Excipients

5.1 Chapter objective

Transport of viral specimens in liquid formulation has historically been done in culture media or in the presence of serums and extracts, as these environments are optimal for viral viability [116,117]. Cell culture media and supplements are optimized to encourage cell growth and product production, but they also serve the function of protecting fragile cellular membranes from various stresses. Chemical stresses such as osmolarity, pH and oxidative stresses, as well as physical stresses such as shear stresses, are all concerns during cell culture and various compounds are added to mitigate these stresses [118,119]. In this chapter, culture media and additives associated with virus production were assayed for their stabilizing properties of ACAM529 in liquid formulation. The media and additives studied were fetal bovine serum (FBS), recombinant human serum albumin (rHSA), OptiPro serum-free media (SFM), cholesterol lipid concentrate solution (CLC), and Pluronic F68 (PF68).

5.2 Materials and methods

5.2.1 Time course assays

5.2.1.1 Effect of FBS

To study the stability of ACAM529 in the presence of FBS, virus Lot B was quickly thawed at 37°C and diluted 1/100 in triplicate into freshly prepared reference buffer with or without 0.01%, 0.1%, 1%, 10%, or 50% (v/v) characterized FBS lot AAF204951 of Canadian origin (HyClone) (see Appendix E), then incubated at 27°C. Samples were taken immediately after (0 hour), and 24, 72, and 120 hours after diluting the virus to monitor the viral titer using plaque assays, described in Chapter 3.

5.2.1.2 Effect of rHSA

To study the stability of ACAM529 in the presence of albumin, frozen stocks of Lot B and Lot C were quickly thawed at 37°C and diluted 1/100 in triplicate into freshly prepared buffer. The time course assay of Lot B with added rHSA compared to Lot C used the reference buffer with or without 1 g/L rHSA (Cellastim, Invitria) at pH 7, and incubation was carried out at either 2-4°C or 25°C. The time course assay analyzing the effects of different concentrations of rHSA on the stability of Lot B used the reference buffer with or without 0.05 g/L, 0.5 g/L, or 5 g/L rHSA at pH 7 and incubation temperatures of 2-4°C or 27°C. Samples were taken immediately after (0 hour), 24, 72, and 120 hours after diluting the virus to monitor the viral titer using plaque assays as described previously in Chapter 3.

5.2.1.3 Effect of OptiPro SFM culture media

To study the stability of ACAM529 in the presence of OptiPro SFM, virus Lot B was quickly thawed at 37°C and diluted 1/100 in triplicate into freshly prepared reference buffer with or without 10% OptiPro SFM (Gibco) or 10% conditioned OptiPro SFM (OptiPro SFM removed from a four-day culture of Vero CCL-81 cells and passed through a 0.2 μm filter), then incubated at 27°C. Samples were taken immediately after (0 hour), and 24, 72, and 120 hours after diluting the virus to monitor the viral titer using plaque assays as described in Chapter 3.

5.2.1.4 Effect of CLC

Two runs were completed to test the effects of a cholesterol solution. In both runs, virus Lot B was quickly thawed at 37°C and diluted 1/100 in triplicate into the freshly prepared buffers. For the first run, the buffers tested were the reference buffer with or without 1x CLC (Gibco). For the second run, the buffers tested were the reference buffer with or without 0.1x or 0.5x CLC. Both runs were incubated at 27°C and samples were taken immediately after (0 hour), and 24, 72, and 120 hours after diluting the virus to monitor the viral titer using plaque assays, described in Chapter 3.

5.2.1.5 Effect of PF68

To study the stability of ACAM529 in the presence of PF68, frozen virus Lot B was quickly thawed at 37°C and diluted 1/100 in triplicate into freshly prepared reference buffer at pH 7 with or without 0.001%, 0.01%, 0.1%, and 1% (w/v) PF68 (Gibco), then incubated at 27°C. Samples were taken immediately after (0 hour), and 120 hours after diluting the virus to monitor the viral titer using plaque assays as described in Chapter 3.

5.2.2 Stability modeling of ACAM529 with buffer containing FBS

5.2.2.1 First order exponential decay model

The stability profiles of Lot B in buffer with or with out 0.01%, 0.1%, 1%, 10%, or 50% FBS (experiment described in section 5.2.1.1) were fit to the first order decay model in equation [7] using R [107–113]. The complete code is presented in Appendix F.

5.2.2.2 Zero order decay model

The stability profiles of Lot B in buffer with or with out 0.01%, 0.1%, 1%, 10%, or 50% FBS (experiment described in section 5.2.1.1) were fit to the following zero order decay model:

$$\frac{d}{dt}V(t) = -k \quad [14]$$

$$V(t) = V_0 - kt \quad [15]$$

where $V(t)$ is the viral titer (PFU/ml) at time t (h), V_0 is the initial viral titer at 0h,and k is the decay rate constant (PFU ml^{-1} h^{-1}). The model was fit using R [107–113] and the complete code is shown in Appendix F.

5.2.3 CD spectrometry

5.2.3.1 Thermal stress effect on rHSA structure

The effects of thermal stresses on rHSA conformation were studied using circular dichroism (CD) spectrometry. Solutions were made by dissolving rHSA in 10 mM phosphate (Sigma-Aldrich) buffer at pH 7, at concentrations of 20 g/L and 2 g/L, then filtered through a 0.2 µm filter. Solutions were split into 1 ml aliquots and each concentration was either: frozen at -80°C for one hour, then thawed at 37°C before incubating on ice; incubated at 56°C for half an hour, then incubated on ice; or incubated at 56°C for half an hour, frozen at -80°C for one hour, then thawed at 37°C before incubating on ice. A control sample that was incubated on ice for the duration of all incubation times was also included. CD scans in the far UV region were collected as described in Chapter 3.

5.3 Results

5.3.1 Effect of FBS on ACAM529 stability

To study the stabilizing effects of FBS, various concentrations of FBS were added to the reference buffer and the stability of ACAM529 at 27°C was monitored using the time course assay. The FBS used in these studies contained approximately 19 g/L BSA (see Appendix E, Figure E.1). There was 0.56 ± 0.10 log loss in virus titer with buffer containing 50% FBS, 0.29 ± 0.08 log loss with 10% FBS, 0.24 ± 0.08 log loss with 1% FBS, 0.30 ± 0.09 log loss with 0.1% FBS, 0.43 ± 0.09 log loss with 0.01% FBS, and 0.61 ± 0.06 log loss in the reference buffer control (Figure 5.1). The addition of any concentration of FBS to the buffer performed equal to or better than the control without FBS. The addition of 0.01%-10% (v/v) FBS to the buffer resulted in significant improvements to the viral stability compared to the control with no FBS. Minimal loss in titer occurred with the buffer containing 1% FBS and as the concentration of FBS was decreased or increased from this point, the stabilizing effects of FBS were less pronounced. The log loss in titer after 120h of the virus in buffer containing 50% FBS was not significantly different from the control. The stability profiles of the virus in buffer containing FBS also appeared more linear over the 120h period.

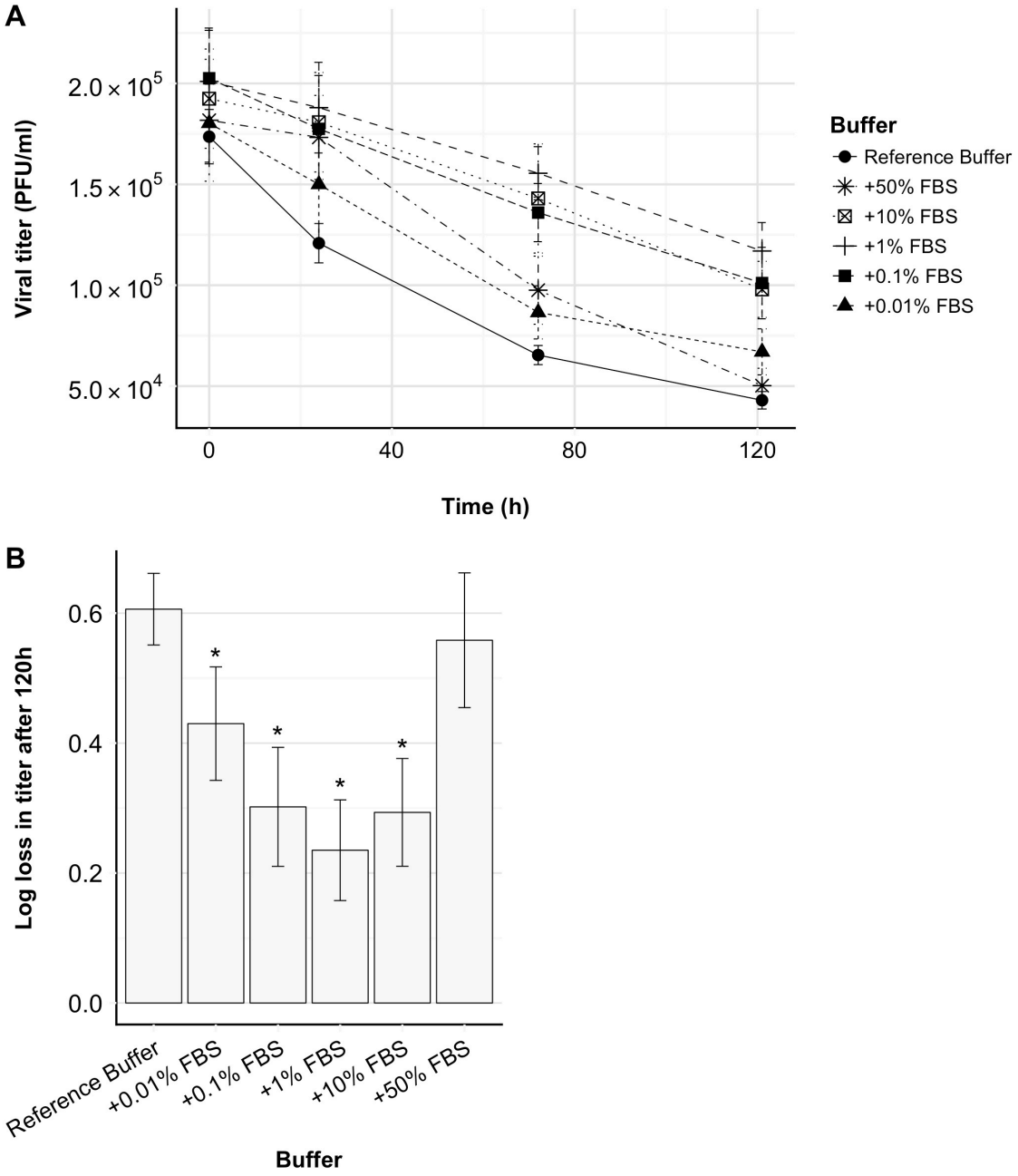

Figure 5.1 Effect of different concentrations of added FBS on ACAM529 stability.

ACAM529 Lot B was diluted into the reference buffer with or without 0.01%, 0.1%, 1%, 10% or 50% FBS, then incubated at 27°C. Viral stability over time was monitored using plaque assays and reported as PFU/ml (**A**). The total log loss in titer (**B**) was determined and buffers which yielded a significant deviation ($\alpha = 0.05$) from the control (reference buffer) are noted with *.

5.3.1.1 Modelling the stability profile of ACAM529 in buffer containing FBS

Several of the viral decay curves observed thus far at conditions above ambient temperatures have followed a first order exponential decay trend. However in this study, buffers containing 0.1%-10% FBS appeared to follow a linear trend over a period of 120 hours as shown in Figure 5.1A. To explore this further, the data was fit to the first order exponential decay model discussed in Chapter 4 (equation [7]), as well as a zero order decay model (equation [15]). As shown in Figure 5.2, the 95% confidence intervals for the zero order models of the 0.1%-10% FBS-containing buffers are much narrower than the control, and the R^2 values are also higher, showing a better fit. The buffers with FBS concentrations on the higher and lower end (50% and 0.01%, respectively) had 95% confidence intervals relatively wider than the other concentrations of FBS but still narrower than the control. With either model, it is clear that the buffer containing 1% FBS resulted in more stable virus as the k values were at a minimum.

A

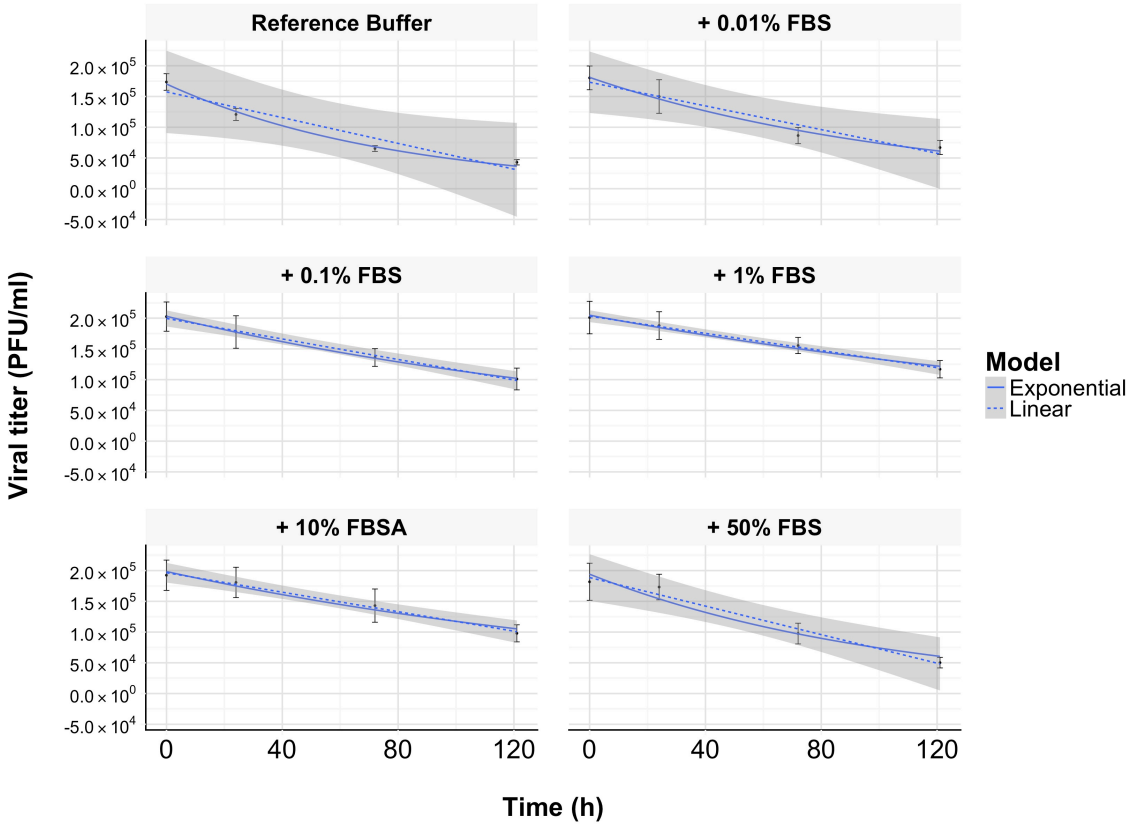

B

Buffer	First order decay model		Zero order decay model		
	V_0 (PFU ml^{-1})	k (h^{-1})	V_0 (PFU ml^{-1})	k (PFU ml^{-1} h^{-1})	Adjusted R^2
Reference Buffer	1.70 x 10^5	12.7 x 10^{-3}	1.58 x 10^5	1048.0	0.8804
+ 0.01% FBS	1.81 x 10^5	8.97 x 10^{-3}	1.73 x 10^5	963.1	0.919
+ 0.1% FBS	2.03 x 10^5	5.68 x 10^{-3}	2.00 x 10^5	834.04	0.9922
+ 1% FBS	2.05 x 10^5	4.30 x 10^{-3}	2.03 x 10^5	698.08	0.994
+ 10% FBS	1.98 x 10^5	5.25 x 10^{-3}	1.97 x 10^5	791.93	0.987
+ 50% FBS	1.94 x 10^5	9.64 x 10^{-3}	1.89 x 10^5	1160.7	0.9667

Figure 5.2 Fitting ACAM529 stability with different concentrations of FBS to decay curves.

Curves from Figure 5.1 were fit to first order exponential and zero order decay curves (**A**). The first order exponential decay model is: $V(t) = V_0 e^{(-kt)}$, where $V(t)$ is the viral titer (PFU/ml) at time t (h), V_0 is the initial viral titer at 0h, and k is the decay rate constant (h^{-1}). The zero order decay model is: $V(t) = V_0 - kt$, where k is the decay rate constant (PFU ml^{-1} h^{-1}). The shaded region in each of the plots indicates the 95% confidence interval for the zero order decay model. The table summarizes the parameter values and the adjusted R^2 value as calculated using R for the linear model fit (**B**).

5.3.2 Effect of adding rHSA to final purified ACAM529 on viral stability

Albumin is the most abundant protein in FBS and it was found in relatively high concentration in the more stable lot of ACAM529. To determine whether it can be used as a stabilizing excipient, rHSA was added to the ACAM529 reference buffer and a time course study was conducted. ACAM529 Lot B, which had minimal albumin (Figure 4.1), was diluted into reference buffer containing 1 g/L rHSA and the stability of the virus was monitored and compared to that of Lot C. At 25°C, the presence of 1 g/L rHSA lead to significantly higher log loss in titer after 120h for Lot B compared to the control with no rHSA, however their stability profiles appeared to be very similar after 24h (Figure 5.3). At 2-4°C, there was also a steeper initial decline in titer for Lot B with 1 g/L rHSA in the first 24h however subsequently there was a less steep decline in titer. The pattern of decay after 24h appeared linear and was more similar to that of Lot C than Lot B without rHSA present. In fact, over the 120h period studied here, there was a significant improvement in the log loss in titer of Lot B with the addition of 1 g/L rHSA at 2-4°C compared to the control but the log loss in titer was not as low as that of Lot C. The addition of 1 g/L rHSA appeared to offer stability to the virus at lower temperatures but was detrimental at higher temperatures.

When different concentrations of rHSA were added to the reference buffer, the stability of Lot B was again significantly improved at 2-4°C with concentrations of 0.05-5 g/L rHSA and significantly poorer at 27°C with the addition of 0.5 g/L and 5 g/L rHSA (Figure 5.4). The stability profiles at 2-4°C were very similar for all samples with rHSA and did not depend on the concentration of rHSA. The stability at 27°C, on the other hand, decreased with increasing concentrations of rHSA, where the steepest decline in viral titer occurred in the first 24h in the presence of 5 g/L rHSA. However, with the addition of 0.05 g/L rHSA, the stability of Lot B at 27°C was significantly improved when compared to the control with no rHSA. At lower temperatures, concentrations of rHSA ranging between 0.05 g/L – 5 g/L aided in viral stability, but at temperatures closer to ambient conditions,

small amounts of rHSA had a protective effect on the virus, whereas increased concentrations accelerated the deactivation of the virus.

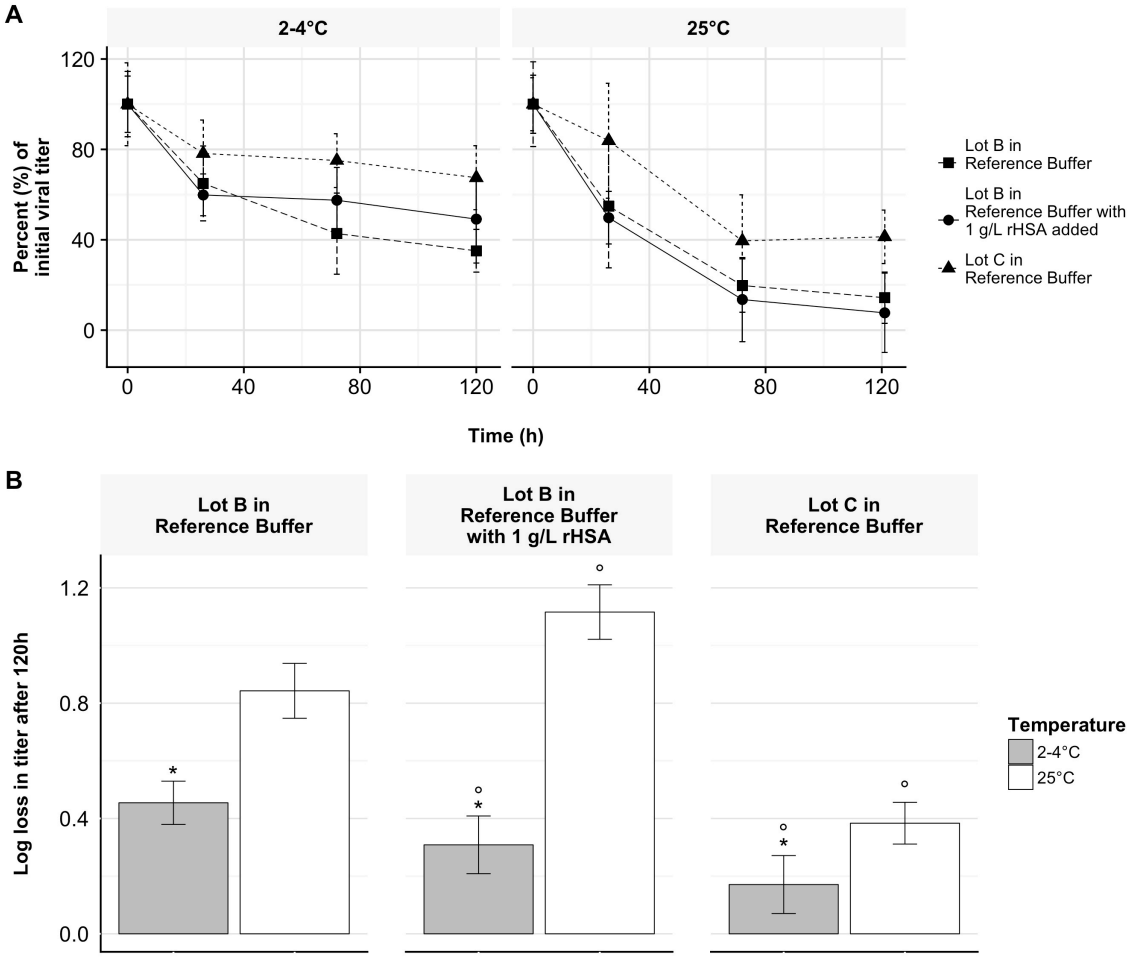

Figure 5.3 Effect of added rHSA on ACAM529 stability.

ACAM529 Lot B was diluted into the reference buffer with or without 1 g/L rHSA and Lot C was diluted into reference buffer, then both were incubated at 2-4°C or 25°C for 120h. Viral stability over time was monitored using plaque assays and reported as PFU/ml (**A**). The total log loss in titer (**B**) was determined and a significant deviation ($\alpha = 0.05$) from the log loss at 25°C is noted with *, and a significant deviation from Lot B at the same temperature is noted with o.

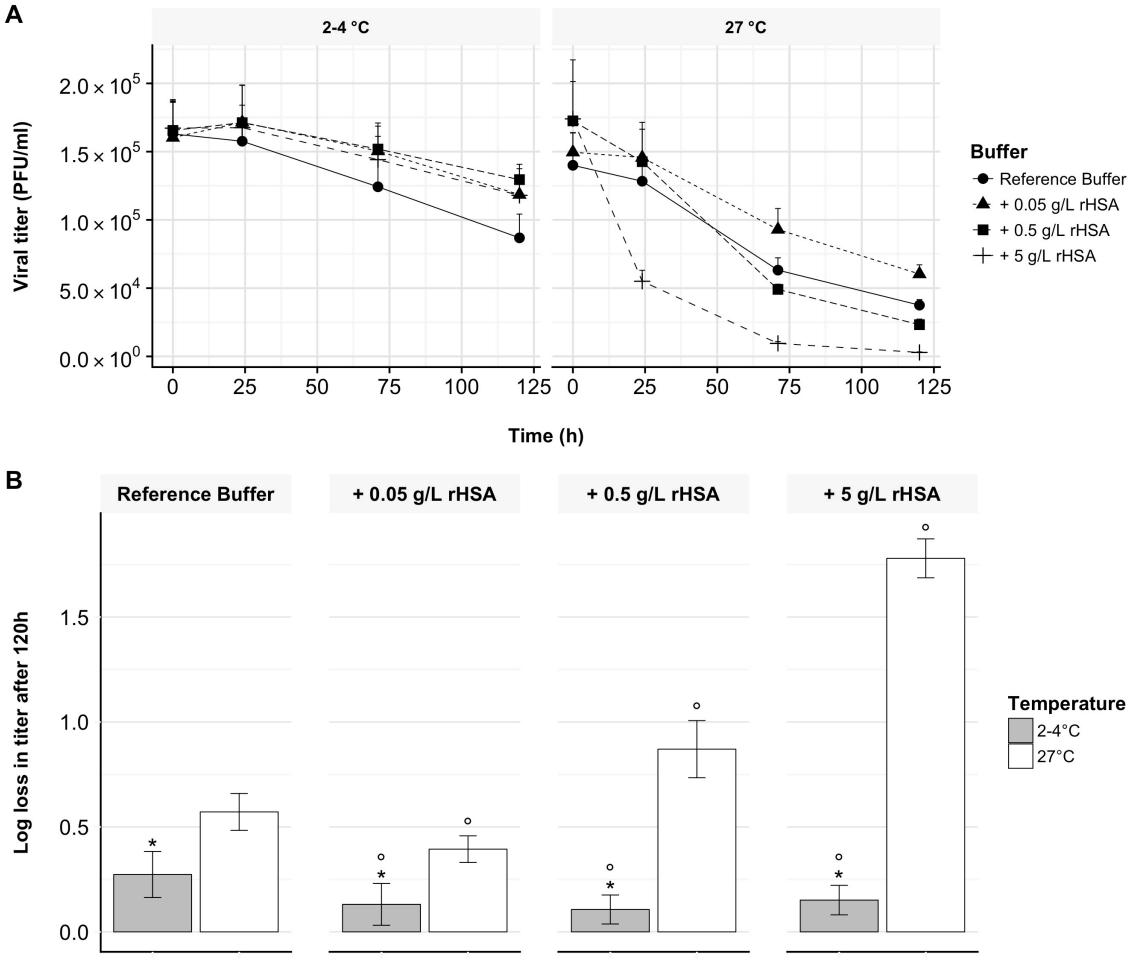

Figure 5.4 Effect of different concentrations of added rHSA on ACAM529 stability.

ACAM529 Lot B was diluted into the reference buffer with or without 0.05 g/L, 0.5 g/L, or 5 g/L rHSA and incubated at 2-4°C or 27°C for 120h. Viral stability over time was monitored using plaque assays and reported as PFU/ml (**A**). The total log loss in titer (**B**) was determined and a significant deviation ($\alpha = 0.05$) from the log loss at 27°C is noted with *, while a significant deviation from the control (reference buffer) at the same temperature is noted with o.

5.3.3 Effect of thermal stress on rHSA structure

The albumin found in FBS compared to albumin found in purified virus may not have the same structural characteristics and one cause is from experiencing different thermal stresses. For example, FBS is often heat-inactivated prior to use, while purified virus is frozen for storage, and then thawed when needed. To study whether thermal stresses due to heating or freezing and thawing cause secondary structure changes in rHSA, far UV CD spectrometry was used. The CD spectra for rHSA subjected to heat-inactivation (56°C for 0.5h) and/or a freeze-thaw cycle (-80°C for 1h then 37°C until thawed) were very similar to that of rHSA incubated on ice at both 2 g/L and 20 g/L rHSA (Figure 5.5). Two strong negative peaks corresponding to alpha helical structure at approximately 208 nm and 222 nm were evident in all conditions tested and there were no discernable differences in the intensities between samples, indicating similar rHSA secondary structure characteristics. Subjecting 2 g/L and 20 g/L rHSA to the different temperature incubation conditions did not cause any permanent changes to secondary structure as seen through CD analysis.

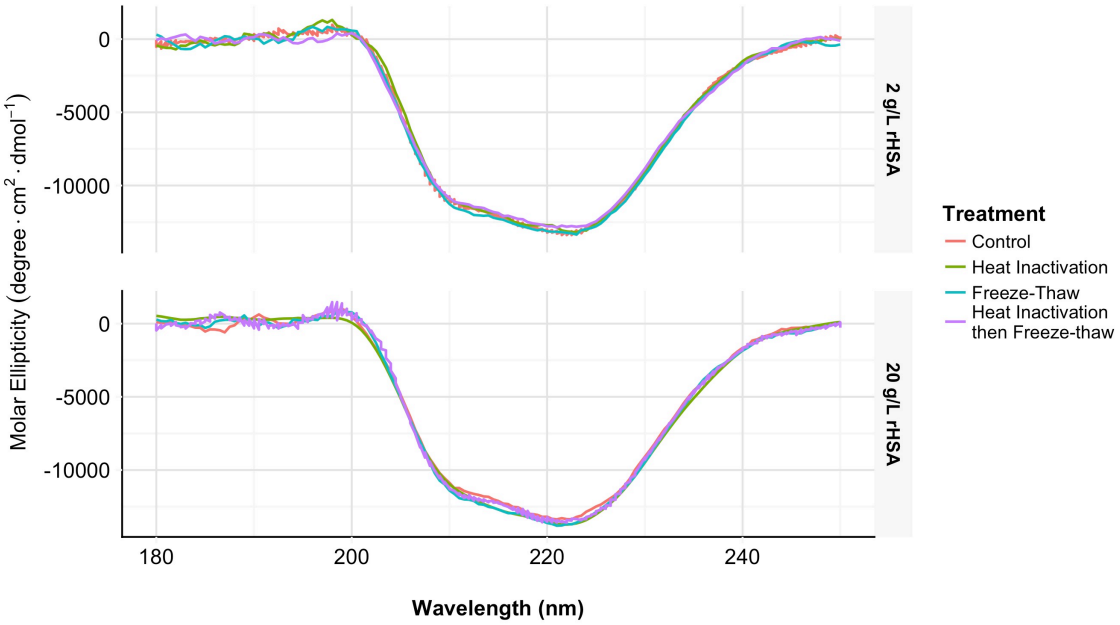

Figure 5.5 Far UV CD spectrometry to analyze the structural effects of thermal stresses on rHSA.

The effect of heat inactivation (56°C for 0.5h), a freeze-thaw cycle (-80°C for 1h, then 37°C until thawed), or a combination of both, on the secondary structure of rHSA was analyzed using CD spectrometry and compared to a control incubated on ice.

5.3.4 Effect of OptiPro SFM culture media on ACAM529 stability

OptiPro SFM is used to culture the complementary Vero cells for ACAM529 production [12] and it replaces components of FBS so that it is not needed in culture. To assess whether OptiPro SFM contains ACAM529 stabilizers, a time course study was conducted. With the addition of 10% (v/v) OptiPro SFM to the reference buffer, no significant changes to viral stability were observed at 27°C when compared to the control over a period of 120 hours (1.05 ± 0.09 log loss compared to 1.03 ± 0.10 log loss) (Figure 5.6). Conditioned OptiPro SFM was also assayed in the same experiment. With the addition of 10% (v/v) conditioned OptiPro SFM, a slight improvement to viral stability was observed after 120 hours, with a 0.70 ± 0.13 log loss in titer (Figure 5.6). The initial titer at 0 hours was slightly lower for the buffer with 10% conditioned OptiPro compared to the control (Figure 5.6B) and this would contribute to the lower overall log loss in titer seen in Figure 5.6C. However it should be noted that the final titer at 120 hours was higher than the control at a significance level of $\alpha = 0.1$.

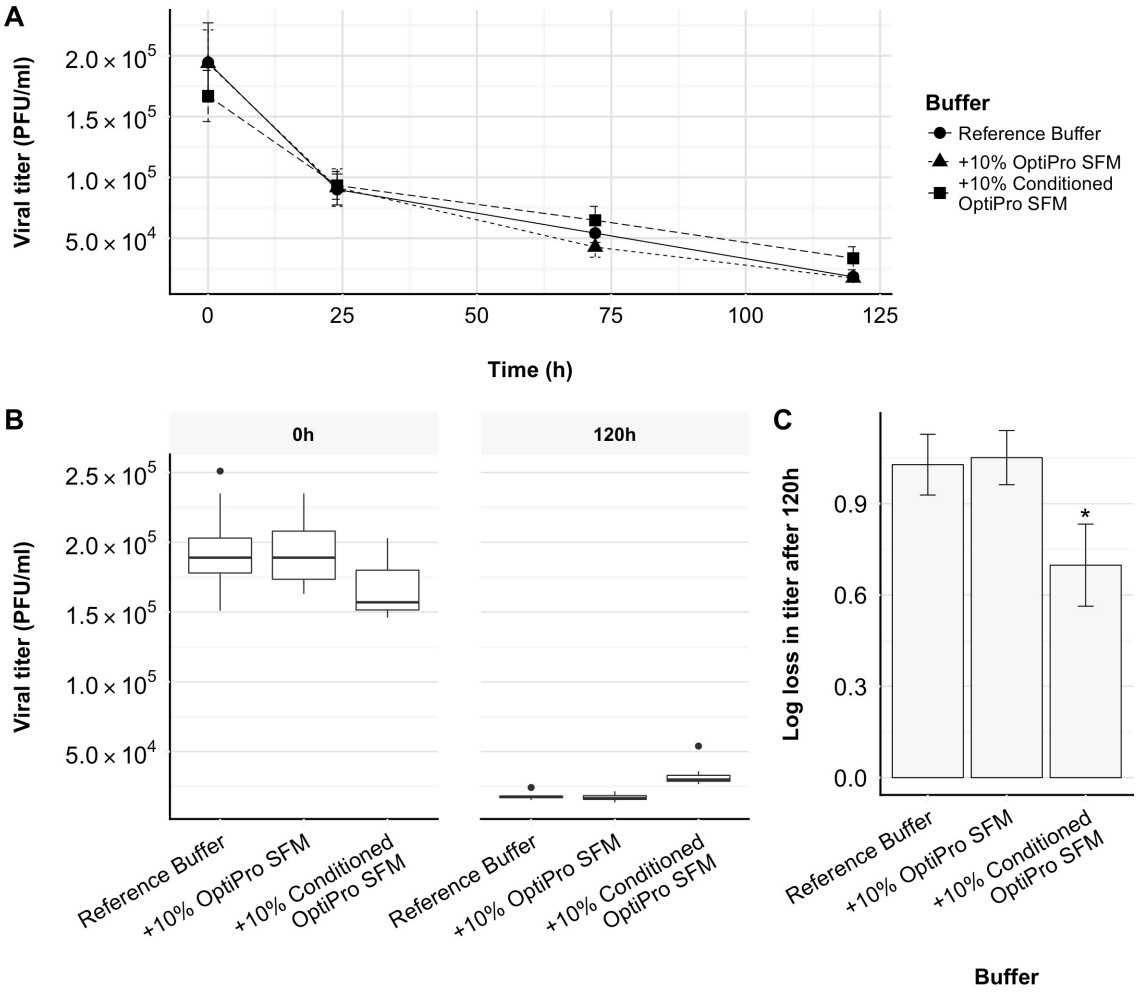

Figure 5.6 Effect of fresh and conditioned OptiPro SFM on ACAM529 stability.

ACAM529 Lot B was diluted into the reference buffer with or without 10% fresh OptiPro serum-free media (SFM) or 10% conditioned OptiPro SFM (filter sterilized media from a 4-day culture of Vero CCL81 cells), then incubated at 27°C. Viral stability over time was monitored using plaque assays and reported as PFU/ml (**A**). The initial and final titers are also displayed as a boxplot (**B**) to show that the titer of the virus in the buffer containing 10% conditioned OptiPro SFM at 120h was higher than the control at a significance level of $\alpha = 0.1$. The total log loss in titer (**C**) was determined and buffers which yielded a significant deviation ($\alpha = 0.05$) from the control (reference buffer) are noted with *.

5.3.5 Effect of CLC on ACAM529 stability

OptiPro SFM is supplemented with CLC for ACAM529 production [12]. CLC is an animal- and protein- free chemically defined lipid solution often used for culturing lipid-dependent cell lines [120,121]. To study whether CLC could protect the virus from degradation at 27°C, time course assays were conducted. When 1x CLC was added to the reference buffer, it had a deleterious effect on viral stability. There was a steep decline in virus titer in the first 24h and titers were too low to quantify after this period (Figure 5.7A). With lower concentrations of CLC (0.5x and 0.1x), there was still a significant decrease in the stability of the virus, with a large drop in titer again occurring in the first 24 hours (Figure 5.7B and C). The loss in titer after 120 hours for solutions containing CLC were both above 2 log, compared to the control with 0.66 ± 0.17 log loss in viral titer.

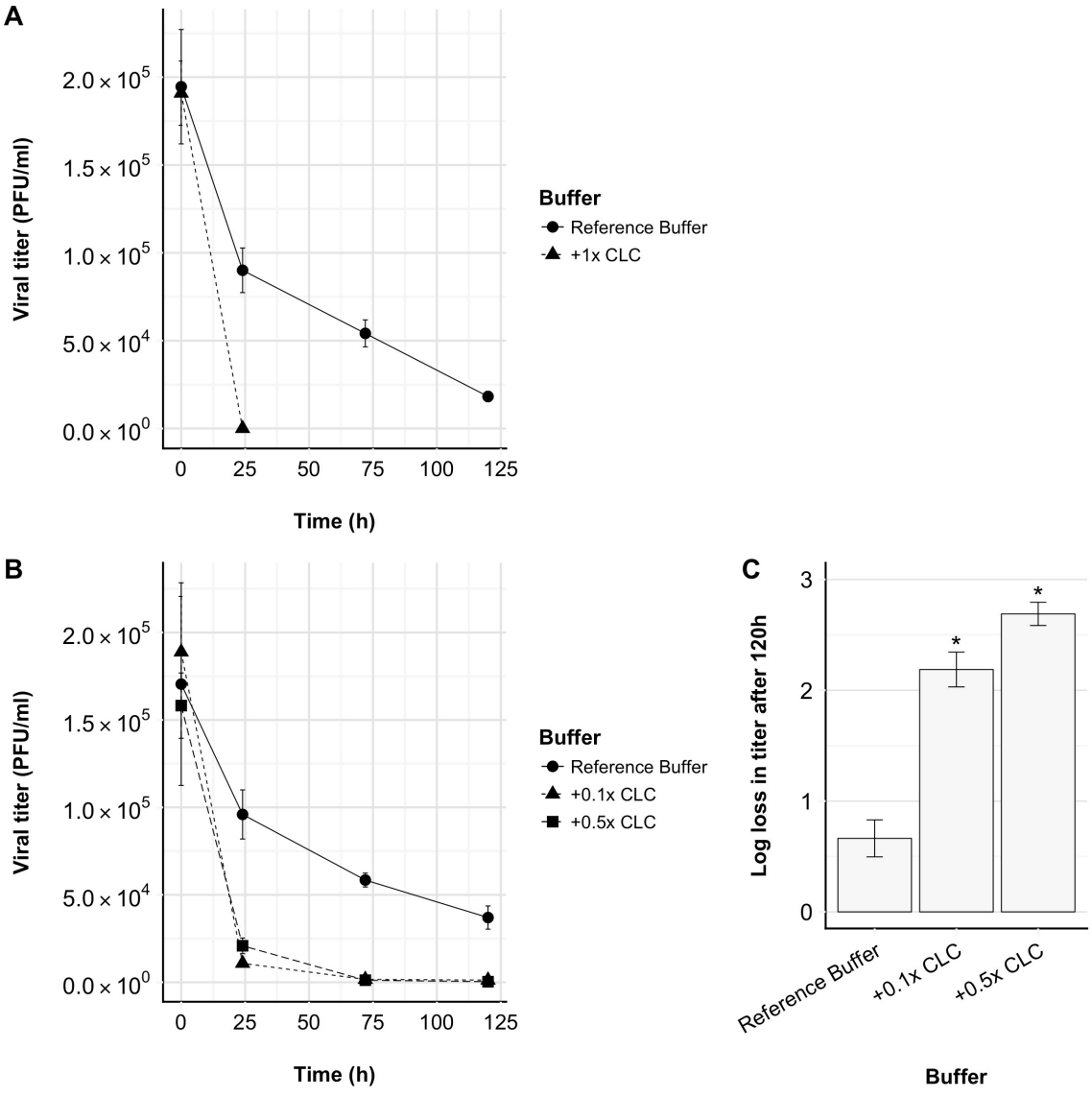

Figure 5.7 Effect of CLC on ACAM529 stability.

ACAM529 Lot B was diluted into the reference buffer with or without 1x CLC then incubated at 27°C. Viral stability over time was monitored using plaque assays and reported as PFU/ml (**A**). Titers for the CLC-containing buffer were unquantifiable beyond 24h. In a second experiment, ACAM529 Lot B was diluted into the reference buffer with or without 0.1x or 0.5x CLC then incubated at 27°C. Viral stability over time was monitored using plaque assays and reported as PFU/ml (**B**). The total log loss in titer (**C**) was determined and buffers which yielded a significant deviation ($\alpha = 0.05$) from the control (reference buffer) are noted with *.

5.3.6 Effect of PF68 on ACAM529 infectivity and stability

Pluronic F68 (PF68) is a non-ionic surfactant that is widely used as a shear protectant in cell culture at a concentration of 0.1%. To study whether PF68 has stabilizing properties for ACAM529, viral stability of Lot B in the reference buffer with the addition of 0.001%, 0.01%, 0.1%, or 1% (w/v) PF68 after 120h at 27°C was assayed and the results are presented in Figure 5.8. Initial viral titers at 0h were similar with or without PF68 at all concentrations indicating no significant effect to viral infection. After 120h, the titer of samples containing 0.01%-0.1% PF68 were higher than the control, with higher titers achieved with higher concentrations of PF68. The overall log loss in titer was significantly decreased compared to the control, where the buffer with 0.01% PF68 had 0.44 ± 0.06 log loss, 0.1% PF68 had 0.38 ± 0.09 log loss and the control with no PF68 had 0.63 ± 0.08 log loss. With 0.001% PF68, there was no significant difference in titers compared to the control. At a concentration of 1% PF68, well above the critical micelle concentration (CMC) of 0.4%, the total log loss in titer after 120h significantly increased to 1.47 ± 0.08. Maximal stability was achieved at a concentration of 0.1% PF68.

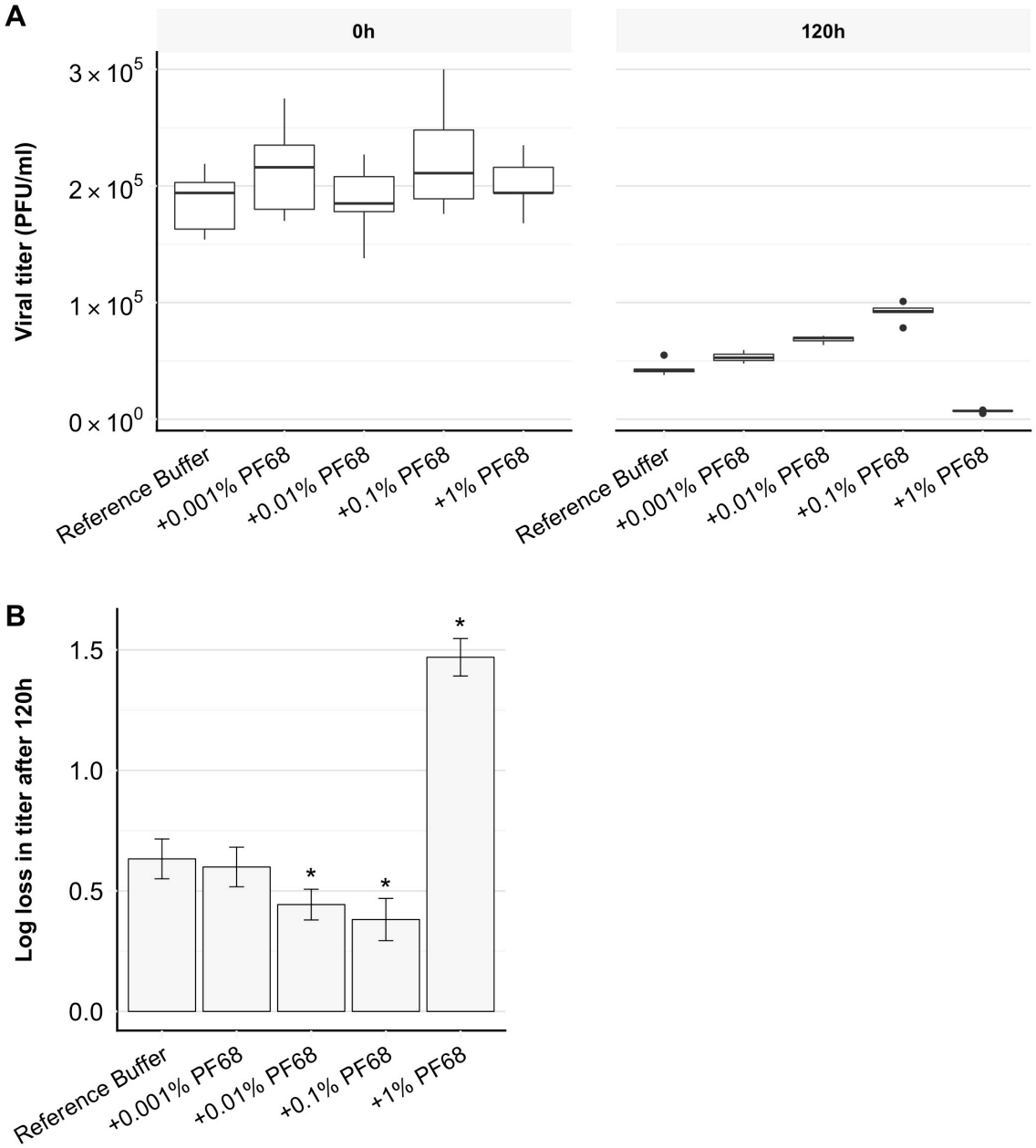

Figure 5.8 Effect of different concentrations of PF68 on ACAM529 stability.

ACAM529 Lot B was diluted into the reference buffer with or without 0.001%, 0.01%, 0.1%, or 1% Pluronic F68 (PF68) and incubated at 27°C for 120h. Viral titer at 0h and 120h was quantified using plaque assays and reported as PFU/ml (**A**). The total log loss in titer (**B**) was determined and a significant deviation ($\alpha = 0.05$) from the control buffer (reference buffer) is noted with *.

5.4 Chapter summary

In this chapter, various defined and complex solutions used in cell culture were assayed for their stabilizing effects on ACAM529. First, FBS and an albumin supplement, rHSA were studied. FBS significantly improved the stability of ACAM529 Lot B at 27°C at concentrations ranging between 0.01%-10%, with a maximum stability achieved using 1% FBS. With 50% FBS, there was no significant change to virus stability compared to the control. The addition of 0.05-5 g/L rHSA to purified ACAM529 Lot B improved virus stability at 2-4°C in a concentration-independent manner. However, at 27°C, 0.5-5 g/L rHSA significantly reduced the stability, where increasing concentrations of rHSA lead to decreasingly stable virus. Low concentrations of rHSA (0.05 g/L) improved stability at 27°C. At both temperatures, the stability of Lot C was significantly better than Lot C with or without 1 g/L rHSA. Thermal stresses to rHSA due to freeze-thaw and/or heat inactivation were assessed using CD spectrometry however no permanent secondary structure changes to rHSA were observed.

The effects of other components used in cell culture were also studied. The addition of 10% conditioned OptiPro SFM resulted in a slight improvement to stability over a period of 120 hours at 27°C, however the same amount of fresh medium resulted in no change to stability. The addition of 0.1x-1x CLC supplements to the buffer resulted in dramatic decreases to ACAM529 stability at 27°C, especially in the first 24h. Lastly, PF68 at concentrations below the CMC, significantly improved viral titers after 120h, with maximal stability achieved at a concentration of 0.1% PF68.

Chapter 6
Screening Excipients for ACAM529 Stability

6.1 Chapter objective

Stabilization formulations have been developed for a number of vaccines, leading to a library of commonly used excipients. Due to differences in structure, composition, and complexity between different vaccines, as well as an incomplete understanding of the mechanisms behind the stabilization properties of some excipients, formulations that work for one vaccine may not necessarily work for another. Even among enveloped virus, differences can arise in membrane composition and glycoprotein structure [100]. Therefore, intensive screening studies are often required for each specific vaccine. Sanofi Pasteur's stabilization buffer, used throughout this work as a reference buffer, was developed partially with screening studies (Patent US 20150150964 A1) [122]. In this chapter, various conditions and excipients that have been implicated in enhancing the stability of protein and lipid-based products, were investigated for ACAM529 stabilization. The effect of pH, trehalose, L-arginine, and Eagle's minimum essential medium (MEM) non-essential amino acid solution (NEAA) were tested in liquid formulation.

6.2 Materials and methods

6.2.1 Effect of buffer pH

To study the stability of ACAM529 at lower buffer pH, virus Lot A was quickly thawed at 37°C and diluted 1/100 into freshly prepared reference buffer adjusted to pH 5, pH 6, or pH 7 with HCl and incubated at room temperature. Samples were taken immediately after (0 hour), and 2, 10, 24, 48, 72, 96, and 120 hours after diluting the virus to monitor the viral titer using plaque assays in triplicate as described in Chapter 3.

6.2.2 Effect of trehalose and interaction effects between pH and the disaccharide

To study the interaction effect between pH and the sugar, virus Lot A was quickly thawed at 37°C and diluted 1/100 in triplicate into freshly prepared reference buffer at pH 6 or pH 7, or in the reference buffer with the 10% sucrose replaced with 10% trehalose (Sigma-Aldrich) at pH 6 or pH 7, then incubated at 27°C. Samples were taken immediately after (0 hour), and 24, 72, and 120 hours after diluting the virus to monitor the viral titer using plaque assays as described above.

To study the effects of increasing concentrations of trehalose, virus Lot C was quickly thawed at 37°C and diluted 1/100 into freshly prepared reference buffer at pH 6, or in the reference buffer with the 10% sucrose replaced with either 10%, 15% or 30% (w/v) trehalose at pH 6, then incubated at 27°C. Samples were taken immediately after (0 hour), and 2, 10, 24, 48, 72, 96, and 120 hours after diluting the virus to monitor the viral titer using plaque assays as described above.

6.2.3 Effect of adding L-arginine

To study the stability of ACAM529 in the presence of L-arginine, virus Lot B was quickly thawed at 37°C and diluted 1/100 in triplicate into freshly prepared reference buffer at pH 7, or in the reference buffer with the addition of 0.01 M or 0.1 M L-arginine (Sigma-Aldrich) at pH 7, then incubated at 27°C. It should be noted that in the process of adjusting to pH 7 for the reference buffer containing 0.01 M and 0.1 M L-arginine, significant amounts of hydrochloric acid (HCl) were required. The concentration of chloride ions was increased by 40 mM and 220 mM, respectively. Samples were taken immediately after (0 hour), and 24, 72, and 120 hours after diluting the virus to monitor the viral titer using plaque assays as described above.

6.2.4 Effect of adding NEAA

To study the stability of ACAM529 in the presence of NEAA, virus Lot B was quickly thawed at 37°C and diluted 1/100 in triplicate into freshly prepared reference buffer at pH 7, or in the reference

buffer with the addition of 0.1x, 0.5x, or 1x NEAA (Sigma-Aldrich) at pH 7, then incubated at 27°C. Samples were taken immediately after (0 hour), and 24, 72, and 120 hours after diluting the virus to monitor the viral titer using plaque assays as described above.

6.3 Results

6.3.1 Effect of changes in buffer pH on ACAM529 stability

To determine the effect that low pH environments have on ACAM529, the pH of the reference buffer was adjusted to either pH 7, pH 6 or pH 5 and the infectivity and stability of Lot A diluted in this buffer was studied. ACAM529 infectivity was assessed by the viral titers at 0h (Figure 6.1A) and it was evident that the low pH buffer significantly improved initial infectivity. The titer of the virus in the reference buffer at pH 5 was $3.9 \pm 0.5 \times 10^4$ PFU/ml whereas the same buffer at pH 7 yielded a titer of $2.9 \pm 0.4 \times 10^4$ PFU/ml. When lowered to pH 6, the viral titer ($3.5 \pm 0.9 \times 10^4$ PFU/ml) was not significantly different from that at pH 7, though there was an increased variability in the data.

To determine whether the reference buffer at pH 5 would be suitable for long-term stability, a 120h time course stability study at room temperature was conducted. Though the pH 5 buffer had an increased titer at the 0h time point, it was clear that the stability of the virus deteriorated much more quickly within the first 24h when compared to the pH 6 and pH 7 buffers (Figure 6.1B). The titer at 120h was $7.9 \pm 1.2 \times 10^3$ PFU/ml for the pH 5 buffer, which was significantly lower than that of the pH 7 and 6 buffers which were $1.2 \pm 0.2 \times 10^4$ PFU/ml and $1.4 \pm 0.2 \times 10^4$ PFU/ml, respectively. The instability of the virus in the acidic buffer is clear from the overall log loss in titer (Figure 6.1C). The viral stability and overall loss in titer were not significantly different in the pH 7 and pH 6 buffers, suggesting that ACAM529 is tolerant of conditions in this pH range, but more acidic conditions result in accelerated deactivation.

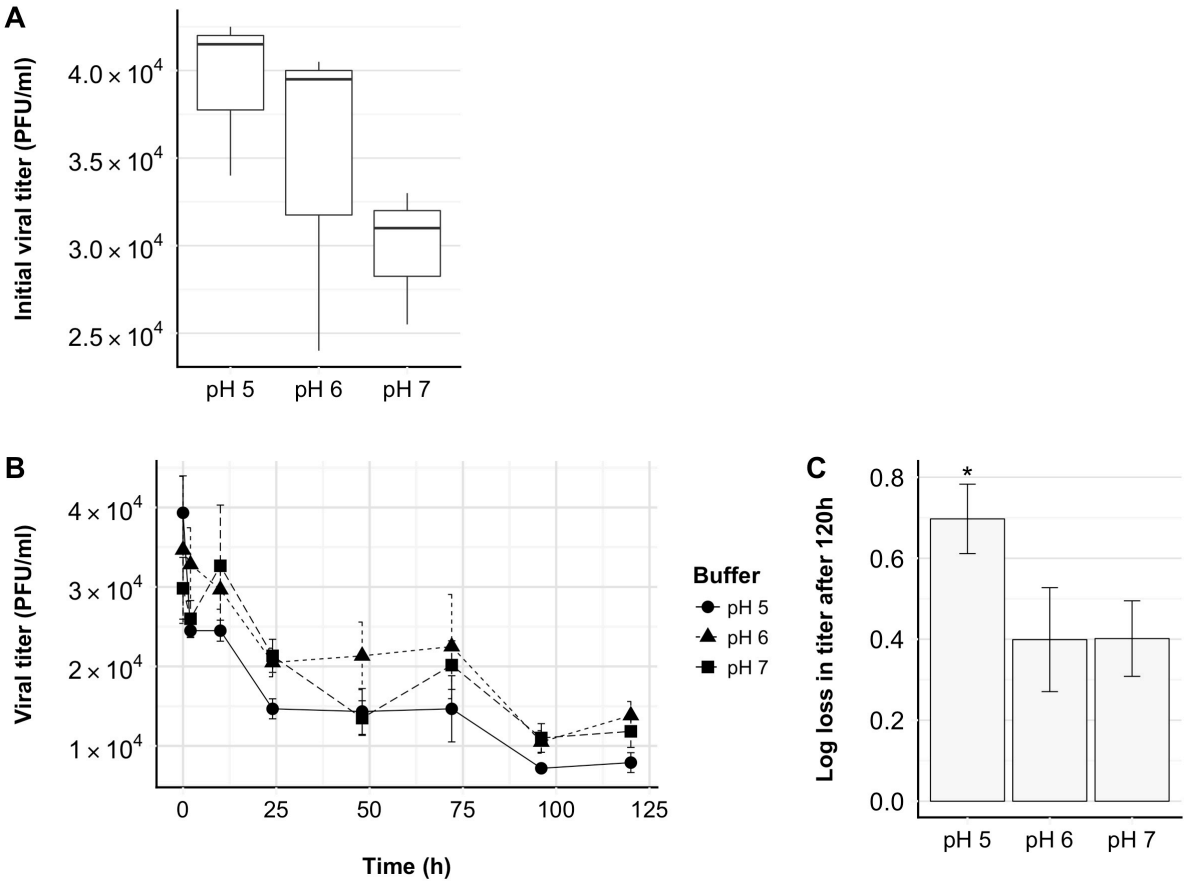

Figure 6.1 Effect of buffer pH on ACAM529 infectivity and stability.

ACAM529 Lot A was diluted into the reference buffer adjusted to pH 5, pH 6, or pH 7 and viral titer in PFU/ml was determined using plaque assays (**A**). The titer at pH 5 was slightly higher than at pH 7 ($\alpha = 0.1$). Viral stability at room temperature was monitored using plaque assays and reported as PFU/ml (**B**). The total log loss in titer was determined (**C**). Buffers that yielded a significant deviation ($\alpha = 0.05$) from the control at pH 7 in terms of log loss in titer after 120h are noted with *.

6.3.2 Effect of trehalose on ACAM529 stability

Trehalose is an increasingly popular disaccharide used in vaccine formulation and it has been shown to demonstrate superior properties over sucrose in some cases [55,66,67,69,70,72,76,77]. To study the effects of trehalose on ACAM529 stability, the disaccharide used in the reference buffer, 10% (w/v) sucrose, was replaced with 10% (w/v) trehalose. In addition, the effect of reducing the pH to 6 from pH 7 was also analyzed to look for any interaction effects between trehalose and buffer pH. The stability profiles of ACAM529 in buffer containing 10% sucrose were very similar to those containing 10% trehalose at 27°C (Figure 6.2A) and there was no significant difference in the overall loss of viral titer after 120 hours (Figure 6.2B). Trehalose offered the same level of stability to ACAM529 as sucrose between pH 6-7. The effect of increasing the concentration of trehalose at pH 6 also did not have a significant effect on the stability at 27°C (Figure 6.3A) or overall loss in titer after 120h (Figure 6.3B) when compared to the control. There was a 0.26 ± 0.12 log loss in titer for the buffer containing 10% trehalose, 0.31 ± 0.10 log loss for 15% trehalose, 0.34 ± 0.12 log loss for 30% trehalose, and 0.31 ± 0.09 log loss for the control buffer with 10% sucrose.

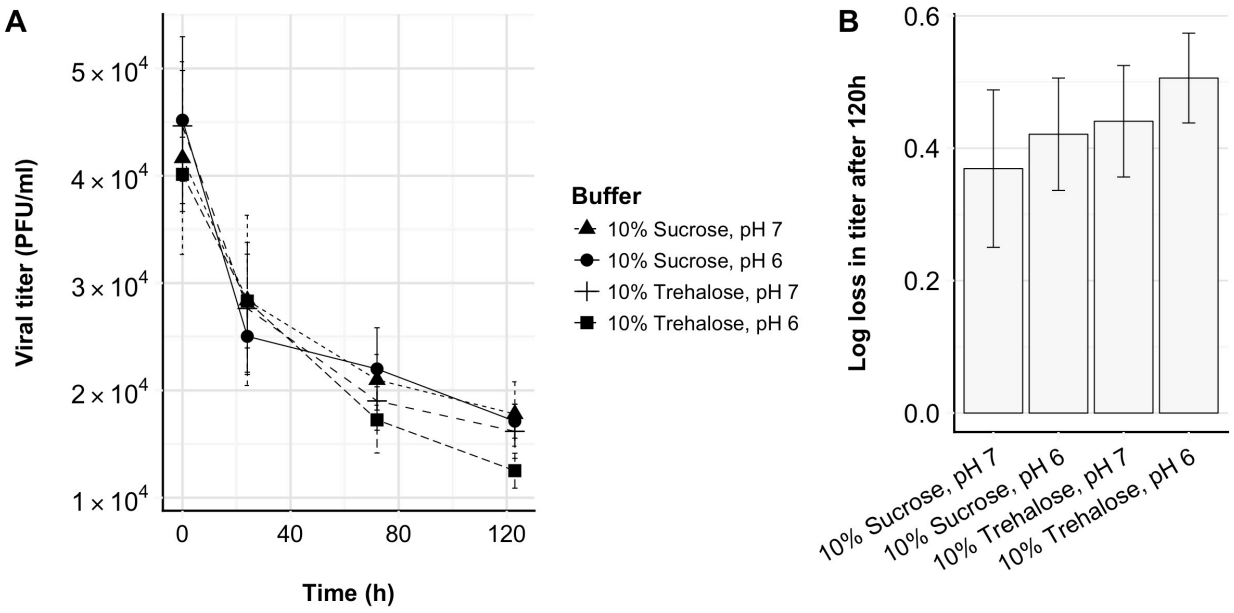

Figure 6.2 Effect of trehalose and pH on ACAM529 stability.

ACAM529 Lot A was diluted into the reference buffer at pH 7 or pH 6, or in the reference buffer with the 10% sucrose replaced with 10% trehalose at pH 7 or pH 6, then incubated at 27°C. Viral stability over time was monitored using plaque assays and reported as PFU/ml (**A**). The total log loss in titer (**B**) was determined and buffers which yielded a significant deviation ($\alpha = 0.05$) from the control buffer (reference buffer at pH 7) are noted with *.

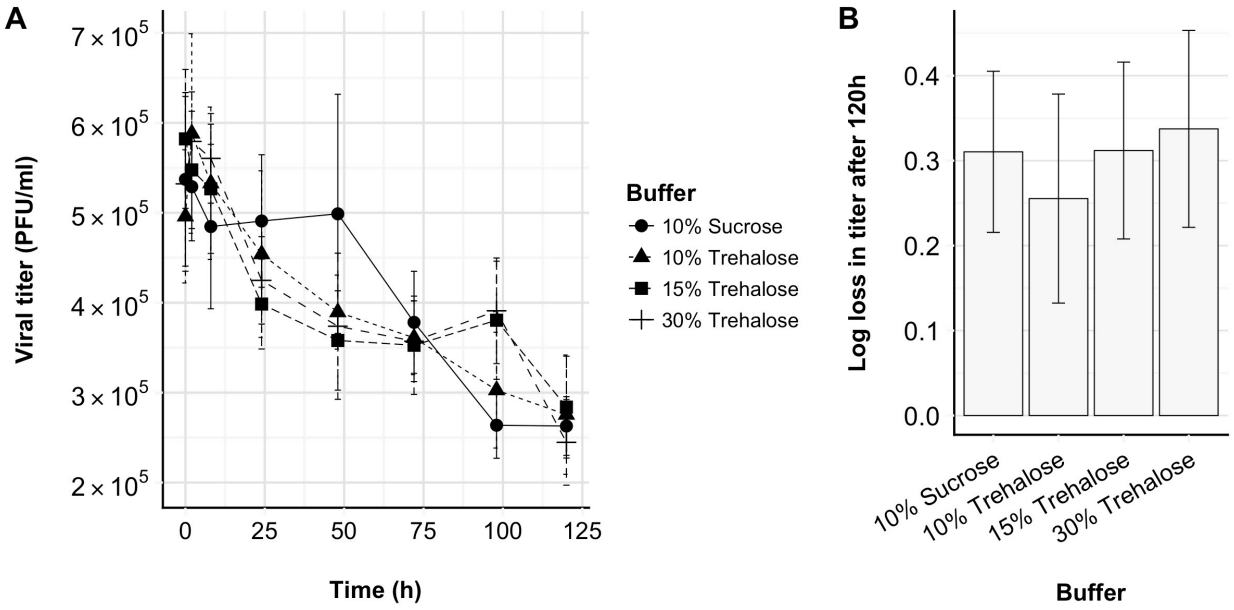

Figure 6.3 Effect of increasing concentrations of trehalose on ACAM529 stability.

ACAM529 Lot C was diluted into the reference buffer at pH 6, or in the reference buffer with the 10% sucrose replaced with either 10%, 15% or 30% trehalose at pH 6, then incubated at 27°C. Viral stability over time was monitored using plaque assays and reported as PFU/ml (**A**). The total log loss in titer (**B**) was determined and buffers which yielded a significant deviation ($\alpha = 0.05$) from the control buffer (reference buffer at pH 6) are noted with *.

6.3.3 Effect of L-arginine and NEAA on ACAM529 stability

Amino acids have been implicated in biological product stabilization due to their buffering capabilities [58], antioxidant properties [85,86], and generally favourable interactions with biochemical compounds [76,81,123]. L-arginine has been used extensively as an excipient to stabilize proteins [80,82] and to discourage protein aggregation [83,124]. To study the stabilizing effect of L-arginine on ACAM529, a time course assay was conducted. The effect of 0.01 M and 0.1 M L-arginine on virus stability at 27°C was not significantly different from the reference buffer control (Figure 6.4). There was no significant difference between the overall log loss in titer between the buffer with 0.1 M L-arginine, 0.01 M L-arginine, and the control (0.80 ± 0.12 log loss, 0.61 ± 0.09 log loss, and 0.66 ± 0.17 log loss, respectively). During buffer preparations, the addition of L-arginine resulted in a more alkaline solution when compared to the control and this necessitated the addition of a significant amount of HCl to adjust the buffer to pH 7. The final 0.1 M L-arginine-containing buffer had ~0.38 M Cl^- ions, more than double the original buffer (~0.16 M), while the 0.01 M arginine-containing buffer had ~0.20 M Cl^- ions. This doubling of the Cl^- ions, and ultimately altering the ionic strength of the buffer, did not negatively affect ACAM529.

Eagle's minimum essential medium (MEM) non-essential amino acid solution (NEAA) is a chemically defined amino acid cell culture supplement shown to have membrane stabilization properties [123]. The effect of NEAA on ACAM529 stability at 27°C was also investigated. It was found that there was no significant change to the stability profiles (Figure 6.5A) or overall loss in titer after 120h (Figure 6.5B) with the 1x, 0.5x or 0.1x concentrations of NEAA when compared to the reference buffer control (0.64 ± 0.10 log loss, 0.69 ± 0.14 log loss, and 0.70 ± 0.10 log loss, respectively, compared to 0.66 ± 0.17 log loss).

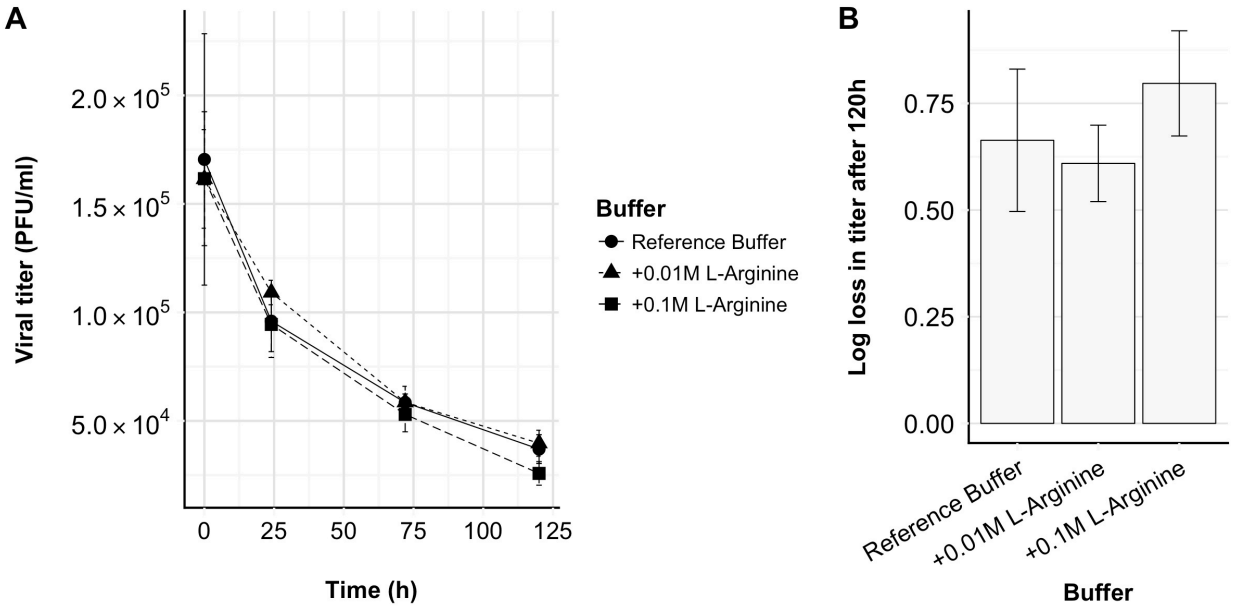

Figure 6.4 Effect of different concentrations of L-arginine on ACAM529 stability.

ACAM529 Lot B was diluted into reference buffer with or without 0.01 M or 0.1 M L-arginine, then incubated at 27°C. Viral stability over time was monitored using plaque assays and reported as PFU/ml (**A**). The total log loss in titer (**B**) was determined and buffers which yielded a significant deviation ($\alpha = 0.05$) from the control buffer (reference buffer) are noted with *.

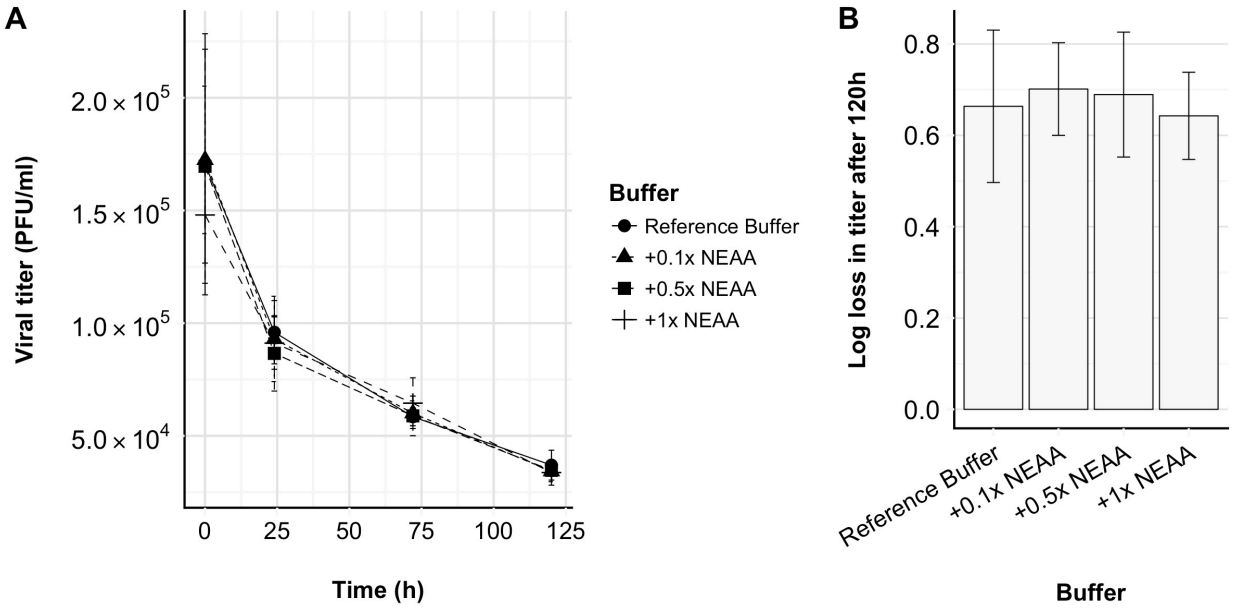

Figure 6.5 Effect of different concentrations of NEAA on ACAM529 stability.

ACAM529 Lot B was diluted into the reference buffer with or without 0.1x, 0.5x, or 1x Eagle's minimum essential medium non-essential amino acid solution (NEAA), then incubated at 27°C. Viral stability over time was monitored using plaque assays and reported as PFU/ml (**A**). The total log loss in titer (**B**) was determined and buffers which yielded a significant deviation ($\alpha = 0.05$) from the control buffer (reference buffer) are noted with *.

6.4 Chapter summary

In this chapter, pH, trehalose, L-arginine, and NEAA were investigated for ACAM529 stabilization. Although an acidic buffer (pH 5) caused an improved initial infectivity of the virus when titered with the plaque assay, it had a negative impact on long-term stability compared to buffers in the range of pH 6-7. The replacement of 10% (w/v) sucrose with 10-30% (w/v) trehalose in the reference buffer did not result in changes to viral stability at pH 6-7 at 27°C. The addition of 0.01-0.1 M L-arginine (along with the resulting increase in buffer ionic strength with the addition of Cl^- ions) and 0.1x-1x NEAA also did not significantly affect the stability of ACAM529.

Chapter 7
Discussion

Stability of the candidate vaccine ACAM529, especially during purification processes, is a major production issue. This work aimed to study the vaccine candidate and identify excipients to improve the effectiveness of the stabilization buffer.

7.1 ACAM529 production and purification processes have resulted in virus with variable titer, albumin content, and stability

The titer of Lot B (2.1 ± 0.4 x 10^7 PFU/ml) was an order of magnitude higher than that of Lot A (3.4 ± 0.6 x 10^6 PFU/ml), and it also had an order of magnitude less albumin (<0.13 g/L and 0.5-1 g/L, respectively). When the stability of the two lots were examined, they had similar stability profiles and losses in titer during a 120h period at 2-4°C and 25°C. Lot C had further improved titers (5.2 ± 0.6 x 10^7 PFU/ml) compared to Lot B and was significantly more stable at 2-4°C, 27°C, and 37°C, with the difference being more apparent with decreasing temperatures; however, higher levels of albumin (approximately 8 g/L) were present.

7.2 ACAM529 stability modelling

Modelling the stability profiles of the virus is beneficial as it allows for quantitative comparisons of the stabilities of the virus lots and provides information about the mechanisms behind the deactivation. However, modelling all aspects of viral decay is challenging, as there are numerous potential mechanisms involved in virus degradation, with each mechanism having its own rate constants. Viral decay, typically follows a characteristic exponential decay [59,115] so the stability profiles were first modeled with a first order decay model. The model estimated initial virus titers, V_0, similar to the experimental values and it also revealed that the reaction rate constant, k, increased with

temperature and was generally higher for Lot B than Lot C. This was consistent with the earlier findings that increased temperature lead to decreased stability and Lot B was less stable than Lot C.

The Arrhenius model describes the dependence of the reaction rate constant on temperature and it can be used to estimate E_a and A. The energy of deactivation, E_a, refers to the energy required for the chemical reaction to proceed forward. In this case, a lower value for E_a would suggest the virus was less stable since less energy is required for deactivation. Though Lot C was found to be more stable than Lot B, the E_a value was slightly higher for Lot B (18.42 kJ mol^{-1} for Lot B and 17.78 kJ mol^{-1} for Lot C). The larger difference was found with the pre-exponential factor, A. The value for A was twice as high in Lot B compared to Lot C (60.91 h^{-1} and 31.07 h^{-1}, respectively).

It should be noted that the estimation of E_a and A for Lot B and Lot C relied on the data obtained from the stability profiles at 2-4°C, which was observed to not fit the model as well as at 27°C and 37°C. It would be beneficial to obtain more accurate estimates of these parameters by repeating the time course assays at more temperature conditions, especially above 20°C since the stability of the virus at ambient conditions is of interest.

Analyzing the E_a and A values for ACAM529 may shed light on the mode of action of different excipients. It would be of interest to repeat the time course studies at multiple temperature conditions with FBS and PF68, both of which improved the stability at 27°C, and determine the changes to E_a and A.

The first order decay model was insufficient to model the ACAM529 stability profiles at 2-4°C as the virus experienced a steep initial decline in titer, followed by a less steep decline thereafter. This biphasic inactivation was also observed by Higashikawa and Chang with two retrovirus vectors [125]. The double decay model proposed here was able to describe the stability profiles at the lower temperature better than the first order decay model. The model proposes the presence of two

subpopulations of virus, each undergoing first order decay at different decay rates. Both Lot B and Lot C were found to have similar proportions of virus subpopulations undergoing the two different rates of decay, where Lot C had the lower decay rate constants in each subpopulation. The smaller subpopulation (29%) in Lot C was found to have a rate constant of 0 h^{-1}, which indicated a stable subpopulation of virus. The cause for the emergence of two subpopulations is unclear. It could be a result of production protocols, a remnant of undergoing freeze-thaw cycles, or how the virus interacts with the contents of the liquid solution. Achieving the conditions that render the 29% subpopulation of Lot C to experience a low rate of deactivation would be ideal for ACAM529 stability.

It is possible that the improved fit of the double decay model could be due to a phenomena that there are indeed two species of virus (or more, which can be modelled by adding more parameters), however it is also possible that the increased number of parameters allowed for the better fit. More data is necessary to validate this model.

It is important to note that the viral stability profiles modelled here are from a time course assay of virus that has been thawed from frozen. A time course assay where a sample was subjected to a freeze-thaw cycle at 24h saw a similar steep decline in viral titer upon thawing (see Appendix A). These profiles may differ from those of fresh virus since samples that have undergone freeze-thaw cycles were subjected to more stresses that could cause accelerated viral inactivation, such as damage from ice crystal formation [55]. Nevertheless, it is evident from the parameter estimates for the decay rate constants that some degradation pathways have been minimized in Lot C. It is possible that the components of Lot C are protecting the virus from specific pathways and this is seen in the reduction of the rate constant values.

When the virus was in buffer with 0.1%-10% FBS, as the stability improved, the decay rate with respect to time appeared more linear instead of following first order or double decay trends. The rate

of decay in a zero order decay model does not depend on the concentration of the virus. The addition of FBS to the reference buffer caused the stability kinetics to deviate from a first-order reaction to a zero-order reaction. The modelling would benefit from more time points to resolve the shape of the curve further, especially in the first 24h, since this is typically where the decay is less linear.

7.3 TEM imaging revealed a high prevalence of unenveloped virus and clumping of ACAM529

TEM images of ACAM529 Lot A and Lot C were taken to identify differences between the lots and to visualize the structure of the virus. There was a high prevalence of naked capsids in both lots imaged. This could indicate uncoating of virus to be a cause for instability since naked capsids are not typically infectious [18]. However, it is unclear whether the prevalence of naked capsids is due to the method of sample preparation or a true representation of the virus in liquid solution. The process of fixing the sample to the grid and staining may damage the viral envelope and it may also cause capsids to rupture, as broken capsids were also observed. Hansen and colleagues [17] quantified the ratio of enveloped HSV-2 and naked capsids on TEM grids and related it to virus titer. This quantification would be informative for ACAM529. It could reveal the cause for lower virus titers over time, whether it was uncoating due to damage to the viral envelope, particle aggregation, or some other mechanism. However, with the difficulties faced with imaging here, such as a poor ability to definitively identify enveloped virus, it would have been immensely challenging to produce such data.

The inner structures of the virus were not as apparent as some reported in the literature [17,126,127]. The capsid and DNA core in most enveloped virus identified were not highly visible. Optimizing the time for fixing or using an alternative fixative that can better preserve ultrastructure, such as glutaraldehyde [128], are areas that can be further explored to improve imaging.

TEM imaging also revealed the presence of clusters of both enveloped virus and naked capsids and this would affect the viral titer quantification. The plaque assay quantifies plaque-forming units (PFU) so an aggregation of viral particles would translate into only one PFU. Aggregates are indistinguishable from free-floating virus using this assay. Identifying the presence of aggregation would therefore be invaluable because excipients targeted for reducing aggregation could be used to improve virus titers. As an alternative to TEM imaging, clustering of enveloped virus and naked capsids could be confirmed using flow cytometry techniques. Flow cytometry has previously been used to study aggregation of baculovirus by tracking the change in particle size [129] and this technique may be transferrable to ACAM529.

7.4 Culture media components as a promising source of stabilizing excipients

In an effort to identify stabilizers for ACAM529, various culture media components were screened using the time course assay.

7.4.1 FBS is an effective stabilizer for ACAM529

ACAM529 Lot C was observed to have improved stability compared to the other lots and the question arose as to whether the significantly higher level of albumin seen in Lot C was contributing to the improved stability. The source of the albumin was unclear as it could be from FBS used commonly to supplement cell culture growth upstream, or a purified albumin could have been added, such as BSA, HSA, or rHSA. Though it is a complex mixture, the stabilization properties of FBS made it an excellent source to screen for stabilizing excipients and historically, serums and culture media have been used to stabilize viral preparations [116,117]. Stability studies with 0.01%-10% FBS added to the reference buffer of ACAM529 Lot B saw significant improvements to the stability at 27°C, with maximal stability achieved at 1% FBS. Replicate experiments with 1% or 10% FBS consistently showed significant protective effects for ACAM529 (Appendix G). This showed there

was substantial promise to further improve the stability of ACAM529 but the cause could be due to numerous factors. The addition of FBS to solutions not only introduced various compounds, such as proteins, vitamins, hormones, lipids, amino acids, and salts, but it also potentially altered other properties of the solution, such as the viscosity, osmolarity, and ionic strength. All or some of these properties may be contributing to the improved stability of ACAM529.

7.4.2 Conditioned OptiPro SFM is a better stabilizer of ACAM529 compared to fresh media

FBS has been used extensively for supporting cell growth, protecting cells from mechanical damage associated with culture mixing [118,119], cryopreservation, and even as a stabilizer for enveloped virus in liquid solution [100]. However, there is an interest to replace serum use with defined mixtures due to high batch-to-batch variation, which can cause inconsistencies in fermentation processes [119], and due to the risk of transferring harmful pathogens since it is of animal origin. Serum-free media (SFM), with chemically defined recipes intended for culturing specific cell lines, have been developed for this purpose. OptiPro SFM is an animal origin-free chemically defined commercial medium optimized for culturing kidney derived cell lines as well as other attachment dependent cell lines, and it is used to culture the complementary Vero cells for ACAM529 production [12]. In this work, it was observed that adding 10% fresh OptiPro SFM to the reference buffer did not significantly affect the stability of Lot B at 27°C, however the same amount of conditioned OptiPro SFM slightly improved the stability. Conditioned OptiPro SFM is a more complex solution containing cellular proteins and metabolites that may protect ACAM529 from degradation pathways. OptiPro SFM has an ultra low (< 10 μg/ml) protein content whereas it is unclear what the protein content of the conditioned media is. Since proteins have been used as stabilizers, it would be of interest to investigate the protein content of conditioned OptiPro SFM to see whether this could be contributing to ACAM529 stability.

7.4.3 The stabilizing effects of rHSA are dependent on temperature and concentration

Albumin is the most abundant protein in FBS and it is a widely used stabilizer [97,98]. This is mainly attributed to its amphiphilic properties as it has the capacity to bind to hydrophobic surfaces, which prevents aggregation and inactivation [57]. Albumin is also able to bind to cellular membranes [130], providing protection against hydrodynamic forces experienced during cell culture [131]. The FBS used in the present study contained 19 g/L albumin so the range of FBS concentrations tested that resulted in significantly improved ACAM529 stability corresponds to 1.9 g/L - 1.9 mg/L albumin. With the addition of 50% FBS to the buffer, which corresponds to 9.5 g/L, the virus stability remained unchanged. The addition of 0.5-5 g/L rHSA to the reference buffer, however, significantly reduced the stability of Lot B at 27°C in a concentration-dependent manner. Significant improvements at 27°C were only observed with 0.05 g/L rHSA. This was not expected since these levels are below what is present in Lot C. Furthermore, a study done by Carmo and colleagues [100] saw improved stability of enveloped viral vectors with the addition of 0.6 g/L-1 g/L rHSA in liquid solution.

One difference between the albumin (rHSA) added to the buffer and the albumin found in Lot C and FBS is that the latter two undergo thermal stresses that could cause conformational changes in the protein. The albumin in Lot C is likely to experience thermal stress from freeze-thaw cycles as the virus samples used in these studies are thawed at 37°C from being frozen at -80°C. Similarly, FBS undergoes freeze-thaw cycles when taken from storage conditions at -80°C and in addition, it is commonly heat inactivated prior to culture use by heating at 56°C for approximately 0.5h. In this work, solutions of rHSA were either subjected to heat inactivation at 56°C for 0.5h; a freeze-thaw cycle by freezing at -80°C for 1h then quickly thawing at 37°C; a heat inactivation followed by a freeze-thaw cycle; or incubated on ice for the duration of all incubations. CD spectrometric analysis of rHSA did not reveal any permanent changes to protein secondary structure in all conditions tested. Albumin is known to undergo reversible conformation changes below 60°C [132], so it is possible that

any structural changes caused by the thermal stresses studied here may have been reversed when the temperature was equilibrated back to ambient conditions prior to analysis. Furthermore, far UV CD spectrometry only reveals information about the protein secondary structure. It would be of interest to see whether these thermal stresses cause changes to the tertiary structure because differences in protein folding could play a role in its viral stabilization properties. CD scans in the near UV region (250 – 350 nm) is commonly used to study protein tertiary structure. Though the information obtained from near UV scans is more qualitative (as it does not provide specific quantifiable tertiary structure characteristics), it is an adequate method for the comparative studies proposed here [105].

At 2-4°C, adding 0.05-5 g/L rHSA improved the stability of Lot B. There is an interaction effect between rHSA and temperature that affects its stabilization properties for ACAM529. Wetzel and colleagues analyzed albumin using CD spectrometry and found reversible structural changes below 60°C, whereas permanent changes were only observed between 65-80°C [132]. Rezaei-Tavirani and colleagues also found reversible albumin conformational changes between 15-65°C through differential scanning calorimetry (DSC) analysis and 25-55°C as determined through far UV CD spectrometry [114]. Again, permanent changes associated with protein unfolding were only observed above 65°C. It is possible that at lower temperatures, rHSA assumes a more favorable conformation to stabilize ACAM529. CD spectrometry studies of rHSA at temperatures between 4-27°C would be beneficial to study these conformation changes. Scans in the far UV region would uncover any secondary structure differences and scans in the near UV region would show any changes to tertiary structure [105,106].

7.4.4 Cholesterol lipid concentrate solution destabilizes ACAM529

Cholesterol lipid concentrate (CLC) is an animal- and protein- free chemically defined lipid solution used for culturing lipid-dependent cell lines [120,121]. Sanofi Pasteur reportedly used it in the production of ACAM529 [12] and they hold a patent (US 20110201087 A1[133]) for its use in the production of alpha

herpes virus, including ACAM529. They found an improved virus yield with the addition of CLC to the culture media. However, this work showed that the addition of 0.1-1x CLC to the reference buffer saw significant decrease in the stability of Lot B at 27°C, especially in the first 24h. Cholesterol is necessary for viral envelope synthesis so it is unsurprising that culture supplementation with cholesterol aids in viral production for numerous enveloped virus such as herpes virus [94] and lentivirus [93]. Lentivirus stability in liquid solution has also been improved with the addition of lipoproteins [100]. Another application for cholesterol is in the production of liposomes as it protects the bilayers from mechanical breakage [95]. However, due to the nonpolar nature of cholesterol, increased levels were shown to decrease the overall surface charge and ion-lipid interactions in synthetic membranes [96]. This reduction in ion-lipid interaction decreases the strength of the membrane as mentioned above [61]. This could explain the negative impact that CLC had on ACAM529 stability. The increased concentrations of cholesterol and lipids may be destabilizing the viral membrane, leading to inactivation. Therefore, it is important to minimize the amount of CLC present after harvesting the virus from the culture. Buffer exchange steps, such as tangential flow filtration, which essentially dilute the solution into a new buffer, should be used to reduce the levels of CLC.

7.4.5 Pluronic F68 is an effective stabilizer for ACAM529

Pluronic F68 (PF68) is a non-ionic surfactant that is widely used as a cell culture shear protectant at a concentration of 0.1%. It associates with cellular membranes and this is thought to provide stability to the membrane and improve the health of the culture [89,91,92]. In this work, PF68 was found to significantly stabilize ACAM529 at concentrations between 0.01%-0.1%, with maximal stability achieved using 0.1% PF68. Replicate experiments with 0.05%-0.1% PF68 were consistent with these results (Appendix G). However at 1% PF68, which is above the CMC for PF68 (0.4%), the virus was destabilized. Povidone was another culture shear protectant studied however it was not as effective as PF68 (see Appendix H). At concentrations typically used during cell culture (0.1% (w/v)), it did not

significantly affect virus stability over 120h. It also did not have any interaction effect with 2 g/L rHSA in its stabilization properties. At concentrations of 1% and 10%, povidone had a significantly negative impact on viral stability.

Though PF68 did not stabilize ACAM529 to the same extent as FBS, it is a promising excipient because it has been used in FDA approved drugs. It has been included as an inactive ingredient in FDA approved intravenous drugs up to 0.6% (w/v) and subcutaneous drugs up to 0.2% (w/v) (https://www.accessdata.fda.gov/scripts/cder/iig/index.cfm, accessed 03/27/2018). Further optimization of the concentration between 0.1% and 0.4% would be beneficial. Furthermore, Mundle and colleagues [12] noted that shear stress contributed significantly to the step yield of ACAM529 during purification processes, so not only would PF68 aid in product stability, but its shear protectant properties could further improve recovery of infectious virus during purification processes.

7.5 Screening of excipients is an important aspect of buffer optimization

Several other buffer conditions and excipients were explored for their stabilization properties for ACAM529 and they were chosen based on their past success with protecting enveloped viruses or proteins. Each biological product is different and conditions that are optimal for one may not necessarily be the case for another. Therefore it is important to test the conditions with the product of interest.

7.5.1 Low pH buffer condition increases ACAM529 infectivity but decreases stability

Physiological pH, approximately 7.4, is a condition in which many biological products are most stable. During the production and purification process, the virus may experience changes in pH. For example, the virus is often frozen at certain stages of the purification process but it has been reported that uneven freezing of a sample has the potential to create pockets of concentrated protons, leading to microenvironments with low pH [55]. HSV-1 was shown to have higher rates of association with

membranes at low pH (<5.3) in the presence of the HVEM receptor on cell membranes [37,134].The lower pH is thought to act as a co-activation signal for HSV membrane fusion and entry. Although beneficial for infection, low pH environments may not necessarily be favourable for longer-term stability [135].

The effect of the pH of the environment on ACAM529 infectivity and stability was studied. Low pH, although beneficial for infection, resulted in accelerated deactivation of Lot A at room temperature when compared to pH 6 and pH 7 conditions. Studies conducted by Lancz and Sample also saw decreased HSV stability below pH 6 and above pH 8 after 90 minutes incubation at 37°C [135]. The low pH is likely to have caused damage to the viral particles, especially the glycoproteins necessary for cell entry. It is hypothesized that gB, a highly conserved glycoprotein necessary for viral entry, along with gH/gL, undergo conformational changes at lower pH (~6.0-5.0), making it more hydrophobic [136]. This is necessary for viral entry however it was observed that prolonged exposure to an acidic environment in the absence of a cell membrane caused HSV to quickly lose infectivity due to irreversible conformational changes [134]. In general, the overall charge of a protein is pH-dependent and this affects not only the structure of the protein but also the enzymatic activity [13]. Here it was observed that ACAM529 is not significantly sensitive to pH shifts between pH 6-7 but effort should be put into controlling the environment to prevent exposure to increased acidic conditions.

7.5.2 Trehalose, L-arginine, and NEAA do not have a significant effect on ACAM529 stability

Disaccharides are commonly used in vaccine formulations due to the role they play in preferential exclusion in liquid solution [65] and for their capacity to remain amorphous during freeze-drying, where they are thought to form a glass around the product [55]. Sucrose is widely used in vaccine formulations [13,55,74] and it is used in the reference buffer for ACAM529. Another increasingly popular disaccharide used in formulation is trehalose [55,66,67,69,70,72,76,77] and it has been shown to have superior properties over sucrose. It has a higher viscosity and a larger hydrated volume, increasing the effect of

preferential exclusion and requiring 3x less molecules than sucrose [69]. In the current study, concentrations of 10%-30% trehalose offered the same level of stability as 10% sucrose to ACAM529 at 27°C. It did not appear as though trehalose was a superior stabilizer over sucrose for ACAM529 in liquid solution. The use of trehalose in lyophilized products is also common and the fact that it does not hydrolyze into reducing monosaccharides at low pH, unlike sucrose [73], is relevant. Product frozen at different stages during the manufacturing process can lead to elevated localized proton concentration, thus promoting the hydrolysis of sucrose into the reducing sugars fructose and glucose. Monosaccharides act as reducing agents in solution and can undergo the Maillard reaction with free amino groups on proteins, altering charge, conformation, and degradation rates [71]. Therefore it would be of interest to study the stabilizing effects of trehalose compared to sucrose through freeze-thaw experiments.

Amino acids have been implicated in biological product stabilization due to their buffering capabilities [58], antioxidant properties [85,86], and generally favourable interactions with biochemical compounds [76,81,123]. The reference buffer in this work contains both histidine and glutamate. Histidine has been shown to stabilize antibodies through non-covalent interactions [56] and be an effective oxygen radical scavenger [85]. L-arginine has become an amino acid of interest as it has been used extensively as an excipient to stabilize proteins [80,82] and to discourage protein aggregation [83,124]. Arginine has previously been shown to have a significant impact on deactivating HSV-1 below pH 4 [137]. In this work, it was found that the addition of 0.01 M-0.1 M L-arginine to the reference buffer did not significantly affect the stability of ACAM529.

Eagle's minimum essential medium (MEM) non-essential amino acid solution (NEAA) is another amino acid source previously shown to have stabilization properties. The 1x NEAA solution contains 10 mM each of glycine, L-alanine, L-asparagine, L-aspartic acid, L-glutamic acid, L-proline, and L-serine. It has been used in culture of hybridoma cells and it was shown to improve membrane stability

as well as improve antibody production [123]. However, when added to ACAM529 reference buffer at 0.1-1x concentrations, it did not have any significant effect on the stability of the virus at 27°C. The study done on hybridoma cultures could have seen improved membrane stability due to improved metabolic activity as increased antibody production was also observed with NEAA [123]. If this were the main mode of action for NEAA, it would be a good indicator as to why it did not induce changes to ACAM529 stability.

Chapter 8
Conclusions

The purpose of this research was to study the stability of ACAM529 vaccine candidate and identify excipients that would further improve the stabilization buffer used for the purification of the virus. The objectives outlined in Chapter 1 were to first study the stability of different lots of virus that vary in the production processes, then screen for potential stabilizing excipients in complex and defined solutions used during cell culture, and finally to screen other common stabilizers used for lipid- and protein-based biologicals.

The first objective was explored in Chapter 4. Virus produced using different production and purification procedures have varying titers, albumin content, and stability. Lot C had the highest titer, highest albumin content, and was the most stable of the three lots studied. Virus stability increased with decreased temperatures and the stability profiles followed a first order exponential decay trend at 27°C and 37°C. At lower temperatures, the stability more closely followed a double decay model, which suggests the presence of two subpopulations of virus, each undergoing different rates of decay.

The second and third objectives were explored in Chapter 5 and Chapter 6, respectively. The results of this work have identified various compounds and conditions that improve viral stability when added to the liquid stabilization buffer and conversely, compounds and conditions that accelerated the deactivation of the virus. There were also several additives that the virus was found to be tolerant to and did not significantly affect the stability.

FBS, PF68, and rHSA in small concentrations or at reduced temperature improve the stability of ACAM529. Minimal log loss in titer at 27°C was achieved with 1% (v/v) FBS or 0.1% PF68. The addition of small amounts (0.05 g/L) rHSA improves stability at 27°C and the addition of 0.05-5 g/L rHSA improves stability at 2-4°C in a concentration-independent manner. Though PF68 was not as

effective as FBS, it is a promising excipient to use for ACAM529, especially as it is present in FDA approved intravenous and subcutaneous drugs.

ACAM529 stability decreases with higher concentrations of rHSA at ambient conditions, CLC, high concentrations of PF68, and acidic pH. Significantly high log loss in titer at 27°C was observed with the addition of 0.5-5 g/L rHSA, 0.1-1x CLC, and 1% (w/v) PF68. Altering the buffer from pH 7 to pH 5, though significantly increased the initial infectivity of the virus, caused destabilization over 120h at room temperature.

Lastly, 50% FBS, 10% OptiPro SFM, buffer pH 6-7, 10-30% trehalose pH 6, 0.01 M-0.1 M L-arginine and the resultant 40-220 mM increase in Cl^- ions, and 0.1x-1x NEAA do not alter the stability of ACAM529 were.

The work presented here has made a substantial contribution towards improving the stability of ACAM529 in liquid solution. Several beneficial compounds have been identified and further research can be directed towards studying and optimizing these compounds to ensure optimal stability with FDA approved excipients.

Chapter 9
Recommendations

Moving forward with the stabilization buffer for ACAM529, several recommendations can be made. The highest level of stability near ambient conditions was observed with 1% FBS. It is of great interest to identify the specific stabilizers in FBS since it is a complex mixture with high batch-to-batch variability. In addition, its presence should be minimized in the final product due to its animal origin. Fractionation studies using ammonium sulfate precipitation and chromatography techniques [138,139] would help identify active fractions of FBS. Also, delipidation of FBS [100] would narrow down whether the lipids are important for stabilization.

The apparent interaction effect between rHSA and temperature is also of interest to explore further because at low temperatures, rHSA significantly improved the stability of the virus. Near and far UV CD spectrometry at temperatures between 4-27°C can be used to study whether there are any changes to rHSA tertiary and secondary structure, respectively. In this work, adding rHSA to the reference buffer at concentrations of 0.5-5 g/L at 27°C reduced the stability of the virus however, virus lots with higher levels of albumin carried over from culturing after purification were more stable. One of the major roles of albumin natively is to bind and transport materials through the circulatory system and it has been well documented to bind various types of compounds, primarily fatty acids, but also heme and many pharmaceutical drugs [101]. The binding of ligands to albumin may induce conformational changes to the protein [101,102], potentially altering the protein's viral stabilization properties. Small ligands that bind to albumin have a higher likelihood of being retained in the various filtration steps during purification. One study found that different sources of albumin, whether they were native BSA and HSA or rHSA produced in rice or yeast, had variable levels of fatty acid content [140]. The number of fatty acids bound to albumin and the chain length of each

molecule was thought to affect the thermal stability because the different types of albumin had variable thermal transition temperatures. It would be of interest to determine the fatty acid content of the rHSA used in this work and perform binding studies with rHSA and various fatty acids to identify whether they can stabilize a more favourable rHSA conformation.

This work identified PF68 as a promising excipient for ACAM529 and moving forward, the optimal concentration, between 0.1%-0.4% (w/v) should be determined. It would also be beneficial to obtain a full stability profile at different temperatures to model the stability and compare it to the stability curves with FBS in the buffer. This could elucidate how similar the mechanisms of stabilization are between the solutions.

Investigating the mechanism by which PF68 is stabilizing the virus would allow for a more directed approach to further improve the stability. To study whether PF68 is affecting the ACAM529 membrane stability, various aspects of the membrane in the presence of PF68 can be studied. The effects of PF68 on the prevalence of intact envelopes could be analyzed using TEM imaging. In addition, laurdan dye, which incorporates into lipid bilayers, can be used to assess differences in membrane fluidity [79]. The emission spectrum of the dye is sensitive to the level of membrane hydration and thus changes to membrane fluidity in the presence of PF68 can be analyzed using fluorescence spectrometry. ACAM529 has also been observed to form aggregates when viewed through TEM. Aggregation would cause an apparent decrease in titer when using the plaque assay. The effect of PF68 on ACAM529 aggregation could be studied qualitatively using TEM imaging. More quantitative approaches to study aggregation include flow cytometry [129] or optical density measurements at 360 nm [79].

Since the primary objective of this work was to identify potential excipients, there was little to no agitation applied to the assayed samples. However, it should be noted that during purification

processes, the virus is likely to experience various physical and chemical stresses from steps such as tangential flow filtration and benzonase treatment for DNA clarification [12]. Therefore, the next step in developing the stabilization buffer, once the concentrations of PF68 have been optimized, is to test whether the protective effects are translatable through the finalized purification protocol.

Another aspect of the purification protocol is that samples are often frozen for storage. Therefore, it would be of interest to study the effects of the stabilizers identified here in protecting the virus through a freeze-thaw cycle. Freezing could cause pockets of low pH environments [55]. Trehalose is not known to hydrolyze into reducing sugars like sucrose at low pH, so it has the potential to be a better choice for disaccharide over sucrose for protection during freeze-thaw cycles. In this study, trehalose was just as effective a stabilizer as sucrose in liquid formulations but it would be interesting to see whether this would hold true after a freeze-thaw step. Trehalose is significantly more expensive than sucrose (ten times the amount compared to sucrose for cell culture-grade material through Sigma-Aldrich) so it would be important to determine whether it aids in recovering a significant level of ACAM529 after a freeze-thaw cycle, before deciding to switch to trehalose.

References

1. Looker, K. J. *et al.* Global estimates of prevalent and incident herpes simplex virus type 2 infections in 2012. *PLoS One* **10,** (2015).
2. Roizman, B., Knipe, D. M. & Whitley, R. J. in *Fields virology* (eds. Knipe, D. M. et al.) 1823–1897 (Lippincott Williams & Wilkins, 2013).
3. Whitley, R. J. & Roizman, B. Herpes simplex virus infections. *Lancet* **357,** 1513–1518 (2001).
4. Freeman, E. E. *et al.* Herpes simplex virus 2 infection increases HIV acquisition in men and women: systematic review and meta-analysis of longitudinal studies. *AIDS* **20,** 73–83 (2006).
5. Wald, A. & Link, K. Risk of human immunodeficiency virus infection in herpes simplex virus type 2–seropositive persons: a meta-analysis. *J. Infect. Dis.* **185,** 45–52 (2002).
6. Chentoufi, A. A., Kritzer, E., Yu, D. M., Nesburn, A. B. & Benmohamed, L. Towards a rational design of an asymptomatic clinical herpes vaccine: The old, the new, and the unknown. *Clin. Dev. Immunol.* **2012,** (2012).
7. Johnston, C., Koelle, D. M. & Wald, A. HSV-2: In pursuit of a vaccine. *J. Clin. Invest.* **121,** 4600–4609 (2011).
8. Belshe, R. B. *et al.* Efficacy results of a trial of a herpes simplex vaccine. *N. Engl. J. Med.* **366,** 34–43 (2012).
9. Corey, L. *et al.* Recombinant glycoprotein vaccine for the prevention of genital HSV-2 infection: two randomized controlled trials. *JAMA* **281,** 331–340 (1999).
10. Da Costa, X. J., Bourne, N., Stanberry, L. R. & Knipe, D. M. Construction and characterization of a replication-defective herpes simplex virus 2 ICP8 mutant strain and its use in immunization studies in a guinea pig model of genital disease. *Virology* **232,** 1–12 (1997).
11. Da Costa, X. J., Jones, C. A. & Knipe, D. M. Immunization against genital herpes with a vaccine virus that has defects in productive and latent infection. *Proc. Natl. Acad. Sci. U. S. A.* **96,** 6994–6998 (1999).
12. Mundle, S. T. *et al.* High-purity preparation of HSV-2 vaccine candidate ACAM529 is immunogenic and efficacious In Vivo. *PLoS One* **8,** (2013).
13. Brandau, D. T., Jones, L. S., Wiethoff, C. M., Rexroad, J. & Middaugh, C. R. Thermal stability of vaccines. *J. Pharm. Sci.* **92,** 218–231 (2003).
14. Akhtar, J. & Shukla, D. Viral entry mechanisms: cellular and viral mediators of herpes simplex virus entry. *FEBS J.* **276,** 7228–7236 (2010).
15. Kumru, O. S. *et al.* Vaccine instability in the cold chain: Mechanisms, analysis and formulation strategies. *Biologicals* **42,** 237–259 (2014).
16. Nicoll, M. P., Proença, J. T. & Efstathiou, S. The molecular basis of herpes simplex virus latency. *FEMS Microbiol. Rev.* **36,** 684–705 (2012).

17. Hansen, R. K. *et al.* Mechanisms of inactivation of HSV-2 during storage in frozen and lyophilized forms. *Biotechnol. Prog.* **21,** 911–917 (2005).

18. Stein, S., Todd, P. & Mahoney, J. Infectivity of herpes simplex virus particles with and without envelopes. *Can. J. Microbiol.* **16,** 953–957 (1970).

19. Fu, X. & Zhang, X. Delivery of herpes simplex virus vectors through liposome formulation. *Mol. Ther.* **4,** 447–453 (2001).

20. Gru, K. *et al.* Three-dimensional structure of herpes simplex virus from cryo-electron tomography. *Science (80-.).* **302,** 1396–1398 (2003).

21. Newcomb, W. W. & Brown, J. C. Time-dependent transformation of the herpesvirus tegument. *J. Virol.* **83,** 8082–8089 (2009).

22. Newcomb, W. W. & Brown, J. C. Structure and capsid association of the herpesvirus large tegument protein UL36. *J. Virol.* **84,** 9408–9414 (2010).

23. Kelly, B. J., Fraefel, C., Cunningham, A. L. & Diefenbach, R. J. Functional roles of the tegument proteins of herpes simplex virus type 1. *Virus Res.* **145,** 173–186 (2009).

24. Laine, R. F. *et al.* Structural analysis of herpes simplex virus by optical super-resolution imaging. *Nat. Commun.* (2015). doi:10.1038/ncomms6980

25. Hsu, H.-Y., Nicholson, A. C., Pomerantz, K. B., Kaner, R. J. & Hajjar, D. P. Altered cholesterol trafficking in herpesvirus-infected arterial cells. *J. Biol. Chem.* **270,** 19630–19637 (1995).

26. Sutter, E. *et al.* Herpes simplex virus 1 induces de novo phospholipid synthesis. *Virology* **429,** 124–135 (2012).

27. Spear, P. G. & Roizman, B. Bouyant density of herpes simplex virus in solutions of caesium chloride. *Nature* **214,** 713–714 (1967).

28. Mettenleiter, T. C., Klupp, B. G. & Granzow, H. Herpesvirus assembly: An update. *Virus Res.* **143,** 222–234 (2009).

29. van Genderen, I. L., Brandimarti, R., Torrisi, M. R., Campadelli, G. & van Meer, G. The phospholipid composition of extracellular herpes simplex virions differs from that of host cell nuclei. *Virology* **200,** 831–836 (1994).

30. Foster, T. P., Rybachuk, G. V. & Kousoulas, K. G. Glycoprotein K specified by herpes simplex virus type 1 is expressed on virions as a Golgi complex-dependent glycosylated species and functions in virion entry. *J. Virol.* **75,** 12431–12438 (2001).

31. Loret, S., Guay, G. & Lippe, R. Comprehensive characterization of extracellular herpes simplex virus type 1 virions. *J. Virol.* **82,** 8605–8618 (2008).

32. Karasneh, G. A. & Shukla, D. Herpes simplex virus infects most cell types in vitro: clues to its success. *Virol. J.* **8,** (2011).

33. WuDunn, D. & Spear, P. G. Initial interaction of herpes simplex virus with cells is binding to heparan sulfate. *J. Virol.* **63,** 52–58 (1989).

34. Spear, P. G. Herpes simplex virus: Receptors and ligands for cell entry. *Cell. Microbiol.* **6,** 401–410 (2004).

35. Carfí, A. *et al.* Herpes simplex virus glycoprotein D bound to the human receptor HveA. *Mol. Cell* **8,** 169–179 (2001).

36. Atanasiu, D., Saw, W. T., Cohen, G. H. & Eisenberg, R. J. Cascade of events governing cell-cell fusion induced by herpes simplex virus glycoproteins gD, gH/gI, and gB. *J. Virol.* **84,** 12292–12299 (2010).

37. Nicola, A. V., McEvoy, A. M. & Straus, S. E. Roles for endocytosis and low pH in herpes simplex virus entry into HeLa and Chinese hamster ovary cells. *J. Virol.* **77,** 5324–5332 (2003).

38. Bauer, D. W., Huffman, J. B., Homa, F. L. & Evilevitch, A. Herpes virus genome, the pressure is on. *J. Am. Chem. Soc.* **135,** 11216–11221 (2013).

39. Copeland, A. M., Newcomb, W. W. & Brown, J. C. Herpes simplex virus replication: roles of viral proteins and nucleoporins in capsid-nucleus attachment. *J. Virol.* **83,** 1660–1668 (2009).

40. Newcomb, W. W., Homa, F. L. & Brown, J. C. Involvement of the portal at an early step in herpes simplex virus capsid assembly. *J. Virol.* **79,** 10540–10546 (2005).

41. Farnsworth, A. *et al.* Herpes simplex virus glycoproteins gB and gH function in fusion between the virion envelope and the outer nuclear membrane. *Proc. Natl. Acad. Sci.* **104,** 10187–10192 (2007).

42. Vittone, V. *et al.* Determination of interactions between tegument proteins of herpes simplex virus type 1. *J. Virol.* **79,** 9566–9571 (2005).

43. Kamen, D. E., Gross, S. T., Girvin, M. E. & Wilson, D. W. Structural basis for the physiological temperature dependence of the association of VP16 with the cytoplasmic tail of herpes simplex virus glycoprotein H. *J. Virol.* **79,** 6134–6141 (2005).

44. Farnsworth, A., Wisner, T. W. & Johnson, D. C. Cytoplasmic residues of herpes simplex virus glycoprotein gE required for secondary envelopment and binding of tegument proteins VP22 and UL11 to gE and gD. *J. Virol.* **81,** 319–331 (2007).

45. Koshizuka, T., Kawaguchi, Y., Goshima, F., Mori, I. & Nishiyama, Y. Association of two membrane proteins encoded by herpes simplex virus type 2, UL11 and UL56. *Virus Genes* **32,** 153–163 (2006).

46. Johnson, D. C. & Huber, M. T. Directed egress of animal viruses promotes cell-to-cell spread. *J. Virol.* **76,** 1–8 (2002).

47. Dingwell, K. S. & Johnson, D. C. The herpes simplex virus gE-gI complex facilitates cell-to-cell spread and binds to components of cell junctions. *J. Virol.* **72,** 8933–8942 (1998).

48. Dingwell, K. S. *et al.* Herpes simplex virus glycoproteins E and I facilitate cell-to- cell spread in vivo and across junctions of cultured cells. *J. Virol.* **68,** 834–845 (1994).

49. Morrison, L. A. & Knipe, D. M. Immunization with replication-defective mutants of herpes simplex virus type 1: sites of immune intervention in pathogenesis of challenge virus infection. *J. Virol.* **68,** 689–696 (1994).

50. Morrison, L. A. & Knipe, D. M. Mechanisms of immunization with a replication-defective mutant of herpes simplex virus 1. *Virology* **220,** 402–413 (1996).

51. Da Costa, X., Kramer, M. F., Zhu, J., Brockman, M. a. & Knipe, D. M. Construction, Phenotypic Analysis, and Immunogenicity of a UL5/UL29 Double Deletion Mutant of Herpes Simplex Virus 2. *J. Virol.* **74,** 7963–7971 (2000).

52. Merten, O.-W., Schweizer, M., Chahal, P. & Kamen, A. A. Manufacturing of viral vectors for gene therapy: part I. Upstream processing. *Pharm. Bioprocess.* **2,** 183–203 (2014).

53. Vicente, T., Roldão, A., Peixoto, C., Carrondo, M. J. T. & Alves, P. M. Large-scale production and purification of VLP-based vaccines. *J. Invertebr. Pathol.* **107,** S42–S48 (2011).

54. Merten, O.-W., Schweizer, M., Chahal, P. & Kamen, A. Manufacturing of viral vectors: part II. Downstream processing and safety aspects. *Pharm. Bioprocess.* **2,** 237–251 (2014).

55. Hansen, L. J. J., Daoussi, R., Vervaet, C., Remon, J. P. & De Beer, T. R. M. Freeze-drying of live virus vaccines: A review. *Vaccine* **33,** 5507–5519 (2015).

56. Kamerzell, T. J., Esfandiary, R., Joshi, S. B., Middaugh, C. R. & Volkin, D. B. Protein – excipient interactions : Mechanisms and biophysical characterization applied to protein formulation development. *Adv. Drug Deliv. Rev.* **63,** 1118–1159 (2011).

57. Crommelin, D. J. A. in *Pharmaceutical Biotechnology: Fundamentals and Applications* (eds. Crommelin, D. J. A., Sindelar, R. D. & Meibohm, B.) 69–99 (Springer, 2013). doi:10.1007/978-1-4614-6486-0

58. Li, S., Schöneich, C., Wilson, G. S. & Borchardt, R. T. Chemical pathways of peptide degradation. V. Ascorbic acid promotes rather than inhibits the oxidation of methionine to methionine sulfoxide in small model peptides. *Pharm. Res.* **10,** 1572–1579 (1993).

59. Cruz, P. E. *et al.* Screening of novel excipients for improving the stability of retroviral and adenoviral vectors. *Biotechnol. Prog.* **22,** 568–576 (2006).

60. Karow, A. R., Bahrenburg, S. & Garidel, P. Buffer capacity of biologics-from buffer salts to buffering by antibodies. *Biotechnol. Prog.* **29,** 480–492 (2013).

61. Garcia-Manyes, S., Oncins, G. & Sanz, F. Effect of ion-binding and chemical phospholipid structure on the nanomechanics of lipid bilayers studied by force spectroscopy. *Biophys. J.* **89,** 1812–1826 (2005).

62. Choi, H.-J. *et al.* Effect of osmotic pressure on the stability of whole inactivated influenza vaccine for coating on microneedles. *PLoS One* **10,** (2015).

63. Barnhart, E. R. & Ash, R. J. Physical characteristics of herpesvirions: Low-temperature and osmotic-shock studies. *Virology* **66,** 563–567 (1975).

64. Burke, C. J. *et al.* The adsorption of proteins to pharmaceutical container surfaces. *Int. J. Pharm.* **86,** 89–93 (1992).

65. Arakawa, T., Kita, Y. & carpen. Protein-solvent interactions in pharmaceutical formulations. *Pharm. Res.* **8,** 285–291 (1991).

66. Lin, T.-Y. & Timasheff, S. N. On the role of surface tension in the stabilization of globular proteins. *Protein Sci.* **5,** 372–381 (1996).

67. Kaushik, J. K. & Bhat, R. Why is trehalose an exceptional protein stabilizer? An analysis of the thermal stability of proteins in the presence of the compatible osmolyte trehalose. *J. Biol. Chem.* **278,** 26458–26465 (2003).

68. Roos, Y. Melting and glass transitions weight carbohydrates of low molecular. *Carbohydr. Res.* **238,** 39–48 (1993).

69. Sola-Penna, M. & Meyer-Fernandes, J. R. Stabilization against thermal inactivation promoted by sugars on enzyme structure and function: Why is trehalose more effective than other sugars? *Arch. Biochem. Biophys.* **360,** 10–14 (1998).

70. Luzardo, M. del C. *et al.* Effect of trehalose and sucrose on the hydration and dipole potential of lipid bilayers. *Biophys. J.* **78,** 2452–2458 (2000).

71. Zhang, Q., Ames, J. M., Smith, R. D., Baynes, J. W. & Metz, T. O. A perspective on the Maillard reaction and the analysis of protein glycation by mass spectrometry: Probing the pathogenesis of chronic disease. *J. Proteome Res.* **8,** 754–769 (2009).

72. Li, S. *et al.* Effects of reducing sugars on the chemical stability of human relaxin in the lyophilized state. *J. Pharm. Sci.* **85,** 873–877 (1996).

73. Karel, M. & Labuza, T. P. Nonenzymatic browning in model systems containing sucrose. *J. Agric. Food Chem.* **16,** 717–719 (1968).

74. Zhai, S. *et al.* Effect of freezing rates and excipients on the infectivity of a live viral vaccine during lyophilization. *Biotechnol. Prog.* **20,** 1113–1120 (2004).

75. Howell, C. L. & Miller, M. J. Effect of sucrose phosphate and sorbitol on infectivity of enveloped viruses during storage. *J. Clin. Microbiol.* **18,** 658–662 (1983).

76. Rudolph, A. S., Crowe, J. H. & Crowe, L. M. Effects of three stabilizing agents - proline, betaine, and trehalose on membrane phospholipids. *Arch. Biochem. Biophys.* **245,** 134–143 (1986).

77. Kissmann, J. *et al.* H1N1 influenza virus-like particles: physical degradation pathways and identification of stabilizers. *J. Pharm. Sci.* **100,** 634–645 (2011).

78. Kreilgaard, L., Frokjaer, S., Flink, J. M., Randolph, T. W. & Carpenter, J. F. Effects of additives on the stability of recombinant human factor XIII during freeze-drying and storage in the dried solid. *Arch. Biochem. Biophys.* **360,** 121–134 (1998).

79. Kissmann, J. *et al.* Stabilization of measles virus for vaccine formulation. *Hum. Vaccin.* **4,** 350–359 (2008).

80. Arakawa, T., Tsumoto, K., Nagase, K. & Ejima, D. The effects of arginine on protein binding and elution in hydrophobic interaction and ion-exchange chromatography. *Protein Expr. Purif.* **54,** 110–116 (2007).

81. Lebon, P., Protat, A. & Molinie, P. L-Arginine elution of measles virus adsorbed on monkey erythrocytes. *Infect. Immun.* **11,** 1407–1408 (1975).

82. Tsumoto, K. *et al.* Role of arginine in protein refolding, solubilization, and purification. *Biotechnol. Prog.* **20,** 1301–1308 (2004).

83. Das, U. *et al.* Inhibition of protein aggregation: supramolecular assemblies of arginine hold the key. *PLoS One* **2,** (2007).

84. Li, S., Schöneich, C. & Borchardt, R. T. Chemical instability of protein pharmaceuticals: Mechanisms of oxidation and strategies for stabilization. *Biotechnol. Bioeng.* **48,** 490–500 (1995).

85. Evans, R. K. *et al.* Development of stable liquid formulations for adenovirus-based vaccines. *J. Pharm. Sci.* **93,** 2458–2475 (2004).

86. Jezek, J. *et al.* A heat-stable hepatitis B vaccine formulation. *Hum. Vaccin.* **5,** 529–535 (2009).

87. Webb, S. D., Golledge, S. L., Cleland, J. L., Carpenter, J. F. & Randolph, T. W. Surface adsorption of recombinant human interferon-gamma in lyophilized and spray-lyophilized formulations. *J. Pharm. Sci.* **91,** 1474–1487 (2002).

88. Thurow, H. & Geisen, K. Stabilisation of dissolved proteins against denaturation at hydrophobic interfaces. *Diabetologia* **27,** 212–218 (1984).

89. Papoutsakis, E. T. Media additives for protecting freely suspended animal cells against agitation and aeration damage. *Trends Biotechnol.* **9,** 316–324 (1991).

90. Wang, J.-Y., Marks, J. & Lee, K. Y. C. Nature of interactions between PEO-PPO-PEO triblock copolymers and lipid membranes: (I) Effect of polymer hydrophobicity on its ability to protect liposomes from peroxidation. *Biomacromolecules* **13,** 2616–2623 (2012).

91. Firestone, M. A., Wolf, A. C. & Seifert, S. Small-angle X-ray scattering study of the interaction of poly(ethylene oxide)-b-poly(propylene oxide)-b-poly(ethylene oxide) triblock copolymers with lipid bilayers. *Biomacromolecules* **4,** 1539–1549 (2003).

92. Gigout, A., Buschmann, M. D. & Jolicoeur, M. The fate of Pluronic F-68 in chondrocytes and CHO Cells. *Biotechnol. Bioeng.* **100,** 975–987 (2008).

93. Campbell, S. M., Crowe, S. M. & Mak, J. Virion-associated cholesterol is critical for the maintenance of HIV-1 structure and infectivity. *AIDS* **16,** 2253–2261 (2002).

94. Bender, F. C. *et al.* Specific association of glycoprotein B with lipid rafts during herpes simplex virus entry. *J. Virol.* **77,** 9542–9552 (2003).

95. Templeton, N. S. *et al.* Improved DNA: Liposome complexes for increased systemic delivery and gene expression. *Nat. Biotechnol.* **15,** 647–52 (1997).

96. Magarkar, A. *et al.* Cholesterol level affects surface charge of lipid membranes in physiological environment. *Nat. Sci. Reports* **4,** (2014).

97. Chuang, V. T. G., Kragh-Hansen, U. & Otagiri, M. Pharmaceutical strategies utilizing recombinant human serum albumin. *Pharm. Res.* **19,** 569–577 (2002).

98. Tarelli, E. *et al.* Recombinant human albumin as a stabilizer for biological materials and for the preparation of international reference reagents. *Biologicals* **26,** 331–346 (1998).

99. He, Y. *et al.* Large-scale production of functional human serum albumin from transgenic rice seeds. *PNAS* **108,** 19078–19083 (2011).

100. Carmo, M. *et al.* Stabilization of gammaretroviral and lentiviral vectors: from production to gene transfer. *J. Gene Med.* **11,** 670–678 (2009).

101. Fasano, M. *et al.* The extraordinary ligand binding properties of human serum albumin. *IUBMB Life* **57,** 787–796 (2005).

102. Curry, S., Mandelkow, H., Brick, P. & Franks, N. Crystal structure of human serum albumin complexed with fatty acid reveals an asymmetric distribution of binding sites. *Nat. Struct. Biol.* **5,** 827–835 (1998).

103. Demoro, B. *et al.* Screening organometallic binuclear thiosemicarbazone ruthenium complexes as potential anti-tumour agents: cytotoxic activity and human serum albumin binding mechanism. *Dalt. Trans.* **42,** 7131–7146 (2013).

104. Iglesias, J. *et al.* Albumin is a major serum survival factor for renal tubular cells and macrophages through scavenging of ROS. *Am. J. Physiol.* **277,** F711–F722 (1999).

105. Kelly, S. M., Jess, T. J. & Price, N. C. How to study proteins by circular dichroism. *Biochim. Biophys. Acta* **1751,** 119–139 (2005).

106. Greenfield, N. J. Using circular dichroism spectra to estimate protein secondary structure. *Nat. Protoc.* **1,** 2876–2890 (2007).

107. R Core Team. *R: A language and environment for statistical computing*. (R Foundation for Statistical Computing, Vienna, Austria, 2017). at <https://www.r-project.org/>

108. Wickham, H., Francois, R., Henry, L. & Müller, K. *dplyr: A grammar of data manipulation*. (R package version 0.7.4, 2017). at <https://cran.r-project.org/package=dplyr>

109. Wickham, H. *ggplot2: Elegant graphics for data analysis*. (Springer-Verlag New York, 2009). at <http://ggplot2.org>

110. Wickham, H. *scales: Scale functions for visualization*. (R package version 0.5.0, 2017). at <https://cran.r-project.org/package=scales>

111. Wickham, H. *gtable: Arrange 'grobs' in tables*. (R package version 0.2.0, 2016).

112. Baptiste, A. *gridExtra: Miscellaneous functions for 'grid' graphics*. (R package version 2.3, 2017). at <https://cran.r-project.org/package=gridExtra>

113. Wilke, C. O. *cowplot: Streamlined plot theme and plot annotations for 'ggplot2'*. (R package version 0.9.0, 2017).

114. Rezaei-Tavirani, M., Moghaddamnia, S. H., Ranjbar, B., Amani, M. & Marashi, S.-A. Conformational study of human serum albumin in pre-denaturation temperatures by differential scanning calorimetry, circular dichroism and UV spectroscopy. *J. Biochem. Mol. Biol.* **39,** 530–536 (2006).

115. Carmo, M. *et al.* Relationship between retroviral vector membrane and vector stability. *J. Gen. Virol.* **87,** 1349–1356 (2006).

116. Johnson, F. B. Transport of viral specimens. *Clin. Microbiol. Rev.* **3,** 120–131 (1990).

117. Jensen, C. & Johnson, F. B. Comparison of various transport media for viability maintenance of herpes simplex virus, respiratory syncytial virus, and adenovirus. *Diagn. Microbiol. Infect. Dis.* **19,** 137–142 (1994).

118. Baker, H., DeAngelis, B. & Frank, O. Vitamins and other metabolites in various sera commonly used for cell culturing. *Experientia* **44,** 1007–1010 (1988).

119. Zheng, X. *et al.* Proteomic analysis for the assessment of different lots of fetal bovine serum as a raw material for cell culture. Part IV. Application of proteomics to the manufacture of biological drugs. *Biotechnol. Prog.* **22,** 1294–1300 (2006).

120. Okonkowski, J. *et al.* Cholesterol delivery to NS0 cells: Challenges and solutions in disposable linear low-density polyethylene-based bioreactors. *J. Biosci. Bioeng.* **103,** 50–59 (2007).

121. Sato, J. D., Kawamoto, T., McClure, D. B. & Sato, G. H. Cholesterol requirement of NS-1 mouse myeloma cells for growth in serum-free medium. *Mol. Biol. Med.* **2,** 121–134 (1984).

122. Anderson, S. *et al.* Herpesvirus compositions and related methods. Patent US 20150150964. (2015).

123. Fassnacht, D., Rössing, S., Ghaussy, N. & Pörtner, R. Influence of non-essential amino acids on apoptotic and necrotic death of mouse hybridoma cells in batch cultures. *Biotechnol. Lett.* **19,** 35–38 (1997).

124. Tsumoto, K., Ejima, D., Kita, Y. & Arakawa, T. Review: Why is arginine effective in suppressing aggregation? *Protein Pept. Lett.* **12,** 613–619 (2005).

125. Higashikawa, F. & Chang, L.-J. Kinetic analyses of stability of simple and complex retroviral vectors. *Virology* **280,** 124–131 (2001).

126. Vernon, S. K., Lawrence, W. C., Long, C. A., Rubin, B. A. & Sheffield, J. B. Morphological components of herpesvirus. IV. Ultrastructural features of the envelope and tegument. *J. Ultrasructure Res.* **81,** 163–171 (1982).

127. Vernon, S. K., Lawrence, W. C., Cohen, G. H., Durso, M. & Rubin, B. A. Morphological components of herpesvirus. II. Preservation of virus during negative staining procedures. *J. Gen. Virol.* **31,** 183–191 (1976).

128. Sabatini, D. D., Bensch, K. & Barnett, R. J. Cytochemistry and electronmicroscopy: The preservation of cellular ultrastructure and enzymatic activity by aldehyde fixation. *J. Cell Biol.* **17,** 19–58 (1963).

129. Jorio, H., Tran, R., Meghrous, J., Bourget, L. & Kamen, A. Analysis of baculovirus aggregates using flow cytometry. *J. Virol. Methods* **134,** 8–14 (2006).

130. Dziarski, R. Cell-bound albumin is the 70-kDa peptidoglycan-, lipopolysaccharide-, and lipoteichoic acid-binding protein on lymphocytes and macrophages. *J. Biol. Chem.* **269,** 20431–20436 (1994).

131. Zhang, Z., Chisti, Y. & Moo-Young, M. Effects of the hydrodynamic environment and shear protectants on survival of erythrocytes in suspension. *J. Biotechnol.* **43,** 33–40 (1995).

132. Wetzel, R. *et al.* Temperature behaviour of human serum albumin. *Eur. J. Biochem.* **104,** 469–478 (1980).

133. Delagrave, S., Oubelaid, R. & Hamberger, J. Compositions and methods for the production of alpha-herpesviruses. Patent US 2011/0201087 A1. (2011).

134. Whitbeck, J. C., Zuo, Y., Milne, R. S. B., Cohen, G. H. & Eisenberg, R. J. Stable association of herpes simplex virus with target membranes is triggered by low pH in the presence of the gD receptor, HVEM. *J. Virol.* **80,** 3773–3780 (2006).

135. Lancz, G. & Sample, J. Thermal-pH inactivation of herpes simplex virus: Interdependence of the medium composition and the pH on the rate of virus inactivation. *Arch. Virol.* **84,** 141–146 (1985).

136. Dollery, S. J., Delboy, M. G. & Nicola, A. V. Low pH-induced conformational change in herpes simplex virus glycoprotein B. *J. Virol.* **84,** 3759–3766 (2010).

137. Yamasaki, H., Tsujimoto, K., Koyama, A. H., Ejima, D. & Arakawa, T. Arginine facilitates inactivation of enveloped viruses. *J. Pharm. Sci.* **97,** 3067–3073 (2008).

138. Chen, L., Mao, S. J. T. & Larsen, W. J. Identification of a factor in fetal bovine serum that stabilizes the cumulus extracellular matrix. *J. Biol. Chem.* **267,** 12380–12386 (1992).

139. Pijuan-Galitó, S., Tamm, C. & Annerén, C. Serum inter-alpha-inhibitor activates the Yes tyrosine kinase and YAP/TEAD transcriptional complex in mouse embryonic stem cells. *J. Biol. Chem.* **289,** 33492–33502 (2014).

140. Lang, B. E. & Cole, K. D. Unfolding properties of recombinant human serum albumin products are due to bioprocessing steps. *Biotechnol. Prog.* **31,** 62–69 (2015).

141. Wallis, C., Trulock, S. & Melnick, J. L. Inherent photosensitivity of herpes virus and other enveloped viruses. *J. Gen. Virol.* **5,** 53–61 (1969).

142. Frahm, G. E. *et al.* Determination of supplier-to-supplier and lot-to-lot variability in glycation of recombinant human serum albumin expressed in Oryza sativa. *PLoS One* **9,** (2014).

143. Suryawanshi, V. D., Walekar, L. S., Gore, A. H., Anbhule, P. V. & Kolekar, G. B. Spectroscopic analysis on the binding interaction of biologically active pyrimidine derivative with bovine serum albumin. *J. Pharm. Anal.* **6,** 56–63 (2016).

144. Andrade, M. A., Chacón, P., Merelo, J. J. & Morán, F. Evaluation of secondary structure of proteins from UV circular dichroism spectra using an unsupervised learning neural network. *Protein Eng. Des. Sel.* **6,** 383–390 (1993).

145. Whitmore, L. & Wallace, B. A. Protein secondary structure analyses from circular dichroism spectroscopy: Methods and reference databases. *Biopolymers* **89,** 392–400 (2008).

146. Bühler, V. in *Polyvinylpyrrolidone excipients for pharmaceuticals: povidone, crospovidone, and copovidone* 5–124 (Springer, 2005).

147. Aurelian, L. Vaccine composition for herpes simplex virus and methods of using. Patent US 6207168 B1. (2001).

148. Wang, W. *Lyophilization and development of solid protein pharmaceuticals*. *International Journal of Pharmaceutics* **203,** (2000).

Appendix A
Time course assay design

Purpose

The following appendix describes the considerations taken into account when designing the time course assay for ACAM529 stability studies. A number of preliminary experiments were also conducted and are presented here.

A.1 General protocol considerations

The purpose of the work was to improve a buffer that would stabilize ACAM529 during purification procedures. A time course assay tracking viral titer over time was determined to be an adequate method for testing various stability buffers and conditions. Decisions about the aspects of the time course assay were made by considering the circumstances of product purification [12]:

- Purification procedures typically take 1-3 days but in order to allow for a complete profile of the viral stability, here the time courses were run for 5 days (120 hours).
- Most steps of the purification, including clarification, buffer exchange, and filtration, are done at ambient temperatures so time course assays were carried out at room temperature, 25°C, or 27°C.
- HSV-2 is known to be photosensitive [141] so all samples were covered in foil for the duration of the experiments.
- Since the primary objective is to identify potential excipients, there was little to no agitation applied to the assayed samples. However, it should be noted that during purification processes, the virus is likely to experience various physical and chemical stresses from steps such as tangential flow filtration and benzonase treatment for DNA clarification.

A.2 Effect of viral dilution into test buffers

A method for suspending the virus in the buffer of interest was needed. To minimize processing of the virus and risk losing viral activity, a simple method of diluting the virus into the buffer was proposed. To determine the effect of diluting the virus on its stability, a time course assay was conducted. Frozen purified virus stock Lot A was quickly thawed at 37°C and was either left undiluted or diluted 1/10 or 1/100 into freshly prepared reference buffer. Samples were incubated at room temperature and plaque assays were performed in triplicate immediately upon dilution (0h), and at 2h, 10h, 24h, 48h, 72h, 97h, and 121h as described in Chapter 3. Results indicated that the virus diluted 1/100 was not as stable as the undiluted or the 1/10 diluted virus after 24h (Figure A.1A) however the overall log loss in titer for each of the different dilutions showed no significant difference (α=0.05) (Figure A.1B). Diluting the virus 1/100 was therefore concluded to be an adequate method for suspending the virus, as it is a simple process. If similar discrepancies from diluting the virus arise in future time course assays similar to the ones observed here, it would show a conservative underestimate of the stability of the virus and avoid inflating the stability of the virus.

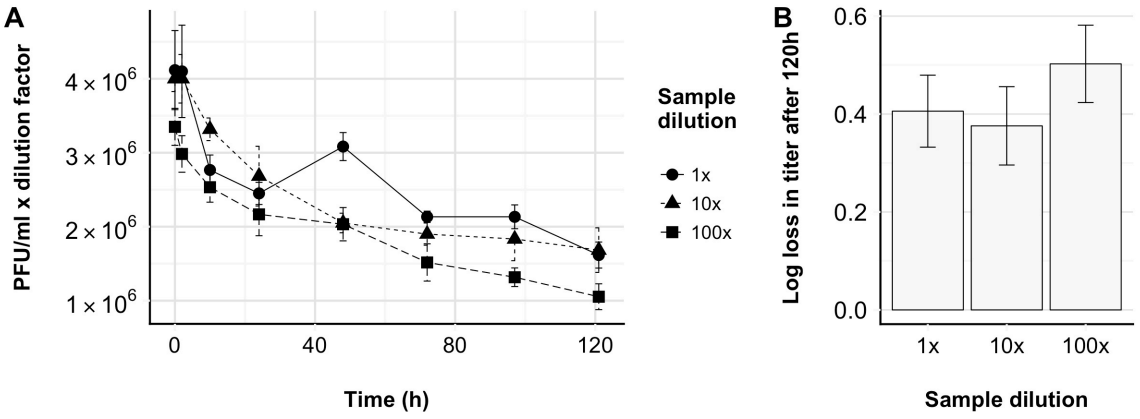

Figure A.1 Effect of different viral dilutions of ACAM529 stability.

A.3 Effects of a freeze-thaw cycle on ACAM529

For time course assays requiring more frequent sampling times, it was not possible to perform plaque assays immediately. For this purpose, it was often necessary to freeze samples taken during the time course and thaw them at a later date to perform the plaque assay. To determine whether this would affect the observed titer, a frozen aliquot of ACAM529 Lot A, Lot B, and Lot C was quickly thawed at 37°C and a sample was diluted in triplicate in the reference buffer, then immediately titered using the plaque assay as described in Chapter 3. The remainder of the aliquot was subjected to a freeze-thaw cycle by freezing at -80°C for approximately 24h, then thawing at 37°C for a plaque assay. Results showed no significant difference in the viral titer before and after the freeze-thaw cycle for all lots (Figure A.2) at a significance level of $\alpha = 0.05$.

To determine the effect of a freeze-thaw cycle on the stability of ACAM529 over a longer period of time a time course study with a freeze-thaw cycle was conducted with Lot C. Frozen virus was quickly thawed at 37°C and diluted 1/100 in the reference buffer. Triplicate samples were taken for tittering using the plaque assay as described in Chapter 3 at 0h, 2h, 8h, 24h, 48h 50h, 56h, 72h, 96h, and 120h. At 24h, a sample was also taken and frozen at -80°C for 24h, then quickly thawed at 37°C. Triplicate samples were titered in a similar manner at the same time points as the original sample. The stability profile is shown in Figure A.3 and results showed that upon thawing the sample that underwent an addition freeze-thaw cycle, the titer was similar to the titer before the cycle (compare 24h data point to 48h data point for the freeze-thaw sample). This was consistent with results shown in Figure A.2. However, a dramatic decrease in titer was observed in the first 2h after the freeze-thaw cycle. The cycle had a negative effect on the stability of the virus and it was most sensitive to degradation 2h after thawing.

Since the titer of the sample before and immediately after a freeze-thaw cycle were very similar, it was concluded that freezing samples prior to titering was an appropriate method for handling a large number of samples. However, it should be assured the plaque assays are preformed immediately upon thawing the frozen samples, as the effect on longer-term viral stability is significant. Furthermore, all samples collected at a time point should be titered at the same time to reduce other variables.

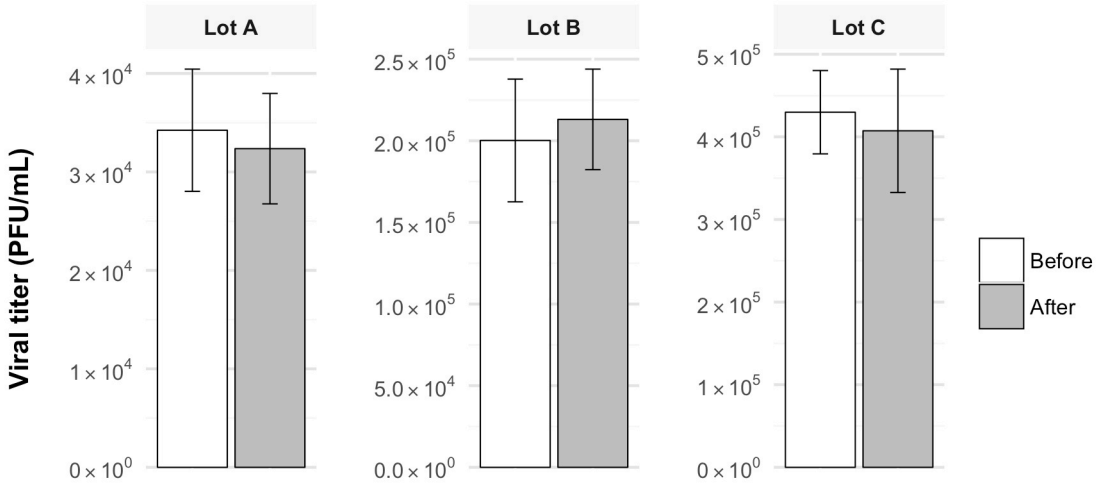

Figure A.2 Effect of a freeze-thaw cycle on initial ACAM529 titer.

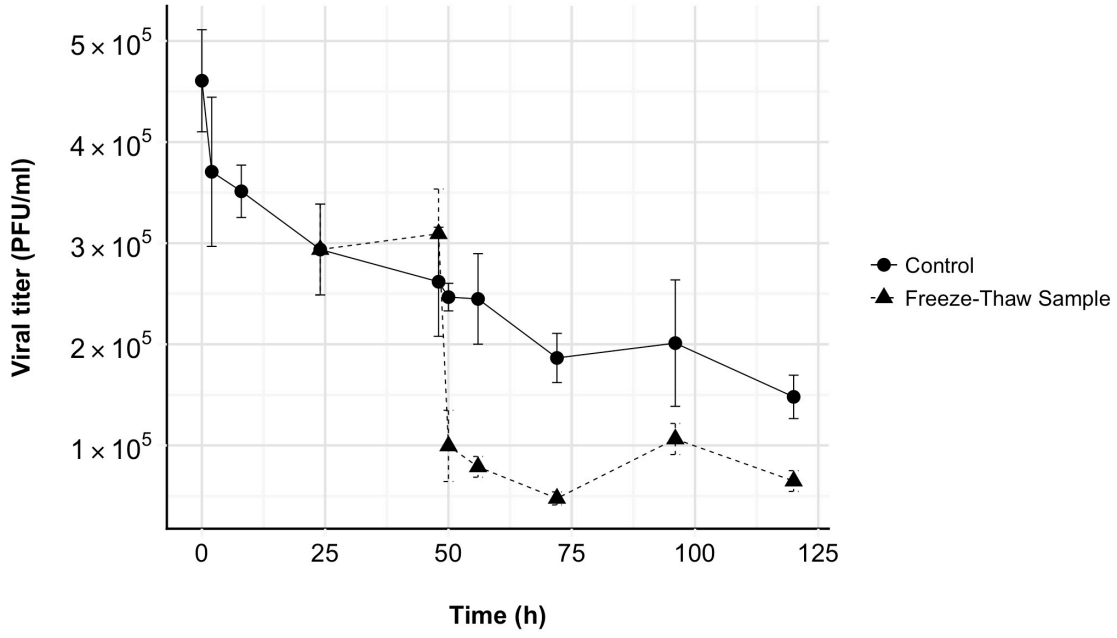

Figure A.3 Effect of a freeze-thaw cycle on ACAM529 stability.

A.4 Effects of complementary Vero cell age on ACAM529 titer

Plaque assays were chosen as the method for tracking ACAM529 activity however a disadvantage of the assay is that it indirectly quantifies the viral particles by counting the effect it has on the monolayer of complementary Vero cells. To determine the working complementary Vero cell passage number range for the time course plaque assays, an experiment studying cell age was performed. A vial of ACAM529 Lot C was aliquoted into 7 cryovials, then frozen at -80°C. A plaque assay was performed at the beginning of each week during an eight-week culture of complementary Vero cells using one of the ACAM529 aliquots to infect the cells in triplicate as described in Chapter 3. Viral titers in PFU/ml were reported at the specified culture passage number (2-3 passages are typically performed each week) and the results are presented in Figure A.4. Though there was variability among the titers at different passage numbers, there was no significant difference between the reported values so it was concluded that cells should be used under passage 25.

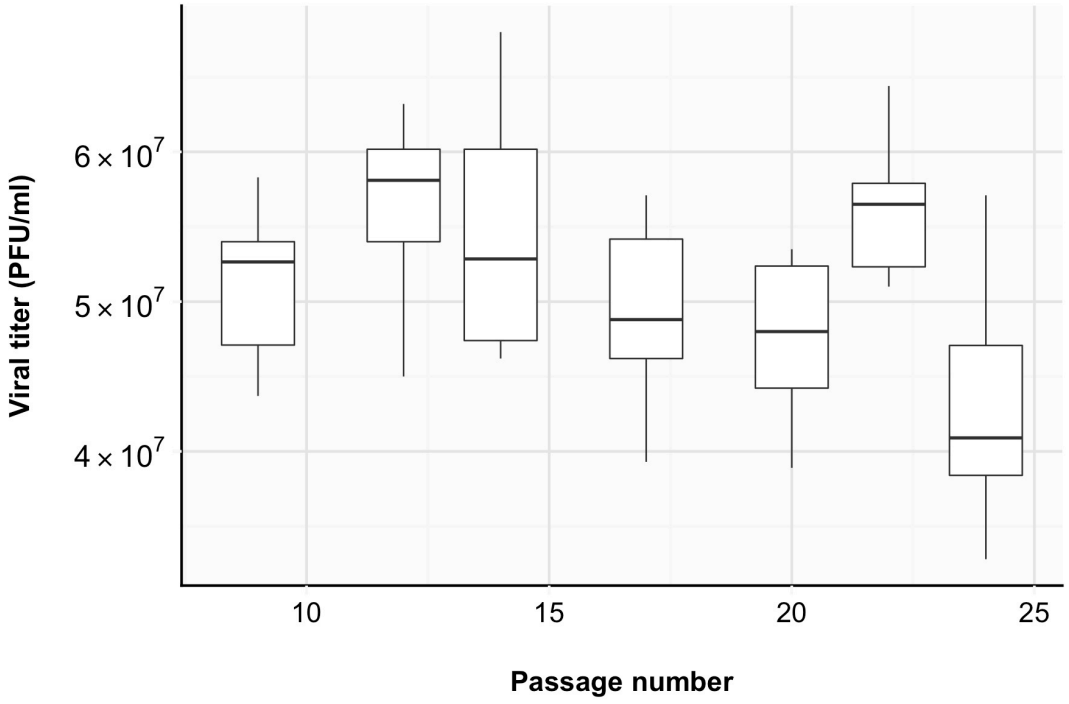

Figure A.4 Effect of cell age on plaque assay-derived ACAM529 titer.

Appendix B

Optimization of conditions for CD spectrometry

B.1 Purpose

Circular dichroism (CD) spectrometry was used to study the secondary and tertiary structure of rHSA. This appendix details the steps taken to determine the optimal choice of buffer and to optimize the concentrations of rHSA to be used in the analysis.

B.2 Experimental protocol

B.2.1 Buffer optimization

Four buffers used in the literature for CD analysis of albumin were tested here to look for minimal signal disruption of the polarized light and for its ability to maintain secondary structure of albumin. The buffers tested were "10 mM Phosphate" (10 mM sodium phosphate (Sigma-Aldrich), pH 7) [114], "25 mM Phosphate" (25 mM sodium phosphate, 150 mM NaCl (Sigma-Aldrich), pH 7.4) [99], "5 mM Phosphate" (5 mM sodium phosphate, pH 7.4) [142], and "100 mM Tris" (100 mM Tris-HCl (Bio-Rad), 100 mM NaCl, pH 7.4) [143]. Buffers were prepared the same day and 2 g/L rHSA (Cellastim, Invitria) was dissolved in each buffer and incubated on ice prior to CD analysis. CD spectra were obtained on a Jasco J-715 CD spectrometer with the accompanying Spectra Manager software. Scans were done at room temperature in quartz SUPRASIL cuvettes (Hellma Analytics, Mullheim, Germany) with 0.1 cm path length for the far UV region (260 nm – 170 nm). Samples containing albumin were diluted with the appropriate buffer immediately before loading into the cuvette to a concentration of 0.5 g/L for scans [132]. The response time used was 0.125 s with a data pitch of 0.5 nm and a scan speed of 100 nm/min. A total of 10 accumulations were acquired for each run and cuvettes were rinsed thoroughly with DI water between runs. Buffer background scans (without albumin) were obtained to establish the baseline. All scans were smoothed using the Spectra Manager software "Means-Movement" method and the baseline spectra were subtracted from the albumin spectra. Molar ellipticity was calculated as described in Chapter 3. Data was visualized by plotting the calculated molar ellipticity against the wavelength using R [107–113].

B.2.2 Concentration of rHSA optimization in the far UV region

The optimal concentration of rHSA for far UV CD spectroscopic analysis was determined. A 2 g/L rHSA sample in 10 mM Phosphate buffer (pH 7) was prepared the same day and incubated on ice prior to dilution and/or analysis. The sample was diluted using 10 mM Phosphate buffer to the following concentrations: 2 g/L (undiluted), 1 g/L, 0.5 g/L, 0.25 g/L, 0.1 g/L, and 0.05 g/L and analysis was done as mentioned above. Secondary structure composition was determined using DichroWeb software with the K2D method [144,145].

B.3 Results and conclusions

B.3.1 Buffer optimization

An appropriate buffer for rHSA analysis using CD spectrometry will have minimal absorbance of the circularly polarized while also stabilizing the structure of the protein. Here, four buffers previously reported in literature for CD analysis of albumin were tested and the results are presented in Figure B.1. The high-tension voltage represents the amount of voltage applied to the sample to gain a signal. With samples that absorb a lot of light, especially at wavelengths below 200 nm, the voltage must be increased but once the value plateaus, the CD signal is no longer reliable in this region. The buffers that contained sodium chloride (25 mM Phosphate and 100 mM Tris) saw a high-tension voltage plateau at higher wavelengths than the buffers without (10 mM Phosphate and 5 mM Phosphate). This would imply that the buffers with sodium chloride absorb more light than those without in that region. This would also cause the reduction in negative CD signal at 208 nm seen with the sodium chloride-containing buffers. The buffers without sodium chloride produced similar CD spectra for rHSA. The 10 mM Phosphate buffer was chosen over the 5 mM Phosphate buffer for further experiments since the increased buffer concentration would allow for increased buffering capacity.

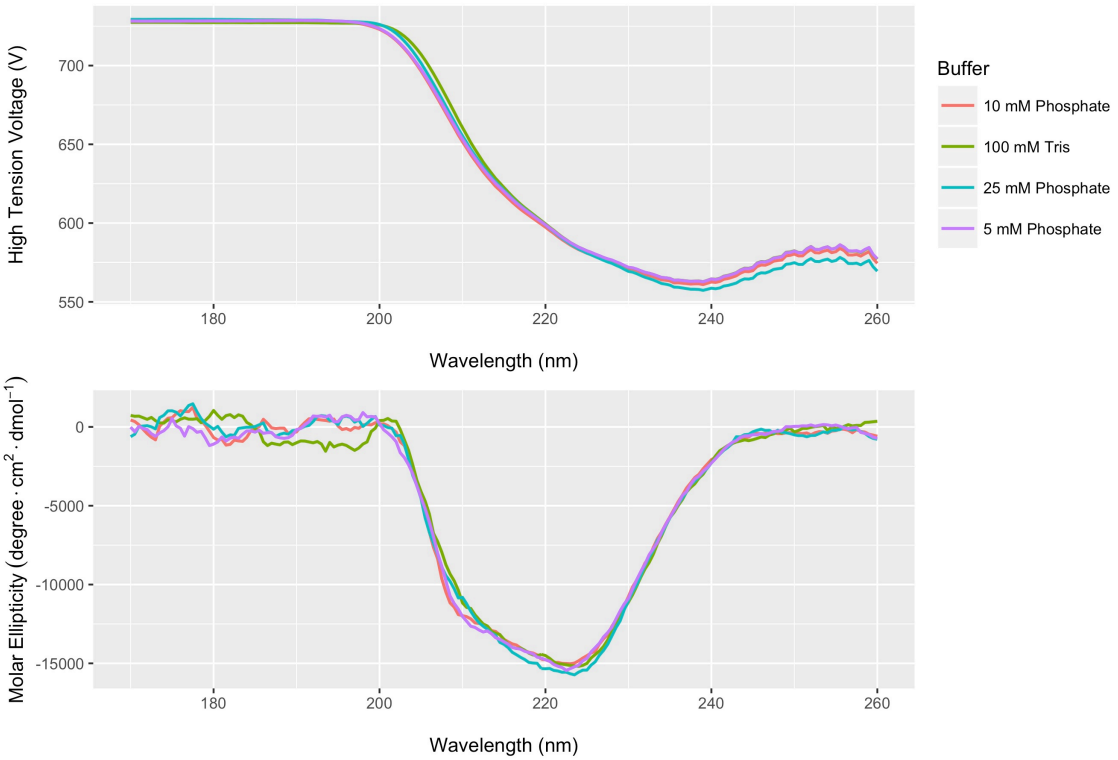

Figure B.1 Buffer optimization for CD spectrometry analysis of rHSA

The high-tension voltage readings (top plot) and calculated molar ellipticities (bottom plot) of CD scans in the far UV region for 0.5 g/L rHSA in different buffers.

B.3.2 Far UV region rHSA concentration optimization

The secondary structure of rHSA is known to be composed predominantly of alpha helices and a CD spectrum reflecting this is ideal. Alpha helical structure causes strong negative peaks at 222 nm and 208 nm, and a strong positive peak at 195 nm. In order to determine the optimal concentration of rHSA to use for analysis, solutions containing 2 g/L, 1 g/L, 0.5 g/L, 0.25 g/L, 0.1 g/L, and 0.05 g/L rHSA in 10 mM Phosphate buffer were analyzed in the far UV region (170 nm-260 nm) using CD spectrometry and the results are presented in Figure B.2. From the high-tension voltage values, it is evident that the higher concentrations of rHSA absorb more light at lower wavelengths and cause the voltage output to plateau at wavelengths ideal for secondary structure analysis. Though the higher concentration of rHSA results in stronger CD signals, the plateau in the high-tension voltage reduces the information that can be gained from the spectra. The negative peak at 208 nm is only observed at concentrations of 0.5 g/L and below, and the expected positive peak at 195 nm is only observed at concentrations of 0.25 g/L and below. After normalizing the spectra for protein concentration, it is evident that the signals from the 0.1 g/L and 0.05 g/L rHSA samples were similar, with the exception of the reduction in peak height at 195 nm for the former. The secondary structure composition was estimated using DichroWeb software with the K2D method (Table B.1) and the plots generated by the software showing the fit are displayed in Figure B.3. The software estimation for the alpha helical content of 0.1 g/L and 0.05 g/L rHSA (60% and 63%, respectively) fit best and was closest to literature values for Cellastim (66.7%-64.7%) [142]. For further experiments in the far UV region, a concentration of 0.1 g/L rHSA was chosen as it has the optimal signal quality.

Table B.1 Secondary structure predictions of rHSA based on CD Spectra at various rHSA concentrations using the K2D method on DichroWeb.

[rHSA]	% Alpha Helix	% Beta Sheet	% Random Coil
2 g/L	5	47	48
1 g/L	32	12	55
0.5 g/L	45	23	31
0.25 g/L	59	7	33
0.1 g/L	60	7	32
0.05 g/L	63	6	31

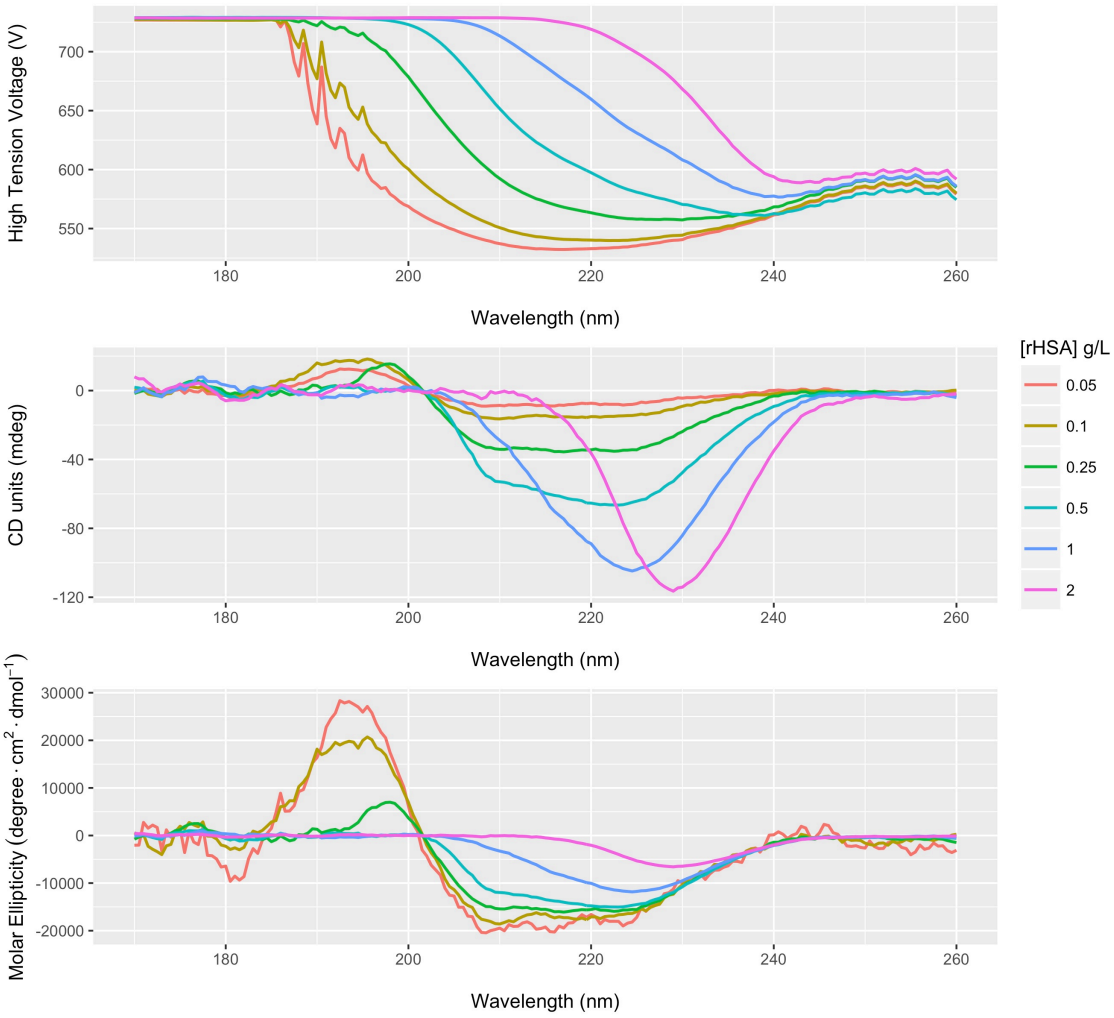

Figure B.2 Optimization of rHSA concentration for far UV CD spectroscopic analysis

The high-tension voltage readings (top plot), smoothed CD values in mdeg (middle plot), and calculated molar ellipticities (bottom plot) for CD scans performed in the far UV region of various concentrations of rHSA in 10 mM Phosphate buffer.

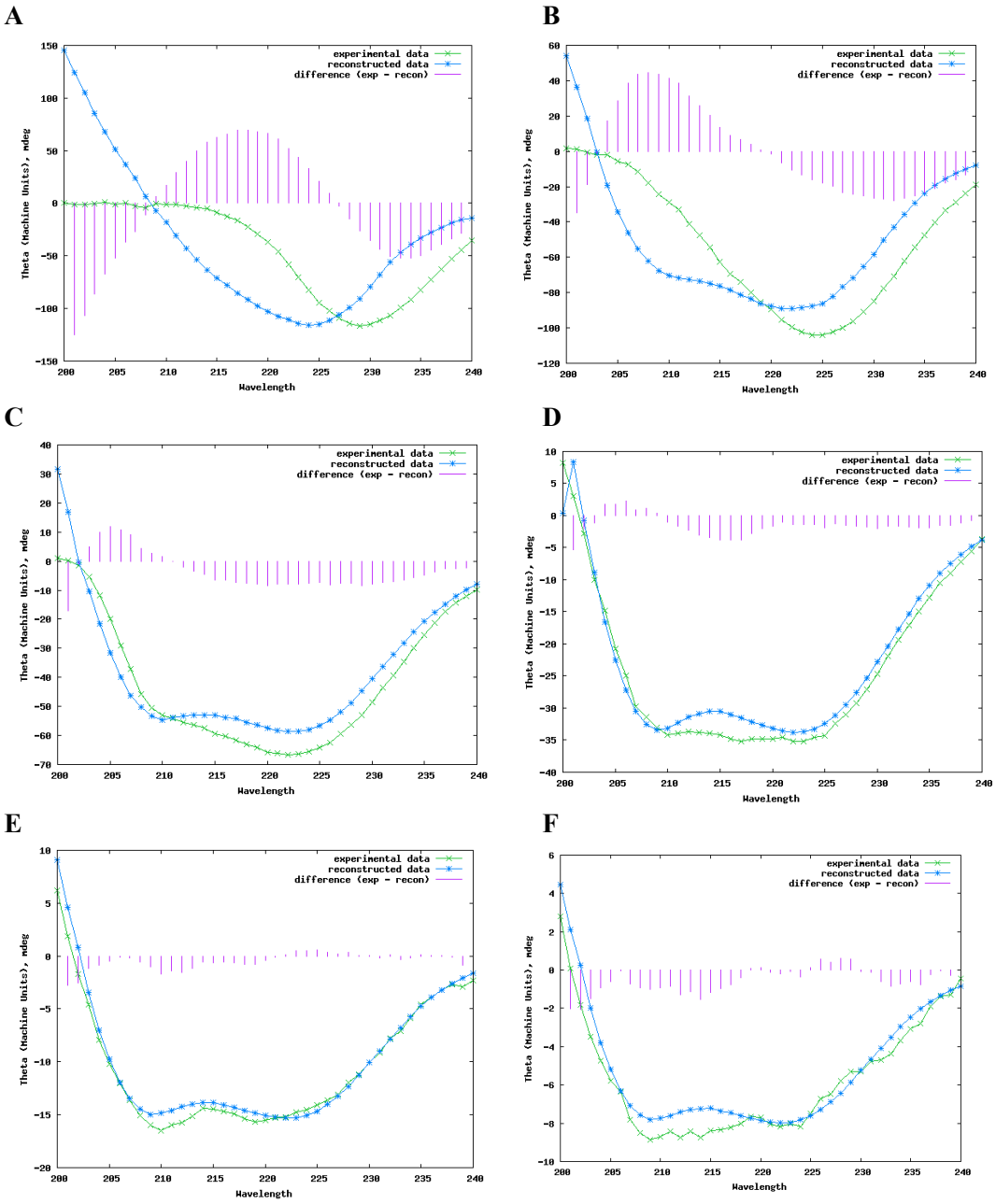

Figure B.3 Fitting CD spectra of various concentrations of rHSA to estimate secondary structure.

DichroWeb's K2D method was used to estimate the secondary structure of rHSA using CD spectra of rHSA at different concentrations. The plots were generated on DichroWeb and show the goodness of fit for rHSA at a concentration of 2 g/L (**A**), 1 g/L (**B**), 0.5 g/L (**C**), 0.25 g/L (**D**), 0.1 g/L (**E**), and 0.05 g/L (**F**).

Appendix C

Analyzing protein content of ACAM529

Various dilutions of Lot A and Lot C were run on SDS-PAGE as described in Chapter 3 to analyse the protein content (Figure C.1). Table C.1 summarizes the size and molar abundance of viral proteins expected to be present in extracellular HSV-1 particles [31].

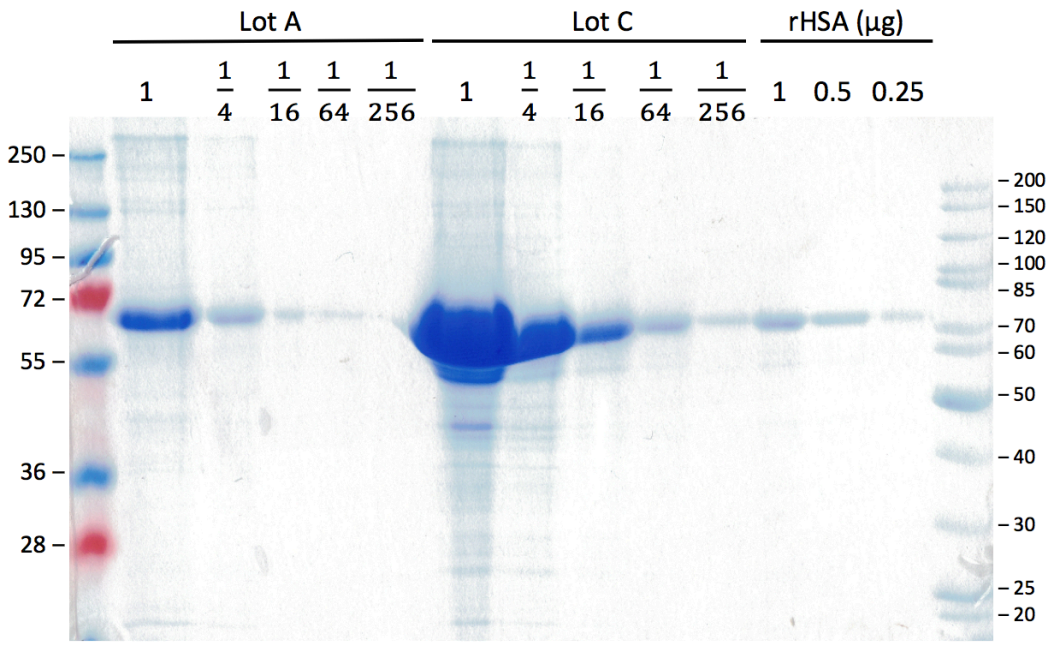

Figure C.1 SDS-PAGE analysis of ACAM529 Lot A and Lot C.

Dilutions of Lot A and Lot B (indicated above each lane) were run on SDS-PAGE, with rHSA used as a protein concentration standard. PageRuler Prestained (first lane) and Unstained (last lane) Protein Ladder were used and protein sizes are indicated (kDa).

Table C.1 Composition of extracellular HSV-1 virion particles [31].

Gene/Protein	Location	Size (amino acids)	Estimated Molecular Weight	Molar Abundance
UL36/Large tegument	Tegument	3164	335.9	5-10%
UL19/VP5 or ICP5	Capsid	1374	149.1	>10%
RS1/ICP4	Tegument	1298	132.8	1-4%
UL37/ICP32	Tegument	1123	120.6	1-4%
UL27/gB	Envelope	904	100.3	5-10%
UL22/gH	Envelope	838	90.4	1-4%
RL2/ICP0	Tegument	776	78.5	1-4%
UL46/VP11/12	Tegument	718	78.2	1-4%
UL17	Capsid	703	74.6	1-4%
UL6	Capsid	676	74.1	<1%
UL47/VP13/14	Tegument	693	73.8	>10%
UL25	Capsid	580	62.7	1-4%
US8/gE	Envelope	550	59.1	1-4%
UL21	Tegument	535	57.6	1-4%
UL13	Tegument	518	57.2	<1%
UL44/gC	Envelope	511	55	1-4%
UL41/vhs	Tegument	489	54.9	1-4%
UL48/VP16/ICP25	Tegument	490	54.3	1-4%
US3	Tegument	481	52.8	<1%
UL10/gM	Envelope	473	51.4	<1%
UL38/VP19C	Capsid	465	50.3	<1%
US6/gD	Envelope	394	43.3	1-4%
US7/gI	Envelope	390	41.4	<1%
UL23/TK	Tegument	376	41	<1%
UL16	Tegument	373	40.4	<1%
UL50/dUTPase	Tegument	371	39.1	1-4%

UL18/VP23	Capsid	318	34.3	5-10%
US10	Tegument	312	34.1	<1%
UL7	Tegument	296	33.1	<1%
US2	Tegument	291	32.5	<1%
UL49/VP22	Tegument	301	32.3	5-10%
UL26/VP24	Capsid	247	26.6	1-4%
RL1/ICP34.5	Tegument	248	26.2	<1%
UL51	Tegument	244	25.5	<1%
US4/gG	Envelope	238	25.2	<1%
UL1/gL	Envelope	224	24.9	<1%
UL20 (+)	Envelope	222	24.2	<1%
UL14	Tegument	219	23.9	<1%
UL56	Envelope	197	21.2	<1%
UL55	Tegument	186	20.5	<1%
UL45	Envelope	172	18.2	1-4%
UL35/VP26	Capsid	112	12.1	1-4%
UL11	Tegument	96	10.5	<1%
US9	Envelope	90	10	<1%

Appendix D

Comparing the stability of different lots of ACAM529 at various temperatures

See section 4.2.3. The data in Figure D.1 below are duplicates of the data found in Figure 4.3, with the exception of the data for ACAM529 Lot B in Figure D.1A and D.1B, which were not presented in Figure 4.3. Here, the data was arranged to better show how the stability of each lot of ACAM529 compared to one another at various temperatures.

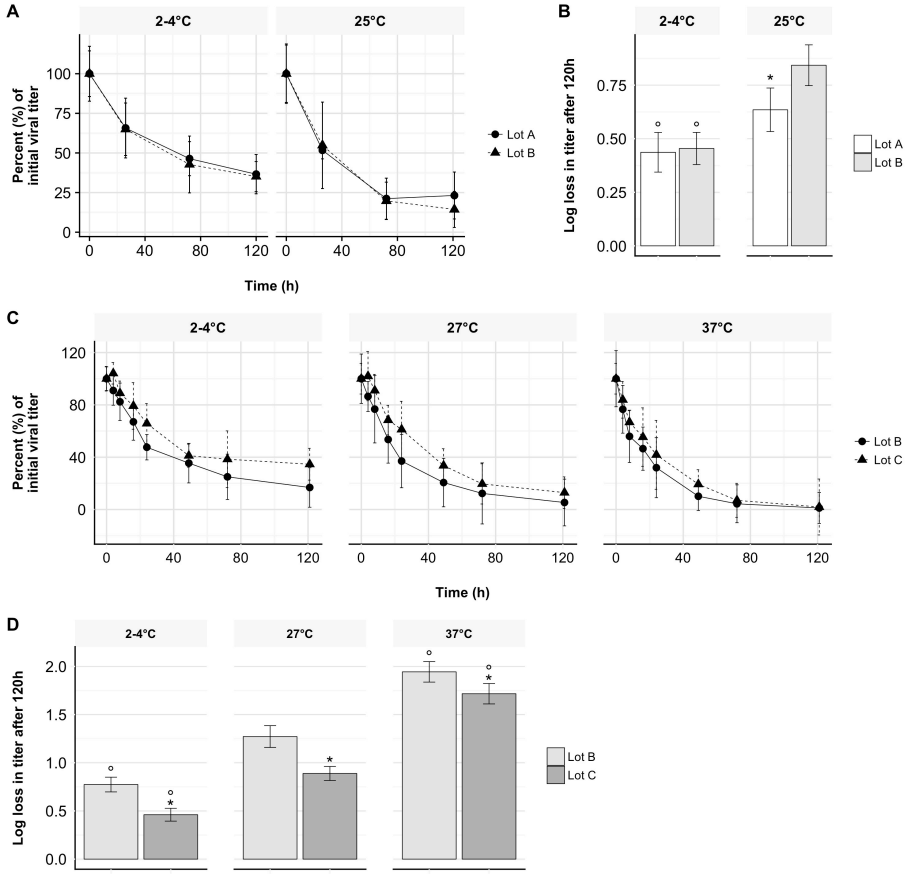

Figure D.1 Stability of different lots of ACAM529 at various temperatures.

Lot A and Lot B were diluted into the reference buffer and incubated at 2-4°C or 25°C. Viral stability (**A**) and the total log loss in titer was determined (**B**). In a second experiment, Lot B and Lot C were diluted into the reference buffer and incubated at 2-4°C, 27°C or 37°C. Viral stability (**C**) and the total log loss in titer was determined (**D**). A significant deviation ($\alpha = 0.05$) from Lot B at the same temperature is noted with *, and a significant deviation from the log loss at 25°C or 27°C is noted with o.

Appendix E

Characterized FBS of Canadian origin

Table E.1 reproduces the certificate of analysis and biochemical analysis performed by HyClone on characterized FBS of Canadian origin (www.gelifesciences.com/en/us/support/quality/certificates, Catalogue: SH30396, Lot: AAF204951). To confirm the levels of albumin in the FBS, SDS-PAGE was performed as described in Chapter 3 (Figure E.1). The albumin content in FBS as determined through SDS-PAGE indeed agreed with HyClone's certificate of analysis, which reports an albumin concentration of 19 g/L.

Table E.1 Certificate of analysis and biochemical assays for FBS

Test	**Lot Value**	**Unit**
Endotoxin	<0.125	EU/ml
Hemoglobin	3	mg/dL
Proteins/Other		
Albumin	1.9	g/dL
Alkaline Phosphatase	283	U/L
Blood Urea Nitrogen	13	mg/dL
Creatinine	2.94	mg/dL
Gamma Globulin	2.8	% tp
Glucose	84	mg/dL
Glutamix Oxaloacetic Transaminase	17	U/L
Glutamic Pyruvic Transaminase	8	U/L
IgG – Nephelometer	0.104	mg/mL
Lactate Dehydrogenase	582	U/L
Osmolality	271	mOsm/kg
pH	7.10	
Total Bilirubin	0.1	mg/dL
Total Protein	3.8	g/dL
Trace Metals/Iron		
Calcium	14.6	mg/dL
Chloride	104	mmol/L
Inorganic Phosphorus	10.7	mg/dL
Iron	155	µg/dL
Percent Saturation (Iron)	57	%
Potassium	>10.0	mmol/L
Sodium	143	mmol/L
Total Iron Binding Capacity	272	µg/dL

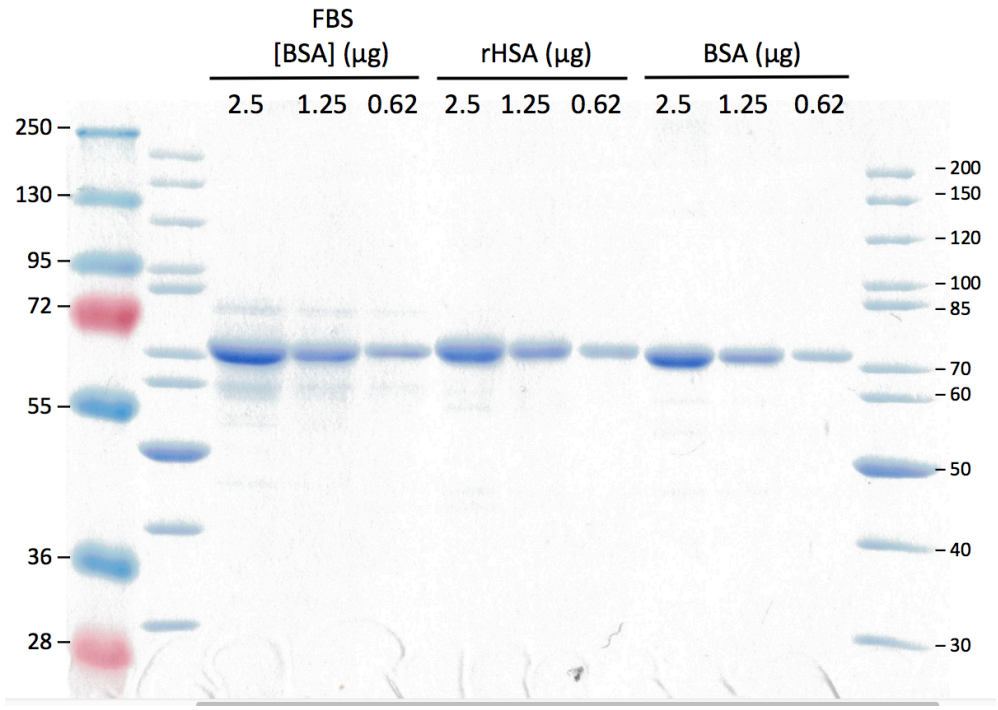

Figure E.1 SDS-PAGE analysis of the albumin content in FBS.

Dilutions of FBS lot AAF204951 were run on SDS-PAGE and the gel is labelled with the expected concentrations of BSA (~66 kDa) in each dilution of FBS (calculated using values reported in the certificate of analysis). The reference standards used were rHSA and BSA. PageRuler Prestained (first lane) and Unstained (second and last lanes) Protein Ladder were used and protein sizes are indicated (kDa).

Appendix F

Supplementary data from model fitting in R

F.1 Modelling ACAM529 stability in the reference buffer with or without FBS:

F.1.1 Summary of parameter estimates

Table F.1 Estimates for V_0 in the first order decay model: $V(t) = V_o\, e^{(-kt)}$

Buffer	V_0	Standard error	t value	Pr (>|t|)
Reference buffer	1.70×10^5	5.73×10^3	29.73	0.00113**
+ 0.01% FBS	1.81×10^5	6.71×10^3	26.985	0.00137**
+ 0.1% FBS	2.03×10^5	0.958×10^3	212.01	2.22×10^{-5} ***
+ 1% FBS	2.05×10^5	5.01×10^3	40.86	0.000599***
+ 10% FBS	1.98×10^5	7.66×10^3	25.921	0.00148**
+ 50% FBS	1.94×10^5	15.4×10^4	12.608	0.00623**

Significance codes: 0 '***' 0.001 '**' 0.01 '*' 0.05 '.' 0.1 ' ' 1

Table F.2 Estimates for k in the first order decay model: $V(t) = V_o\, e^{(-kt)}$

Buffer	k	Standard error	t value	Pr (>|t|)
Reference buffer	12.7×10^{-3}	1.04×10^{-3}	12.19	0.00667**
+ 0.01% FBS	8.97×10^{-3}	8.99×10^{-4}	9.986	0.00988**
+ 0.1% FBS	5.68×10^{-3}	9.22×10^{-5}	61.65	0.000263***
+ 1% FBS	4.30×10^{-3}	4.38×10^{-4}	9.81	0.010232*
+ 10% FBS	5.25×10^{-3}	7.33×10^{-4}	7.154	0.01899*
+ 50% FBS	9.64×10^{-3}	2.01×10^{-3}	4.795	0.04085*

Significance codes: 0 '***' 0.001 '**' 0.01 '*' 0.05 '.' 0.1 ' ' 1

Table F.3 Parameter estimates for the zero order decay model: $V(t) = V_o - kt$

Buffer	V_0	k	R^2	Adjusted R^2
Reference buffer	1.58×10^5	1048.0	0.9203	0.8804
+ 0.01% FBS	1.73×10^5	963.1	0.946	0.919
+ 0.1% FBS	2.00×10^5	834.04	0.9948	0.9922
+ 1% FBS	2.03×10^5	698.08	0.996	0.994
+ 10% FBS	1.97×10^5	791.93	0.9914	0.987
+ 50% FBS	1.89×10^5	1160.7	0.9778	0.9667

F.1.2 Complete R code and modelling outputs

```
> library(tidyr)
> library(grid)
> library(gridExtra)
> library(scales)
> library(gtable)
> library(cowplot)
>
> # Loading data-----
> data<- read.csv('compiledstudies.csv', header=TRUE)
>
> #Axis scales----
> fancy_scientific <- function(l) {
+   # turn in to character string in scientific notation
+   l <- format(l, scientific = TRUE)
+   # quote the part before the exponent to keep all the digits
+   l <- gsub("^(.*)e", "'\\1'e", l)
+   # remove + after exponent, if exists. E.g.: (3x10^+2 -> 3x10^2)
+   l <- gsub("e\\+","e",l)
+   # convert 1x10^ or 1.000x10^ -> 10^
+   l <- gsub("\\'1[\\.0]*\\'\\%\\*\\%", "", l)
+   # turn the 'e+' into plotmath format
+   l <- gsub("e", "%*%10^", l)
+   # return this as an expression
+   parse(text=l)
+ }
> #Study8 ([FBS])-------------------------------------------------------
> #Plaque count range setting
> plq8<-data[data$EXP==8 & data$PlaqueCount>19 & data$PlaqueCount < 235,]
>
> #get averages
> grouped8<- plq8%>%
+   group_by(Time, Name) %>%
+   mutate(avg8=mean(PFUperml), stdev8=sd(PFUperml))
>
> #calculate percentages
> final8 <- filter(grouped8, Replicate==1, SampleDilutionN==2)
>
> #Calculating Log losses in titer
> #Calculate  Logarithms 0h-121h
> groupedlog8<- final8%>%
+   group_by(Time, Name) %>%
+   mutate(avglog8=log10(avg8), stdevlog8=(log10(avg8+stdev8)-log10(avg8-
stdev8))/2)
>
> #Calculate Differences
> finallog8 <- groupedlog8 %>%
+   group_by(Name) %>%
+   mutate(logdiff8= (-1)*(avglog8-log10(avg8[Time==0])),
+
logdiffstdev8=sqrt((1/avg8/log(10))^2*stdev8^2+(1/avg8[Time==0]/log(10))^2
*stdev8[Time==0]^2))
>
```

```
> study8logdiff <- filter(finallog8, Time>110)

> #Chapter 5 Plots (5.3-4) [FBS] (Study 8)-----------------------------
>
> plotJ <- final8
>
> plotlogJ <- study8logdiff
>
> #PFU vs. Time
> J1<-ggplot(plotJ, aes(x=Time, y=avg8, linetype=factor(Buffer)))+
+   labs(x="\nTime (h)", y="Viral titer (PFU/ml)\n")+
+   geom_line(aes(y=avg8), size=0.25)+
+   geom_point(aes(Time, avg8, shape=factor(Buffer)), size=2.5)+
+   scale_y_continuous(labels=function(n){format(n, scientific = TRUE)})+
+   scale_y_continuous(labels=fancy_scientific)+
+   scale_linetype_discrete(breaks=c("Sanofi Buffer", "Sanofi Buffer FBS
50%", "Sanofi Buffer FBS 10%", "Sanofi Buffer FBS 1%", "Sanofi Buffer FBS
0.1%", "Sanofi Buffer FBS 0.01%"),
+                           labels=c("Reference Buffer", "+50% FBS", "+10%
FBS", "+1% FBS", "+0.1% FBS", "+0.01% FBS"),
+                           name="Buffer")+
+   scale_shape_discrete(breaks=c("Sanofi Buffer", "Sanofi Buffer FBS
50%", "Sanofi Buffer FBS 10%", "Sanofi Buffer FBS 1%", "Sanofi Buffer FBS
0.1%", "Sanofi Buffer FBS 0.01%"),
+                        labels=c("Reference Buffer", "+50% FBS", "+10%
FBS", "+1% FBS", "+0.1% FBS", "+0.01% FBS"),
+                        name="Buffer")+
+   theme(text=element_text(size=11),
legend.title=element_text(face="bold"), axis.text.x=element_text(size=11),
+         axis.title=element_text(face="bold"),
strip.text=element_text(face="bold"),
axis.ticks=element_line(color="gray97"),
+         strip.background=element_rect(fill="gray97"),
panel.background=element_rect(fill="white"),panel.margin.x=unit(0.3,
"in"),
+         panel.grid.major=element_line(colour="gray90"),
panel.grid.minor=element_line(colour="gray97")) +
+   geom_errorbar(aes(ymin = avg8-stdev8, ymax = avg8+stdev8), width=2,
size=0.25)
Scale for 'y' is already present. Adding another scale for 'y', which will
replace the existing scale.
Warning messages:
1: `panel.margin` is deprecated. Please use `panel.spacing` property
instead
2: `panel.margin.x` is deprecated. Please use `panel.spacing.x` property
instead
> ggsave("//Users//juliamanalil//Dropbox/Aucoin
Lab//Thesis//Figures//v3//5.3A.jpg", plot=J1, dpi=300, width=6,
height=3.5)
>
> #log loss in titer after 120h
> J2<-ggplot(plotlogJ, aes(factor(Buffer), logdiff8)) +
+   labs(x="Buffer",y="Log loss in titer after 120h\n") +
+   geom_bar(stat="identity", colour="black", fill="gray97", size=0.25) +
```

```
+   annotate("text", x=c(2,3,4,5), y=c(0.53, 0.41, 0.33, 0.39),
label=c("*", "*", "*", "*"), size=5)+
+   scale_x_discrete(breaks=c("Sanofi Buffer", "Sanofi Buffer FBS 50%",
"Sanofi Buffer FBS 10%", "Sanofi Buffer FBS 1%", "Sanofi Buffer FBS 0.1%",
"Sanofi Buffer FBS 0.01%"),
+                    labels=c("Reference Buffer", "+50% FBS", "+10% FBS",
"+1% FBS", "+0.1% FBS", "+0.01% FBS"))+
+   theme(text=element_text(size=11),
legend.title=element_text(face="bold"), axis.text.x=element_text(angle=30,
hjust=1, size=11, colour="black"),
+         axis.title=element_text(face="bold"),
strip.text=element_text(face="bold"),
axis.ticks=element_line(color="gray97"),
+         strip.background=element_rect(fill="gray97"),
panel.background=element_rect(fill="white"),panel.margin.x=unit(0.3,
"in"),
+         panel.grid.major.y=element_line(colour="gray90"),
panel.grid.minor.y=element_line(colour="gray97")) +
+   geom_errorbar(aes(ymin = logdiff8-logdiffstdev8, ymax =
logdiff8+logdiffstdev8), width = 0.2, size=0.25)
Warning messages:
1: `panel.margin` is deprecated. Please use `panel.spacing` property
instead
2: `panel.margin.x` is deprecated. Please use `panel.spacing.x` property
instead
> ggsave("//Users//juliamanalil//Dropbox/Aucoin
Lab//Thesis//Figures//v3//5.3B.jpg", plot=J2, dpi=300, width=3,
height=3.5)
>
> JFinB<-plot_grid(J2, NULL, nrow=1)
> JFin<-plot_grid(J1, JFinB, nrow=2, labels=c('A', 'B'), rel_heights =
c(5,6))
> ggsave("//Users//juliamanalil//Dropbox/Aucoin
Lab//Thesis//Figures//v3//5.3.jpg", plot=JFin, dpi=300, width=7, height=8)
>
> #Modelling
> SBS507278<-filter(final8, Name=="8S50SB7.27")
> SBS107278<-filter(final8, Name=="8S10SB7.27")
> SBS17278<-filter(final8, Name=="8S1SB7.27")
> SBS0.17278<-filter(final8, Name=="8S0.1SB7.27")
> SBS0.017278<-filter(final8, Name=="8S0.01SB7.27")
> SB7278<-filter(final8, Name=="8SB7.27")
>
> #add xlabs, fix theme
> xlabs8<-c('Sanofi Buffer'="Reference Buffer",
+           'Sanofi Buffer FBS 50%'="+ 50% FBS",
+           'Sanofi Buffer FBS 10%'="+ 10% FBSA",
+           'Sanofi Buffer FBS 1%'="+ 1% FBS",
+          'Sanofi Buffer FBS 0.1%'="+ 0.1% FBS",
+          'Sanofi Buffer FBS 0.01%'="+ 0.01% FBS")
> J3<-ggplot(final8, aes(x=Time, y=avg8))+
+   labs(x="\nTime (h)", y="Viral titer (PFU/ml)\n")+
+   geom_point(aes(Time, avg8), size=0.25)+
+   facet_wrap(~Buffer, ncol=2,labeller=as_labeller(xlabs8))+
+   scale_y_continuous(labels=function(n){format(n, scientific = TRUE)})+
```

```
+   scale_y_continuous(labels=fancy_scientific)+
+   theme(text=element_text(size=16),
legend.title=element_text(face="bold"),
axis.text.x=element_text(colour="black", size=16),
+         axis.title=element_text(face="bold"),
strip.text=element_text(face="bold"),
axis.ticks=element_line(color="gray97"),
+         strip.background=element_rect(fill="gray97"),
panel.background=element_rect(fill="white"),panel.margin.x=unit(0.3,
"in"),
+         panel.grid.major=element_line(colour="gray90"),
panel.grid.minor=element_line(colour="gray97")) +
+   geom_errorbar(aes(ymin = avg8-stdev8, ymax = avg8+stdev8), width = 2,
size=0.25, position="dodge")+
+   scale_linetype_discrete(name="Model")+
+   geom_smooth(method="nls", aes(linetype = 'Exponential'),
#color="black",
+               formula='y~e*exp(-f*x)',
+               method.args=list(start=c(e=2e7, f=0)), size=0.5,
se=FALSE)+ #
+   geom_smooth(method="lm", aes(linetype = 'Linear'),size=0.5,
#color="black",
+               formula='y~x')
Scale for 'y' is already present. Adding another scale for 'y', which will
replace the existing scale.
Warning messages:
1: `panel.margin` is deprecated. Please use `panel.spacing` property
instead
2: `panel.margin.x` is deprecated. Please use `panel.spacing.x` property
instead
> ggsave("//Users//juliamanalil//Dropbox/Aucoin
Lab//Thesis//Figures//v3//5.4.jpg", plot=J3, dpi=300, width=11, height=8)
>
> #SB7
> y=SB7278$avg8
> x=SB7278$Time
> mSB7278<-nls(y~(e*exp(-f*x)), data = SB7278, start = list(e=2e7, f = 0))
Warning messages:
1: In min(x) : no non-missing arguments to min; returning Inf
2: In max(x) : no non-missing arguments to max; returning -Inf
> summary(mSB7278)

Formula: y ~ (e * exp(-f * x))

Parameters:
   Estimate Std. Error t value Pr(>|t|)
e 1.704e+05  5.730e+03   29.73  0.00113 **
f 1.271e-02  1.043e-03   12.19  0.00667 **
---
Signif. codes:  0 ‘***’ 0.001 ‘**’ 0.01 ‘*’ 0.05 ‘.’ 0.1 ‘ ’ 1

Residual standard error: 6406 on 2 degrees of freedom

Number of iterations to convergence: 8
Achieved convergence tolerance: 8.555e-07
```

```
>
> y=SB7278$avg8
> x=SB7278$Time
> lSB7278<-lm(y~x, data = SB7278)
> summary(lSB7278)

Call:
lm(formula = y ~ x, data = SB7278)

Residuals:
     1      2      3      4
 16054 -11584 -16712  12242

Coefficients:
            Estimate Std. Error t value Pr(>|t|)
(Intercept) 157570.7    15577.7  10.115  0.00963 **
x            -1048.0      218.1  -4.805  0.04069 *
---
Signif. codes:  0 ‘***’ 0.001 ‘**’ 0.01 ‘*’ 0.05 ‘.’ 0.1 ‘ ’ 1

Residual standard error: 20260 on 2 degrees of freedom
Multiple R-squared:  0.9203,  Adjusted R-squared:  0.8804
F-statistic: 23.09 on 1 and 2 DF,  p-value: 0.04069

>
> #0.01% FBS
> y=SBS0.017278$avg8
> x=SBS0.017278$Time
> mSBS0.017278<-nls(y~(e*exp(-f*x)), data = SBS0.017278, start =
list(e=2e7, f = 0))
Warning messages:
1: In min(x) : no non-missing arguments to min; returning Inf
2: In max(x) : no non-missing arguments to max; returning -Inf
> summary(mSBS0.017278)

Formula: y ~ (e * exp(-f * x))

Parameters:
   Estimate Std. Error t value Pr(>|t|)
e 1.811e+05  6.711e+03  26.985  0.00137 **
f 8.973e-03  8.986e-04   9.986  0.00988 **
---
Signif. codes:  0 ‘***’ 0.001 ‘**’ 0.01 ‘*’ 0.05 ‘.’ 0.1 ‘ ’ 1

Residual standard error: 7772 on 2 degrees of freedom

Number of iterations to convergence: 6
Achieved convergence tolerance: 5.278e-06

>
> y=SBS0.017278$avg8
> x=SBS0.017278$Time
> lSBS0.017278<-lm(y~x, data = SBS0.017278)
> summary(lSBS0.017278)
```

```
Call:
lm(formula = y ~ x, data = SBS0.017278)

Residuals:
        1         2         3         4
  7083.33    -87.11 -17319.06  10322.83

Coefficients:
            Estimate Std. Error t value Pr(>|t|)
(Intercept) 173202.4    11617.7  14.909  0.00447 **
x              -963.1      162.7  -5.921  0.02736 *
---
Signif. codes:  0 ‘***’ 0.001 ‘**’ 0.01 ‘*’ 0.05 ‘.’ 0.1 ‘ ’ 1

Residual standard error: 15110 on 2 degrees of freedom
Multiple R-squared:  0.946,   Adjusted R-squared:  0.919
F-statistic: 35.05 on 1 and 2 DF,  p-value: 0.02736

>
> #0.1% FBS
> y=SBS0.17278$avg8
> x=SBS0.17278$Time
> mSBS0.17278<-nls(y~(e*exp(-f*x)), data = SBS0.17278, start = list(e=2e7,
f = 0))
Warning messages:
1: In min(x) : no non-missing arguments to min; returning Inf
2: In max(x) : no non-missing arguments to max; returning -Inf
> summary(mSBS0.17278)

Formula: y ~ (e * exp(-f * x))

Parameters:
   Estimate Std. Error t value Pr(>|t|)
e 2.031e+05  9.579e+02  212.01 2.22e-05 ***
f 5.685e-03  9.220e-05   61.65 0.000263 ***
---
Signif. codes:  0 ‘***’ 0.001 ‘**’ 0.01 ‘*’ 0.05 ‘.’ 0.1 ‘ ’ 1

Residual standard error: 1151 on 2 degrees of freedom

Number of iterations to convergence: 5
Achieved convergence tolerance: 1.163e-06

>
> y=SBS0.17278$avg8
> x=SBS0.17278$Time
> lSBS0.17278<-lm(y~x, data = SBS0.17278)
> summary(lSBS0.17278)

Call:
lm(formula = y ~ x, data = SBS0.17278)

Residuals:
    1     2     3     4
```

```
 3024 -2014 -3481  2471

Coefficients:
             Estimate Std. Error t value Pr(>|t|)
(Intercept) 199531.26    3047.37   65.48 0.000233 ***
x             -834.04      42.67  -19.55 0.002607 **
---
Signif. codes:  0 ‘***’ 0.001 ‘**’ 0.01 ‘*’ 0.05 ‘.’ 0.1 ‘ ’ 1

Residual standard error: 3964 on 2 degrees of freedom
Multiple R-squared:  0.9948,  Adjusted R-squared:  0.9922
F-statistic:   382 on 1 and 2 DF,  p-value: 0.002607

>
> #1% FBS
> y=SBS17278$avg8
> x=SBS17278$Time
> mSBS17278<-nls(y~(e*exp(-f*x)), data = SBS17278, start = list(e=2e7, f =
0))
Warning messages:
1: In min(x) : no non-missing arguments to min; returning Inf
2: In max(x) : no non-missing arguments to max; returning -Inf
> summary(mSBS17278)

Formula: y ~ (e * exp(-f * x))

Parameters:
   Estimate Std. Error t value Pr(>|t|)
e 2.049e+05  5.014e+03   40.86 0.000599 ***
f 4.301e-03  4.384e-04    9.81 0.010232 *
---
Signif. codes:  0 ‘***’ 0.001 ‘**’ 0.01 ‘*’ 0.05 ‘.’ 0.1 ‘ ’ 1

Residual standard error: 6130 on 2 degrees of freedom

Number of iterations to convergence: 6
Achieved convergence tolerance: 2.369e-07

>
> y=SBS17278$avg8
> x=SBS17278$Time
> lSBS17278<-lm(y~x, data = SBS17278)
> summary(lSBS17278)

Call:
lm(formula = y ~ x, data = SBS17278)

Residuals:
    1     2     3     4
-2238  1516  2524 -1803

Coefficients:
             Estimate Std. Error t value Pr(>|t|)
(Intercept) 203237.77    2236.79   90.86 0.000121 ***
x             -698.08      31.32  -22.29 0.002007 **
```

```
---
Signif. codes:  0 ‘***’ 0.001 ‘**’ 0.01 ‘*’ 0.05 ‘.’ 0.1 ‘ ’ 1

Residual standard error: 2909 on 2 degrees of freedom
Multiple R-squared:  0.996,   Adjusted R-squared:  0.994
F-statistic: 496.8 on 1 and 2 DF,  p-value: 0.002007

>
> #10% FBS
> y=SBS107278$avg8
> x=SBS107278$Time
> mSBS107278<-nls(y~(e*exp(-f*x)), data = SBS107278, start = list(e=2e7, f
= 0))
Warning messages:
1: In min(x) : no non-missing arguments to min; returning Inf
2: In max(x) : no non-missing arguments to max; returning -Inf
> summary(mSBS107278)

Formula: y ~ (e * exp(-f * x))

Parameters:
   Estimate Std. Error t value Pr(>|t|)
e 1.985e+05  7.657e+03  25.921  0.00148 **
f 5.246e-03  7.333e-04   7.154  0.01899 *
---
Signif. codes:  0 ‘***’ 0.001 ‘**’ 0.01 ‘*’ 0.05 ‘.’ 0.1 ‘ ’ 1

Residual standard error: 9249 on 2 degrees of freedom

Number of iterations to convergence: 6
Achieved convergence tolerance: 1.186e-06

>
> y=SBS107278$avg8
> x=SBS107278$Time
> lSBS107278<-lm(y~x, data = SBS107278)
> summary(lSBS107278)

Call:
lm(formula = y ~ x, data = SBS107278)

Residuals:
    1     2     3     4
-4056  3283  3518 -2744

Coefficients:
             Estimate Std. Error t value Pr(>|t|)
(Intercept) 196500.92    3732.54   52.65 0.000361 ***
x             -791.93      52.26  -15.15 0.004327 **
---
Signif. codes:  0 ‘***’ 0.001 ‘**’ 0.01 ‘*’ 0.05 ‘.’ 0.1 ‘ ’ 1

Residual standard error: 4855 on 2 degrees of freedom
Multiple R-squared:  0.9914,  Adjusted R-squared:  0.987
F-statistic: 229.6 on 1 and 2 DF,  p-value: 0.004327
```

```
>
> #50% FBS
> y=SBS507278$avg8
> x=SBS507278$Time
> mSBS507278<-nls(y~(e*exp(-f*x)), data = SBS507278, start = list(e=2e7, f
= 0))
Warning messages:
1: In min(x) : no non-missing arguments to min; returning Inf
2: In max(x) : no non-missing arguments to max; returning -Inf
> summary(mSBS507278)

Formula: y ~ (e * exp(-f * x))

Parameters:
   Estimate Std. Error t value Pr(>|t|)
e 1.941e+05  1.539e+04  12.608  0.00623 **
f 9.635e-03  2.009e-03   4.795  0.04085 *
---
Signif. codes:  0 ‘***’ 0.001 ‘**’ 0.01 ‘*’ 0.05 ‘.’ 0.1 ‘ ’ 1

Residual standard error: 17710 on 2 degrees of freedom

Number of iterations to convergence: 7
Achieved convergence tolerance: 5.472e-06

>
> y=SBS507278$avg8
> x=SBS507278$Time
> lSBS507278<-lm(y~x, data = SBS507278)
> summary(lSBS507278)

Call:
lm(formula = y ~ x, data = SBS507278)

Residuals:
    1     2     3     4
-6916 12440 -7548  2024

Coefficients:
            Estimate Std. Error t value Pr(>|t|)
(Intercept) 188665.8     8827.3   21.37  0.00218 **
x            -1160.7      123.6   -9.39  0.01115 *
---
Signif. codes:  0 ‘***’ 0.001 ‘**’ 0.01 ‘*’ 0.05 ‘.’ 0.1 ‘ ’ 1

Residual standard error: 11480 on 2 degrees of freedom
Multiple R-squared:  0.9778,  Adjusted R-squared:  0.9667
F-statistic: 88.18 on 1 and 2 DF,  p-value: 0.01115
```

Appendix G

Effects of FBS and PF68: Replicate ACAM529 stability studies

The following figures show the results of replicate stability studies of ACAM529 with 10% or 1% FBS, or 0.05% or 0.1% PF68. Each figure is a separate experiment and includes run-specific details.

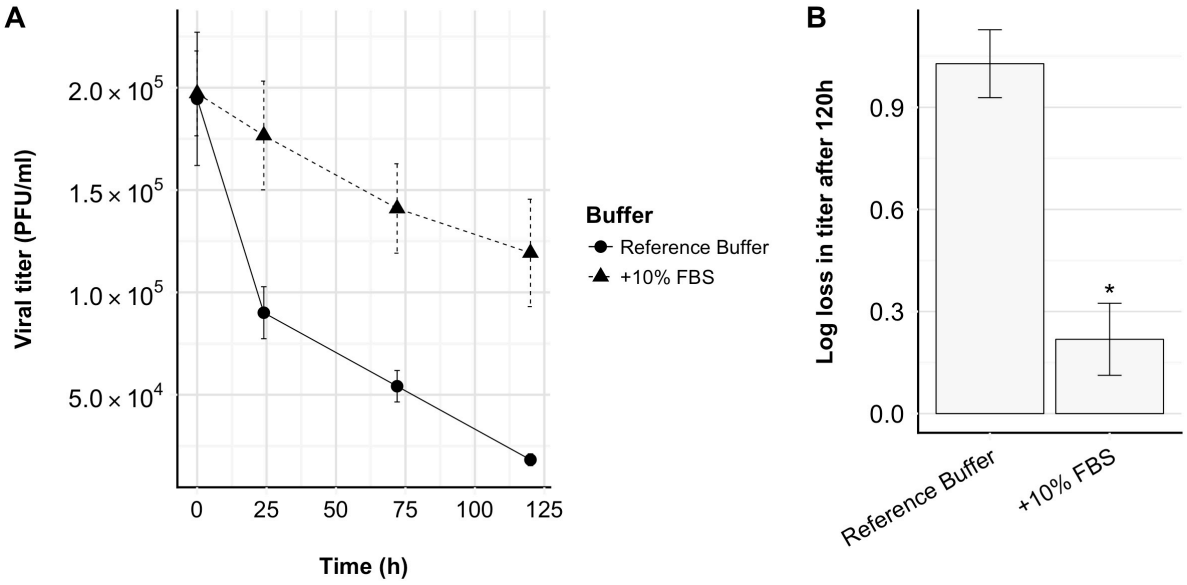

Figure G.1 Effect of 10% FBS on ACAM529 stability.

Frozen virus Lot B was quickly thawed at 37°C and diluted 1/100 in triplicate into freshly prepared reference buffer at pH 7 with or without 10% (v/v) FBS, then incubated at 27°C. Samples were taken immediately after (0 hour), 24, 72, and 120 hours after diluting the virus to monitor the viral titer using plaque assays and titers were reported as PFU/ml (**A**). The total log loss in titer (**B**) was determined and a significant deviation ($\alpha = 0.05$) from the control (reference buffer) is noted with *.

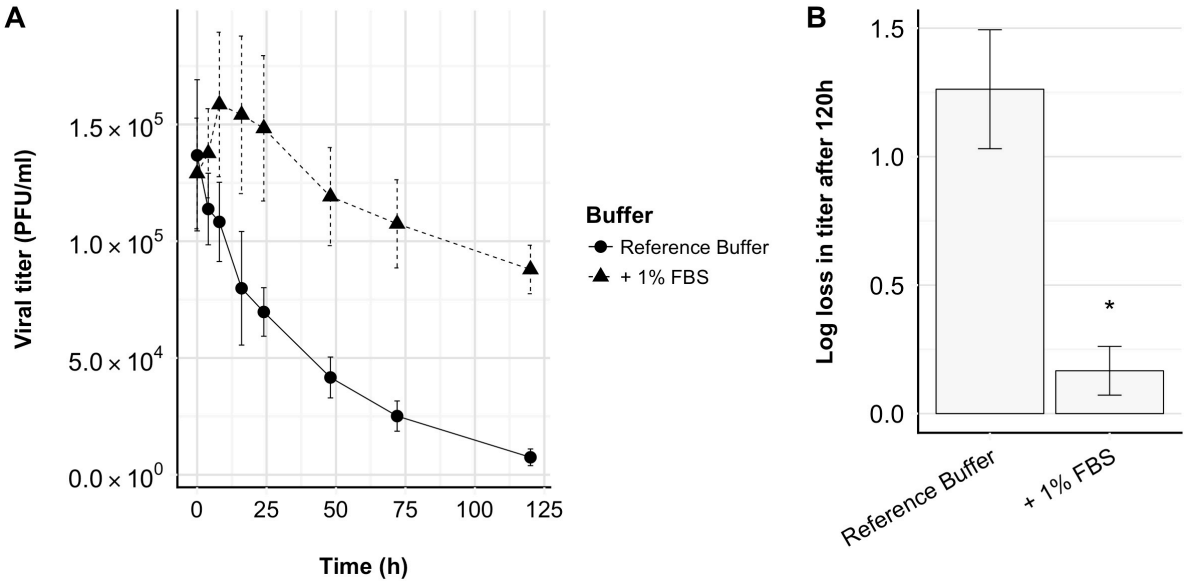

Figure G.2 Effect of 1% FBS on ACAM529 stability.

Frozen virus Lot B was quickly thawed at 37°C and diluted 1/100 in triplicate into freshly prepared reference buffer at pH 7 with or without 1% (v/v) FBS, then incubated at 27°C. Samples were taken immediately after (0 hour), 4, 8, 16, 24, 48, 72, and 120 hours after diluting the virus to monitor the viral titer using plaque assays and titers were reported as PFU/ml (**A**). The total log loss in titer (**B**) was determined and a significant deviation ($\alpha = 0.05$) from the control (reference buffer) is noted with *.

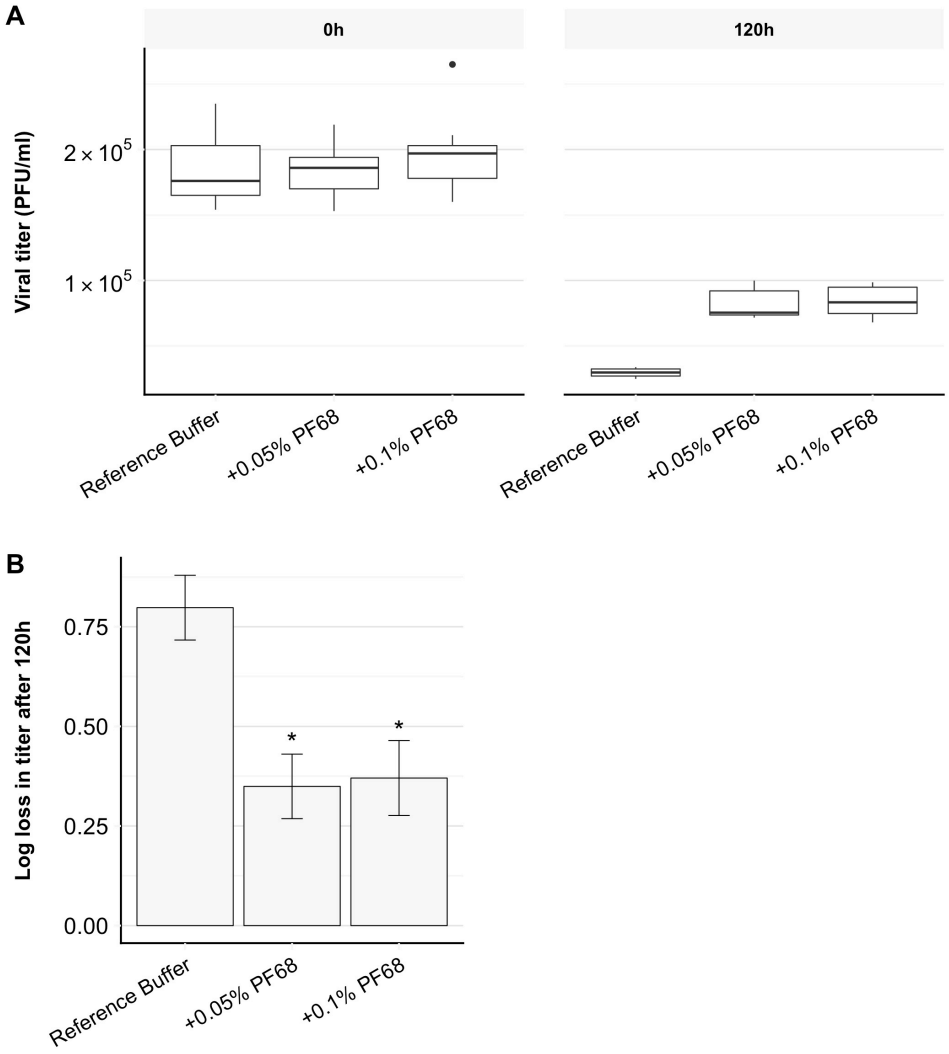

Figure G.3 Effect of 0.05% and 0.1% PF68 on ACAM529 stability: Replicate 1.

Frozen virus Lot B was quickly thawed at 37°C and diluted 1/100 in triplicate into freshly prepared reference buffer at pH 7 with or without 0.05% or 0.1% (w/v) PF68, then incubated at 27°C. Samples were taken immediately after (0 hour) and 120 hours after diluting the virus to monitor the viral titer using plaque assays and titers were reported as PFU/ml (**A**). The total log loss in titer (**B**) was determined and a significant deviation ($\alpha = 0.05$) from the control (reference buffer) is noted with *****.

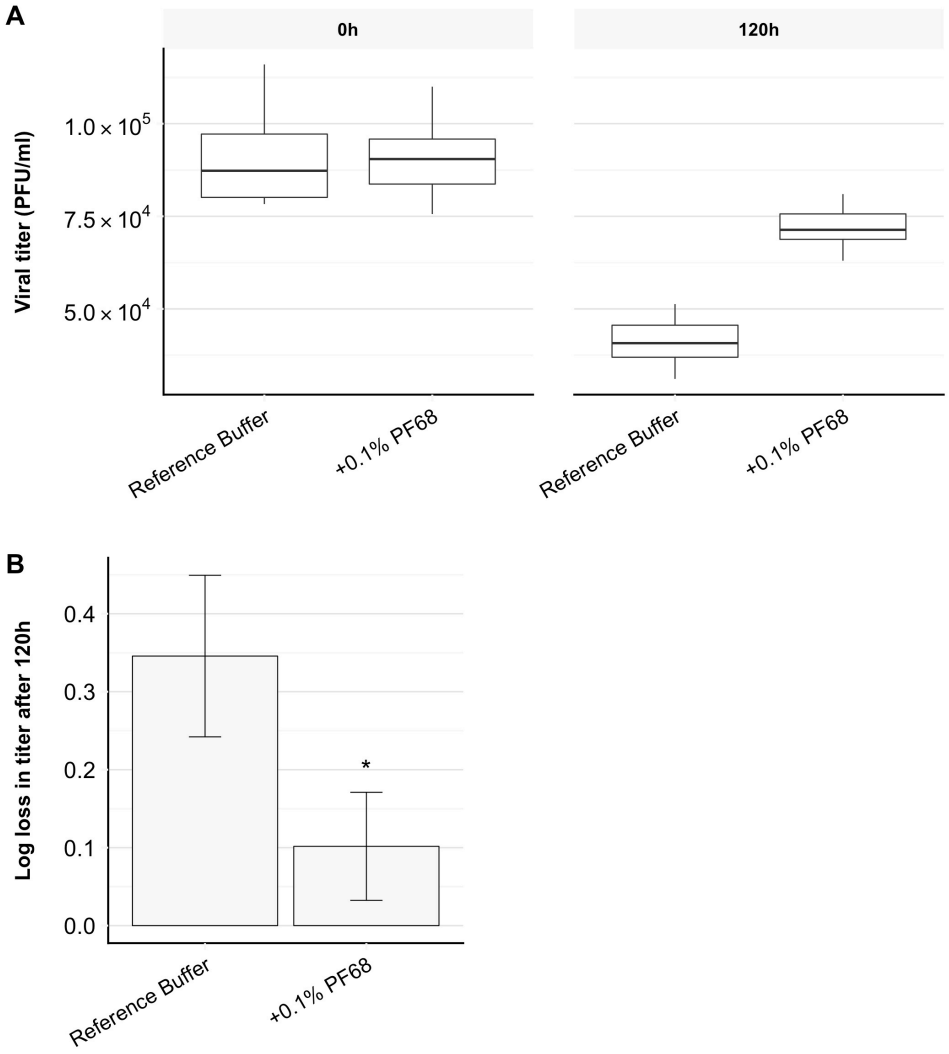

Figure G.4 Effect of 0.1% PF68 on ACAM529 stability: Replicate 2.

Frozen virus Lot B was quickly thawed at 37°C and diluted 1/100 in triplicate into freshly prepared reference buffer at pH 7 with or without 0.1% (w/v) PF68, then incubated at 27°C. Samples were taken immediately after (0 hour) and 120 hours after diluting the virus to monitor the viral titer using plaque assays and titers were reported as PFU/ml (**A**). The total log loss in titer (**B**) was determined and a significant deviation ($\alpha = 0.05$) from the control (reference buffer) is noted with *.

Appendix H
Additional ACAM529 stability studies

H.1 Povidone as an excipient

Polyvinylpyrrolidone or povidone is used commonly for pharmaceuticals for its adhesive, film-forming, dispersing, and thickening properties. It is used as a tablet binding and sugar coating agent, solubilizer, and stabilizer. It has reportedly been used to stabilize enzymes by forming a complex such as with asparaginase, beta-interferon, catalase, pyruvate carboxylase, peroxidase, and urease [146]. Povidone has also been used as a shear protectant in cell culture so it may possess desirable properties for stabilizing ACAM529. Shear protectants are employed in cell culture for the purposes of protecting membranes from harsh hydrodynamic forces, and it may be able to offer stability to the ACAM529 membrane.

H.1.1 Materials and methods

Frozen virus Lot B was quickly thawed at 37°C and diluted 1/100 in triplicate into freshly prepared reference buffer at pH 7 with or without 0.1%, 1%, and 10% (w/v) povidone (Sigma-Aldrich), then incubated at 27°C. For the stability study investigating the interaction effect between povidone and rHSA, frozen Lot A virus was quickly thawed at 37°C and diluted 1/100 in triplicate into the following freshly prepared buffers: reference buffer at pH 7; reference buffer at pH 7 with 0.1% (w/v) povidone; reference buffer at pH 7 with 0.1% (w/v) povidone and 2 g/L rHSA (Cellastim, Invitria); and reference buffer at pH 7 with 2 g/L rHSA, then incubated at 27°C. For both experiments, samples were taken immediately after (0 hour), and 120 hours after diluting the virus to monitor the viral titer using plaque assays as described previously in Chapter 3.

H.1.2 Results

To test whether povidone stabilizes ACAM529, virus Lot B was diluted in the reference buffer with the addition of 0.1%, 1% and 10% (w/v) povidone and incubated at 27°C for 120h. Initial viral titers at 0h were similar with or without povidone at all concentrations except with 10% povidone, which showed a slight decrease in titer (Figure H.1A). After 120h, increasing concentrations of povidone resulted in increasingly larger losses in viral titer, with concentrations above 0.1% leading to significantly lower viral titers compared to the control with no povidone (Figure H.1B). The addition

of 10% povidone lead to a log loss in titer three times larger than the control. The presence of 0.1% povidone did not significantly affect the initial titer or the overall log loss in titer after 120h when compared to the control with no povidone.

In order to investigate whether there was an interaction event between rHSA and povidone, ACAM529 was incubated in the reference buffer containing 2 g/L rHSA and 0.1% povidone for 120 hours at 27°C and the results are presented in Figure H.2. The log loss in titer of the virus in the buffer containing povidone and rHSA was 1.19 ± 0.10, which was not significantly different from that of the virus in the reference buffer with 2 g/L rHSA (1.13 ± 0.08). Povidone did not have any interaction effect on viral stability with rHSA but instead, the same significant reduction in stability with the addition of rHSA seen in section 5.3.2 was observed here.

H.1.3 Conclusion

Povidone did not significantly affect the infectivity or the overall stability of ACAM529 after 120h at concentrations used in cell culture (0.1%). Also, 0.1% povidone did not have any interaction effect with 2 g/L rHSA in stabilizing ACAM529. However, the presence of 1-10% povidone lead to significantly less stable virus.

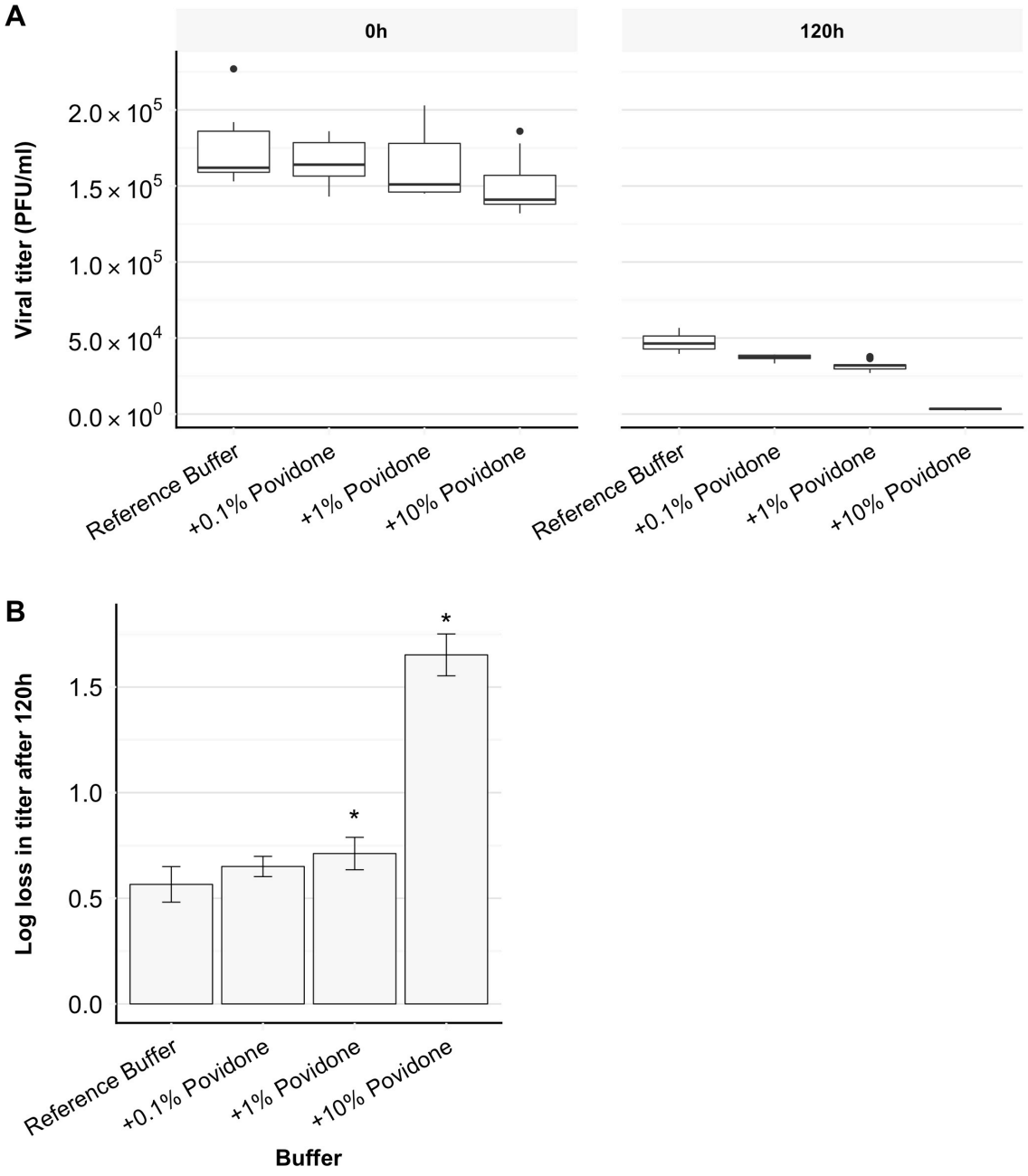

Figure H.1 Effect of different concentrations of povidone on ACAM529 stability.

ACAM529 Lot B was diluted into the reference buffer with or without 0.1%, 1%, or 10% povidone and incubated at 27°C for 120h. Viral titer at 0h and 120h was quantified using plaque assays and reported as PFU/ml (**A**). The total log loss in titer (**B**) was determined and a significant deviation (α = 0.05) from the control (reference buffer) is noted with *.

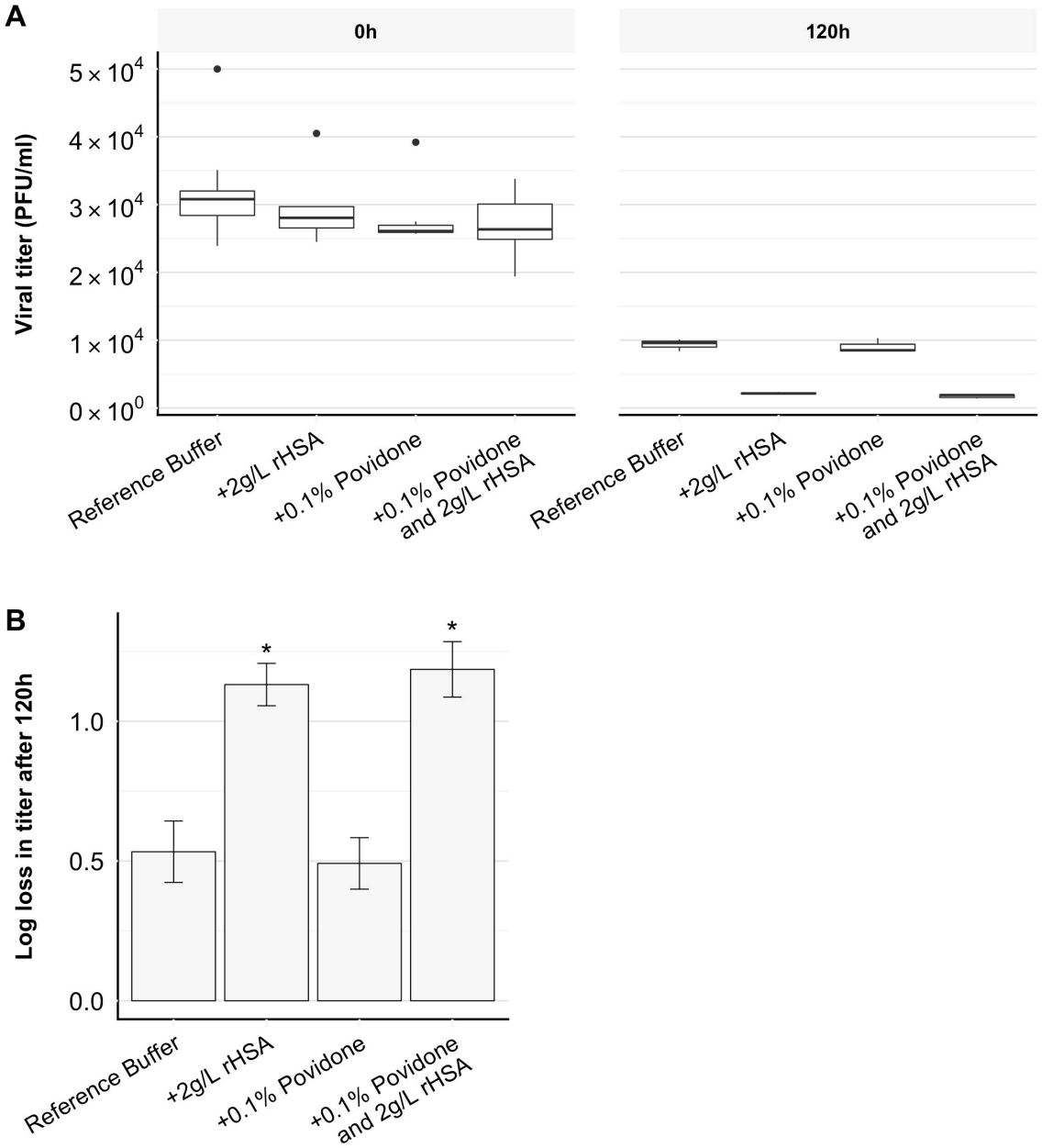

Figure H.2 Effects of povidone and rHSA on ACAM529 stability.

ACAM529 Lot A was diluted into the reference buffer with or without 0.1% povidone, or 2 g/L rHSA, or 0.1% povidone and 2 g/L rHSA, then incubated at 27°C for 120h. Viral titer at 0h and 120h was quantified using plaque assays and reported as PFU/ml (**A**). The total log loss in titer (**B**) was determined and a significant deviation ($\alpha = 0.05$) from the control buffer (reference buffer) is noted with *.

H.2 Effects of whole buffer formulations: Assaying HSV-2 lyophilization buffer

One of the most damaging processes to lipid membranes is freeze-drying and extensive research has gone into developing strategies and libraries of excipients that will protect biological products from such damage [55,59,74]. Cantab Pharmaceuticals Research Ltd. owns a 2001 patent (US 6258362 B1 [147]) for stabilization formulations for herpesvirus, more specifically, a disabled HSV-2 vaccine. It describes several formulations that claim to retain within 0.5 log of the starting titer of a lyophilized sample after a period ranging from 16-52 weeks at 8°C. Here, two representative example buffers presented in the patent were screened for stabilizing properties for ACAM529

H.2.1 Materials and methods

ACAM529 Lot A was quickly thawed at 37°C and diluted 1/100 into freshly prepared reference buffer at pH 7, Cantab Pharmaceuticals buffer Example 1 (CP1) (5% (w/v) lactose (Sigma-Aldrich), 5% (w/v) sucrose (Sigma-Aldrich), 1.8% (w/v) sorbitol (Sigma-Aldrich), 0.1% (w/v) sodium glutamate (Sigma-Aldrich), 2% (w/v) vegetable peptone, 0.1 M Tris-HCl (Bio-Rad), pH 7), or Cantab Pharmaceuticals buffer Example 2 (CP2) (2.5% (w/v) sucrose, 0.5% (w/v) sodium glutamate, 2.5% (w/v) dextran (MW 9,000 - 11,000) (Sigma-Aldrich), 0.1 M Tris-HCl, pH 7), then incubated at room temperature. Samples were taken in triplicate immediately after (0 hour), and 2, 10, 24, 48, 72, 96, and 120 hours after diluting the virus to monitor the viral titer using plaque assays as described in Chapter 3.

H.2.2 Results

Two representative variations of the Cantab Pharmaceutical's patented formulation with components of interest were assayed for stabilization of ACAM529 at room temperature using a time course assay. The Cantab buffers demonstrated sharper decreases in viral stability over the first 48 hours when compared to the control (Figure H.3A). CP2 had a higher titer loss after 120 hours compared to CP1, at 0.72 ± 0.04 log compared to 0.61 ± 0.08 log loss in titer, respectively, but both were significantly higher than the control, which only had a 0.40 ± 0.09 log loss in titer (Figure H.3B). The combination of components of the Cantab buffers was insufficient for stabilizing ACAM529 in liquid solution compared to the reference buffer.

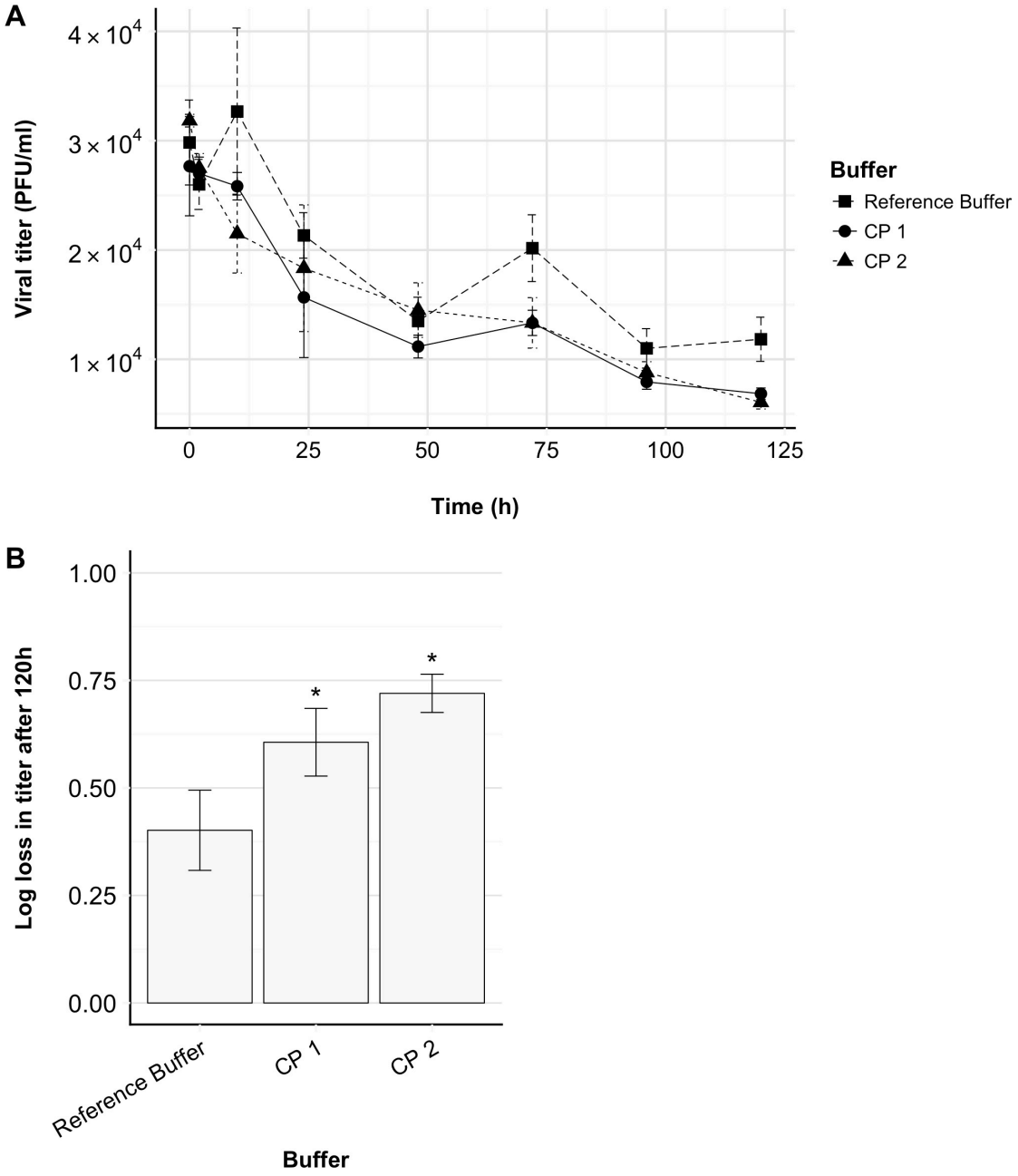

Figure H.3 Effect of two sample formulations for a lyophilized HSV-2 vaccine on ACAM529 stability.

ACAM529 LOT A was diluted into either the reference buffer, Cantab Pharmaceuticals Example buffer 1 (CP1), or Cantab Pharmaceuticals Example buffer 2 (CP2), then incubated at room temperature. Viral stability over time was monitored using plaque assays and reported as PFU/ml (**A**). The total log loss in titer (**B**) was determined and buffers which yielded a significant deviation (α = 0.05) from the control buffer (reference buffer) are noted with *.

H.2.3 Discussion

The Cantab buffers are optimized for lyophilized HSV and its stabilizing effects may not be sufficient for virus in liquid form. The lyophilization process significantly reduces the moisture levels around the product so formulations would aim to mitigate the negative effects by providing excipients that would take the place of water molecules on the product surface [57]. Also, the product would experience less motility in the lyophilized form and would not be subjected to the same deleterious pathways it would encounter in liquid solution so it would not always require the same type of stabilizers. The glutamate level in CP1 was two orders of magnitude lower than that in the reference buffer, and one order of magnitude lower than that in CP2. Also CP2, which had the worst stabilizing properties, had half the amount of sugars (by weight) compared to CP1 and the reference buffer. Furthermore, Tris buffers have been known to have difficulty with pH fluctuations during freezing steps[56,58] yet it is listed as a component of Cantabs formulation buffer. It is clear that formulations that stabilize one type of biological do not necessarily stabilize another, which makes developing formulations a challenge.

Nevertheless, there are components of the Cantab buffers that are of interest to study further. For example, sorbitol, found in CP1, is a sugar alcohol that is not easily crystalized and acts as a plasticizer, increasing mobility but improving stability [56]. Sorbitol and gelatin formulations are effective for many vaccines [55]. Dextran, used in CP2, is a hygroscopic polysaccharide made up of glucose monomers and it is able to increase solution viscosity. It is used commonly for lyophilization as it acts as a bulking agent and lyoprotectant [148]. Despite the Cantab buffers performing poorly in these studies, the potential stabilization properties of the components can not be completely ruled out. Controlled studies where excipients are added to the ACAM529 base purification buffer would provide better information as to whether the excipient is contributing to the stabilization of the virus.